

**REAL TIME MONITORING OF MICROCLIMATIC PARAMETERS OF
POLYHOUSE USING IOT EMBEDDED SENSOR SYSTEMS**

BY

ABHIRAM BABU (2021-02-029)

BHAVANA P (2021-02-030)

ANJALY ANAND (2021-02-039)

KEERTHI NATH R (2021-02-044)



Kerala Agricultural University

**DEPARTMENT OF SOIL AND WATER CONSERVATION ENGINEERING
KELAPPAJI COLLEGE OF AGRICULTURAL ENGINEERING AND FOOD
TECHNOLOGY**

Tavanur-679573, Malappuram

Kerala, India

2025

**REAL TIME MONITORING OF MICROCLIMATIC PARAMETERS OF
POLYHOUSE USING IOT EMBEDDED SENSOR SYSTEMS**

BY

ABHIRAM BABU (2021-02-029)

BHAVANA P (2021-02-030)

ANJALY ANAND (2021-02-039)

KEERTHI NATH R (2021-02-044)

PROJECT REPORT

Submitted in partial fulfilment of the requirement for the degree of

BACHELOR OF TECHNOLOGY IN AGRICULTURAL ENGINEERING

Faculty of Agricultural Engineering and Technology

Kerala Agricultural University



**DEPARTMENT OF SOIL AND WATER CONSERVATION ENGINEERING
KELAPPAJI COLLEGE OF AGRICULTURAL ENGINEERING AND FOOD
TECHNOLOGY**

Tavanur-679573, Malappuram

Kerala, India

2025

DECLARATION

We hereby declare that this Project entitled **“REAL TIME MONITORING OF MICROCLIMATIC PARAMETERS OF POLYHOUSE USING IOT EMBEDDED SENSOR SYSTEMS”** is a Bonafide record of the project work done by us during the course of study and that the report has not previously formed the basis for the award to us of any degree, diploma, associateship, fellowship or other similar title of another university or society.

Place: Tavanur

Date:

Abhiram Babu
(2021-02-029)

Bhavana P
(2021-02-030)

Anjaly Anand
(2021-02-039)

Keerthi Nath R
(2021-02-044)

CERTIFICATE

This is to certify that the project entitled **“REAL TIME MONITORING OF MICROCLIMATIC PARAMETERS OF POLYHOUSE USING IOT EMBEDDED SENSOR SYSTEMS”** is a record of the project work done jointly by **Mr. ABHIRAM BABU (2021-02-029), Ms. BHAVANA P (2021-02-030), Ms. ANJALY ANAND (2021-02-039) and Ms. KEERTHI NATH R (2021-02-044)** under my guidance and supervision and that it has not been previously formed the basis for the award of any degree, diploma, fellowship or associateship or other similar title of any other university or society to them.

Place: Tavanur

Date:

Guide

Dr. Sathian K K

Professor

KCAEFT, Dept. of SWCE

Co-Guide

Dr. Shaheemath Suhara K K

Assisstant Professor (C)

KCAEFT, Dept. of SWCE

ACKNOWLEDGEMENT

First of all, I offer million gratitude to The Almighty who made us to do this task and made every job a success for us. He was the greatest source of all resources and provision, moral or without whose grace nothing is possible.

We are deeply grateful to our esteemed guide, **Dr. Sathian K K**, Professor, Department of Soil and Water Conservation Engineering, KCAEFT, for his invaluable guidance, constant encouragement, and constructive feedback throughout the project. His expertise and mentorship were instrumental in shaping this project work.

We would also like to extend our heartfelt thanks to our co-guide, **Dr. Shaheemath Suhara K K**, Assistant Professor (C), Department of Soil and Water Conservation Engineering, KCAEFT, for her continuous support, insightful suggestions, and motivating presence that helped us overcome various challenges during the project.

It is our pleasure to pay tribute to **Dr. Jayan P R**, Dean of Faculty and Professor & Head, Department of Farm Machinery and Power Engineering, KCAEFT, Tavanur, for his valuable advices and help rendered during this study.

A special word of appreciation goes to **Er. Siddharam**, Young Professional of Precision Farming Development Centre (PFDC), KCAEFT, Tavanur for his technical assistance and practical insights, which greatly contributed to the implementation and refinement of the IoT-based sensor system used in this project.

Finally, we extend our gratitude to all the faculty members, staffs and friends who directly or indirectly supported us throughout the duration of this work.

| | |
|----------------|---------------|
| Abhiram Babu | (2021-02-029) |
| Bhavana P | (2021-02-030) |
| Anjaly Anand | (2021-02-039) |
| Keerthi Nath R | (2021-02-044) |

**DEDICATED TO OUR
AGRICULTURAL
ENGINEERING
PROFESSION**

CONTENT

| Chapter No. | Title | Page No. |
|-------------|------------------------|----------|
| | LIST OF FIGURES | i |
| | LIST OF TABLES | iii |
| | LIST OF PLATES | iv |
| I | INTRODUCTION | 1 |
| II | REVIEW OF LITERATURE | 3 |
| III | MATERIALS AND METHODS | 45 |
| IV | RESULTS AND DISCUSSION | 85 |
| V | SUMMARY AND CONCLUSION | 113 |
| VI | REFERENCES | 117 |
| | ABSTRACT | 130 |

LIST OF FIGURES

| Figure No. | Title | Page No. |
|-------------------|--|-----------------|
| 2.1 | Classification of CO ₂ control methods in the greenhouse | 26 |
| 2.2 | Smart IoT controller for greenhouse automation | 28 |
| 3.1 | Location of study area | 48 |
| 3.2 | Experimental plot | 49 |
| 3.3 | SHT10 Soil temperature & Humidity sensor | 52 |
| 3.4 | Arduino IDE windows interface | 56 |
| 3.5 | Arduino account creation | 58 |
| 3.6 | ESP32-S board connection with USB cable | 58 |
| 3.7 | Arduino dash board | 59 |
| 3.8 | Selecting the board | 60 |
| 3.9 | Sketch files | 60 |
| 3.10 | Successful upload printed in the console | 61 |
| 3.11 | Successful compilation printed in the console | 62 |
| 3.12 | Serial monitoring of data | 62 |
| 3.13 | ThingSpeak windows interface | 63 |
| 3.14 | Channels | 65 |
| 3.15 | API keys interface | 65 |
| 3.16 | System overview | 69 |
| 3.17 | Pins of ESP32-S, DHT22 sensor and their interfacing | 70 |
| 3.18 | Pins of ESP32-S, BH1750 light intensity sensor and their interfacing | 72 |
| 3.19 | Schematic circuit diagram of sensor connected to microcontroller | 73 |
| 3.20 | Source code for reading temperature and relative humidity | 74-78 |
| 4.1 | DHT22 sensor temperature calibration curve | 86 |
| 4.2 | Calibration chart for DHT22 sensor for relative humidity | 88 |
| 4.3 | Incorporation of calibration equation into Arduino code | 89 |
| 4.4 | Calibration chart for BH1750 voltage vs. lux meter reading | 90 |

| | | |
|------|---|---------|
| 4.5 | Code used for light intensity using lux meter reading and voltage | 91 |
| 4.6 | Calibration chart of lux meter reading vs. BH1750 sensor reading | 92 |
| 4.7 | Calibration chart for lux meter reading vs. BH1750 sensor's resistance reading | 93 |
| 4.8 | Code used for light intensity using lux meter reading and resistance | 94 |
| 4.9 | Weather data apps | 96 |
| 4.10 | Datasheet of wind speed sensor | 96 |
| 4.11 | Wind speed sensor calibration chart | 98 |
| 4.12 | Code used for wind speed sensor | 99 |
| 4.13 | Windspeed sensor calibration chart (Inverse code) | 100 |
| 4.14 | Inverse code used for windspeed sensor | 101 |
| 4.15 | Code used for SHT10 soil temperature sensor | 102 |
| 4.16 | Obtained results of temperature and humidity from different poles | 104-105 |
| 4.17 | Vertical variation | 106 |
| 4.18 | Time based microclimate variation | 108 |

LIST OF TABLES

| Table No. | Title | Page No. |
|------------------|---|-----------------|
| 2.1 | General overview with brief description of models | 20 |
| 3.1 | Details of study area | 46 |
| 3.2 | Specifications of the Polyhouse | 47 |
| 3.3 | Specifications of DHT22 Temperature & Humidity sensor | 50 |
| 3.4 | Specifications of BH1750 Light sensor | 51 |
| 3.5 | Specifications of SHT10 Soil temperature & Humidity sensor | 52 |
| 3.6 | Specifications of wind speed sensor | 53 |
| 3.7 | Specifications of microcontroller | 54 |
| 3.8 | Specifications of Jio WI-FI modem | 55 |
| 3.9 | ESP32-S pins and its connections with DHT22 Temperature & Humidity sensor | 71 |
| 3.10 | ESP32-S pins and its connections with BH1750 light intensity sensor | 72 |
| 3.11 | Estimated cost of wire required at different microcontroller position | 79 |
| 3.12 | Estimated cost of components | 79 |
| 3.13 | Overall cost estimation of the system | 80 |
| 4.1 | DHT22 Sensor reading and dry bulb temperature reading | 86 |
| 4.2 | DHT22 Sensor reading and calculated reading for relative humidity | 87 |
| 4.3 | Lux meter and voltage reading | 90 |
| 4.4 | Lux meter reading and BH1750 sensor reading | 91 |
| 4.5 | Lux meter reading and sensor resistance reading | 92 |
| 4.6 | Readings from wind compass pro app and wind speed sensor | 97 |
| 4.7 | Readings from wind compass pro app and wind speed sensor (Inverse Code) | 99 |
| 4.8 | Challenges faced during the installation of different components in polyhouse | 109 |

LIST OF PLATES

| Plate No. | Title | Page No. |
|-----------|--|----------|
| 3.1 | Polyhouse | 46 |
| 3.2 | DHT22 Temperature & Humidity sensor | 50 |
| 3.3 | BH1750 Light sensor | 51 |
| 3.4 | Wind speed sensor | 53 |
| 3.5 | NODE MCU ESP32-S microcontroller | 54 |
| 3.6 | Jio WI-FI modem | 55 |
| 3.7 | Preparations for the experiment | 84 |
| 4.1 | Readings obtained from soil temperature sensor | 102 |
| 4.2 | Sensor readings | 103 |
| 4.3 | Sensor damages | 112 |
| 5.1 | Project team | 116 |

INTRODUCTION

CHAPTER-I

INTRODUCTION

The global population has reached 8 billion and is projected to rise to 9.8 billion by the year 2050 (FAO, 2020). This population surge presents a major challenge in ensuring for global food security, requiring a significant increase in agricultural productivity. Concurrently, rapid urbanization and expanding infrastructure are contributing a significant reduction in arable land due to the conversion of farmlands into residential and industrial areas. These changes are intensifying problems such as hunger, poverty, and the increasing demand for nutritious and fresh produce.

Traditional methods of crop monitoring, such as manual scouting, are labour-intensive, time-consuming, and costly. However, monitoring key environmental parameters like temperature, relative humidity (RH), and light intensity are critical for optimal plant growth and ensuring higher crop productivity. Continuous observation of these parameters helps farmers understand how different environmental factors influence plant health and to adopt more effective cultivation strategies.

In this context, smart farming techniques, particularly those based on IoT (Internet of Things) technologies, have become essential tools in modern agriculture. IoT-based sensors and data analytics support precision agriculture by collecting and analysing real-time field data (Kagan *et al.*, 2022). IoT integration allows precise regulation of internal conditions such as temperature, humidity, and light. Greenhouses, typically made of transparent materials like glass or plastic, protect crops from adverse weather and pests while promoting optimal growth (FAO, 2020).

Maintaining optimal microclimatic conditions within a greenhouse is key to ensuring healthy plant growth and maximizing productivity (Maraveas *et al.*, 2022). While greenhouse automation is gaining traction for its role in enhancing resource efficiency and crop output, our focus is solely on monitoring these parameters.

The emergence of IoT has significantly influenced agricultural practices in recent years. IoT refers to a network of interconnected physical devices equipped with sensors, microcontrollers, or processors that can communicate and share data over the internet without human intervention (Gillis, 2021). These smart devices, embedded with

sensors, collect critical environmental data that can be accessed and monitored remotely in real-time. IoT systems reduce the need for manual labor and mitigate risks associated with accessing remote or hazardous areas.

The integration of IoT in greenhouse environments has opened new avenues for sustainable agriculture by enabling real-time monitoring of environmental conditions. A well-designed IoT-based system involves sensor networks and cloud computing to continuously collect and process data related to temperature, humidity, light intensity, and other relevant parameters (Dhanaraju *et al.*, 2022). This data-driven approach equips farmers with valuable insights, allowing them to track and analyse the crop environment over time, identify trends, and make informed decisions to improve crop health and productivity.

In light of these advancements, the present study Entitled "**Monitoring of microclimatic parameters using IoT Embedded sensor systems and introducing control systems**" was undertaken with the following specific objectives:

- Design of an IoT-based embedded sensor system for real-time monitoring of critical environmental parameters in a polyhouse
- Implementation of the IoT-based embedded sensor system for real-time monitoring
- To evaluate the real time variation of microclimatic variation

REVIEW OF LITERATURE

CHAPTER-II

REVIEW OF LITERATURE

In recent years, there has been a lot of interest in the integration of IoT-based embedded sensor systems in agriculture, especially in polyhouse environments. Optimising crop productivity, resource use, and disease prevention all depend on real-time monitoring of microclimatic factors including temperature, humidity, and light intensity.

2.1 EFFECT OF TEMPERATURE ON GREENHOUSE FARMING

Temperature is a critical environmental factor that significantly influences greenhouse crop production. The interaction between day and night temperatures, climate management strategies, solar radiation, pest dynamics, and broader climate changes all play vital roles in shaping plant growth, reproductive success, and yield quality (Myser and Moe, 1995).

The difference between day and night temperature (DIF) influences multiple plant morphological traits, including internode length, plant height, leaf orientation, shoot orientation, chlorophyll content, lateral branching and petiole and flower stalk elongation in plants (Myser and Moe, 1995).

Internode length increases as DIF increases. The response of stem elongation to DIF is greater when DIF increases from zero to positive, than from negative to zero DIF. DIF has the greatest effect on plant height during the period of rapid growth in determinant crops. Furthermore, the responses to DIF are rapid, and most plants respond to a change in day and night temperature within 24 h. These morphological changes are attributed to enhanced cellular elongation rather than increased cell division. DIF influences flower initiation minimally in some long-day plants, it delays flowering in short-day species like poinsettia (Myser and Moe, 1995).

Furthermore, DIF interacts with light intensity, quality, and photoperiod, though it does not significantly interact with water stress. Physiologically, DIF influences endogenous gibberellin (GA) concentrations, which modulate growth responses (Myser and Moe, 1995).

In subtropical regions, greenhouses often face the challenge of extremely high internal temperatures due to intense solar radiation, which hinder crop growth and survival. Two primary shading systems are employed to mitigate heat stress: internal shading nets and external shading nets (Chen *et al.*, 2011). Internal shading nets, placed just below the greenhouse roof, filter sunlight after it enters, whereas external shading nets, positioned above the structure, intercept solar radiation before it penetrates the greenhouse. While both types protect crops from heat stress and sunburn, external shading nets are more effective in reducing internal temperatures by preventing heat buildup. Internal shading nets, while still effective, may not reduce temperatures as much since some heat is already inside before being filtered. Additionally, internal nets may obstruct airflow, potentially reducing ventilation efficiency, while external nets maintain better air circulations. Overall, both nets contribute to creating a more stable and suitable microclimate for plant growth by moderating temperature fluctuations and reducing water loss through transpiration (Chen *et al.*, 2011).

Tomato yield in warm climates is particularly sensitive to night temperatures. Willits and Peet (1998) demonstrated that maintaining night temperatures (NT) below 21°C during fruit set significantly enhances fruit weight. Their findings showed that keeping NT below this threshold increased fruit weight by 28% in spring, 53% in summer, and 11% in fall, compared to higher night temperatures. High night temperatures (above 21°C) are detrimental to fruit set and yield in tomatoes. When NT exceeds this limit, fruit set declines, leading to reduced overall yields. Conversely, maintaining NT within the optimal range of 15°C to 21°C supports better reproductive development and significantly improves tomato yields (Willits and Peet, 1998).

High temperatures have a predominantly negative impact on reproductive development in many plant species, including tulip, iris, chrysanthemum, and tomato. Elevated temperatures typically above 30°C to 35°C can disrupt key reproductive processes such as pollen development, pollen viability, and pollen tube growth, often leading to pollen sterility. For example, in rice, more than 50% of pollen fails to germinate when temperatures exceed this range, and similar reductions in pollen viability are observed in wheat and other crops (Willits and Peet, 1998).

Increasing temperature under low radiation conditions in greenhouse-grown broccoli significantly affects the levels of phytochemicals and ascorbic acid (Vitamin C). Schonhof *et al.* (2006) found that elevated temperatures under low radiation reduce ascorbic acid levels and alter glucosinolate profiles, compromising both nutritional value and defence mechanisms. The concentration and composition of glucosinolates are sensitive to temperature changes. Some glucosinolates may decrease, while others may increase, depending on the specific compound and temperature regime. The interaction between temperature and light is crucial; low radiation combined with higher temperatures tends to have a more pronounced negative effect on ascorbic acid and can shift the balance of phytochemicals, potentially affecting both crop quality and health-promoting properties.

Solar radiation plays a fundamental role in shaping the internal climate of greenhouses, particularly by influencing temperature, ventilation, and humidity interactions. It remains a critical driver of internal climate dynamic (Frausto *et al.*, 2003). In greenhouse cultivation, maintaining appropriate temperature and humidity is crucial for optimal crop growth, particularly during cold weather when heating is needed to create a suitable environment, and during warm weather when humidity control is also essential. Research indicates that temperature distribution within a greenhouse is not uniform: the highest temperatures are typically found at the centre, while the sides exhibit variation based on orientation (Tang *et al.*, 2020).

Specifically, the south side of the greenhouse is usually the warmest among the sides, followed by the east side, with the north and west sides generally having the lowest and quite similar temperatures (Tang *et al.*, 2020). The south side receives the most direct sunlight throughout the day, leading to higher temperatures due to increased solar gain. The east side warms up quickly in the morning as it is exposed to the rising sun, but does not retain heat as long as the south side. The north and west sides receive less direct sunlight, resulting in cooler temperatures. The north side is often shaded for most of the day in the northern hemisphere, while the west side only receives afternoon sun, which is less effective in raising the temperature compared to the sustained exposure on the south side.

This uneven temperature distribution is a direct result of the greenhouse's orientation to the sun and the way solar radiation interacts with the structure. Proper management of heating, ventilation, and humidity control systems is therefore necessary to ensure a uniform and optimal environment for plant growth throughout the greenhouse (Tang *et al.*, 2020).

Raising the average daily temperature (ADT) by increasing daytime temperatures has a stronger effect on plant elongation compared to increasing both day and night temperatures equally. However, according to Grimstad *et al.*, (1993), if daytime temperatures are raised to extreme levels, this positive effect on elongation does not continue indefinitely. At excessively high temperatures, plant growth and elongation can actually be inhibited due to heat stress, reduced photosynthetic efficiency, and possible damage to cellular processes. Thus, while moderate increases in daytime temperature stimulate elongation, extreme daytime temperatures can negatively impact plant growth and development.

For flower bud development, more negative DIF values (where nights are warmer than days) lead to a sharper decrease in the number of flower buds, compared to increasing positive DIF values (where days are warmer than nights). Overall plant dry weight increases as ADT rises. However, when daytime temperatures are lower than nighttime temperatures, plants tend to have significantly lower fresh and dry weights, poorer root development, and shorter height (Grimstad *et al.*, 1993).

Kocourek *et al.* (1994) demonstrated that temperature is a key factor influencing the development, reproductive period, fecundity, and population growth rate of *Aphis gossypii* (cotton aphid) on greenhouse cucumbers. The optimal temperature range for *A. gossypii* development was found to be between 20°C - 30°C. At temperatures below or above this optimal range, both the developmental rate and reproduction rate of *A. gossypii* declined. Extreme high temperatures (above 32°C–35°C) negatively impacted aphid survival and fecundity, with heat stress causing a continuous decrease in the number of offspring and adult survival over time.

At warmer temperatures (up to 30°C), aphids developed faster and produced more offspring. In fact, total fecundity the number of larvae produced per female increased from 36 larvae at 10°C to 76 larvae at 30°C (Kocourek *et al.*, 1994).

Rising greenhouse gas (GHG) levels have led to increased temperatures and reduced temperature fluctuations in high-latitude regions. The decrease in variability is partly attributed to the diminishing presence of insulating elements such as snow and ice, which historically helped buffer temperature changes (Stouffer *et al.*, 2007).

For greenhouses, this shift means that, despite generally warmer conditions, the loss of natural insulation can allow cold outside air to penetrate more easily particularly in winter and spring. This is especially problematic for greenhouses with poor insulation, where sudden drops in outside temperature can quickly translate to abrupt temperature declines inside, increasing the risk of cold stress for crops (Stouffer *et al.*, 2007).

To manage heat buildup inside greenhouses, four main strategies are typically used: ventilation, shading, evaporative cooling, and composite systems that combine multiple methods. Chen *et al.* (2011) found that the most effective approach for lowering greenhouse temperatures during hot summer months was the combination of shading with increased ventilation rates.

Key Findings from Chen *et al.* (2011) are listed out below:

- a. Temperature reduction: The combined use of shading nets and mechanical ventilation (using exhaust fans) was able to reduce the interior greenhouse temperature to nearly the same level as the ambient outdoor temperature, even under intense summer heat. In some experimental conditions, the difference between internal and external temperatures was minimized to as little as 1°C, effectively preventing dangerous heat accumulation that could otherwise exceed 40°C levels at which no commercial crop could survive.
- b. Type of ventilation: The study tested both natural ventilation (roof and side vents partially open, with an air exchange rate of about 0.15/h) and mechanical ventilation (exhaust fans in the upper layer). Mechanical ventilation, when combined with shading, was significantly more effective in expelling accumulated heat than natural ventilation alone.
- c. Shading configuration: Both internal and external shading nets were used, with internal nets having a transmittance of 50%. The combination of shading and

ventilation was crucial, as shading alone could reduce solar radiation but also restricted airflow, limiting heat release if not paired with adequate ventilation.

- d. Climatic conditions and greenhouse structure: The experiments were conducted in a greenhouse exposed to high summer temperatures, focusing on conditions relevant for growing high-value crops. The structure included upper and lower air layers, and the methodology involved monitoring temperature differences at various heights and with different control strategies.
- e. Context-dependence: The effectiveness of any cooling strategy is highly context-dependent, varying with greenhouse design, geographic location, crop type, and local climate. For example, in regions with intense solar radiation and limited natural airflow, mechanical ventilation combined with shading is especially beneficial.

2.2 EFFECT OF WIND VELOCITY ON GREENHOUSE MICRO CLIMATE

Wind direction significantly affects ventilation and internal climate that crosses the ridge of the greenhouse at an angle, it influences inflow and outflow through roof openings. Wind flowing parallel with the ridge creates inflow at the downwind terminus and outflow at the windward terminus. Airflow inside the greenhouse is irregular, with varying velocities and asymmetric distribution. Air velocities were higher near the ground and roof, Internal wind velocities were directly proportional to external wind velocities when the roof vents were open. Internal velocities were higher near the floor and lower at the crop canopy position. Internal air speeds were highly correlated with ventilation flux, which includes both wind-induced and buoyancy-induced ventilation driven by the temperature gradients. The combination of these produced more accurate prediction of the speeds of the internal air compared to wind speeds alone (Wang *et al.*, 1999).

Equation to calculate average air speed,

$$V_{\text{Cal}} = \frac{\phi_v}{A}$$

Where, V_{Cal} = calculated average air speed

ϕ_v = ventilation flux (m^3/s)

A = greenhouse cross-sectional area (Wang *et al.*, 1999).

The wind pressure coefficient represents the force acting along the surface of the greenhouse caused by fluid flow on the surface of the greenhouse (Hur *et al.*, 2018).

Buoyant forces are excluded when ventilation rate is directly proportional with wind speed. That justifies classical ventilation theory that explains airflow due to pressure gradients caused by wind. Wind direction influences the rate of ventilation heavily. A 10-degree shift of wind direction influences ventilation rates by up to 50%. Ventilation rates are most rapid when the wind impinges directly upon the window (windward) and least rapid when wind runs with the roofline (leeward). Rollup and flap roof windows were the roof window types that were examined. Rollup roof windows provided more ventilation rates on average since the openings' area increased (Campen *et al.*, 2003).

Warm air exited by the roof vents at the top and cool dry air entered by the roof vents at the bottom, establishing periodic convective currents caused by the thermal gradients. The above highlights the combined effect of wind-induced ventilation and buoyancy-induced airflow. Insect screens reduced the internal air speeds considerably and raised temperatures and humidities, especially beneath the crop canopy. Ventilation rate decreased, which meant poor elimination of heat and humidities (Majdoubi *et al.*, 2009).

Traditional cup anemometers and hot-wire sensors are not appropriate for greenhouses for the reasons (Li *et al.*, 2023) that:

- Inability to monitor airflow patterns.
- Sensitivity to temperature changes.
- Expensive and requiring servicing under moist green-house conditions

Rong *et al.* (2015) evaluated the impact of wind speed, wind direction and nearby maize field on the rate of air exchange (ACH) and the rate of indoor air velocity within the hybrid vented dairy cow facility utilizing auto-regulated natural and mechanical pit. The wind speed had a strong impact on ACH while the modelling of the maize field had a negligible effect on ACH with the wind of low speed. At a wind speed

of 3.86 m s^{-1} during validation, with modelling of the maize field lowered the total ACH by 24%, ACH through the lower openings of the sidewall by 89.7%, and the upwind measured air speed by 71%. The results showed that the most important effect of the plant canopy was on ACH by the opening at the sidewall. When wind direction changed from 0° to 90° , ACH varied by up to 60%.

2.2.1 Wind/Air velocity inside greenhouse

Under greenhouse condition, inside flow of air influences several important aspects of microclimate which have great influence on the growth regulating processes of crop / plant viz. photosynthesis and transpiration.

Due to photosynthesis and respiration, the microclimate around the leaf is changing regularly. In daytime CO_2 status of this microclimate reduces significantly due to increasing photosynthesis rate, which subsequently leads to gradual reduction in photosynthesis. At the same time the Relative humidity around the leaf increases due to transpiration eventually reducing the rate of transpiration. This ultimately affect the root uptake adversely (Gastra ,1959).

The increased air circulation inside a greenhouse improves the air movement around the leaf, reducing the humidity and increasing the CO_2 status around stomata. As a result, rate of photosynthesis and root uptake increase, promoting crop growth (Gastra ,1959).

Gastra (1959) explored the relationship between CO_2 uptake, the rate of photosynthesis, and wind velocity in various greenhouse vegetables. The study observed that, there is a continuing increase in the rate of CO_2 uptake by leaf as wind velocity increases. Wind velocity influences the resistance to CO_2 diffusion from air to leaf.

2.2.2 Wind/Air velocity outside greenhouse

High wind speed and storm events can cause significant structural damage to greenhouses and severely impact the crops inside. Therefore, the greenhouses must be built to resist such extreme conditions. If the high-wind penetrates the greenhouse through windows the crop, particularly the trellising crop, can be severely damaged (Gastra ,1959).

Analysing long-term (20 to 50 years) climatic data, the average wind speed can be estimated. Depending on that estimate the structural design should be made (Gastra, 1959)

It should be made in such a way that it can take care of the extreme adverse effect of wind/storm. In general, 100 to 150 km/h wind speed is considered for greenhouse construction depending upon the area.

2.3 EFFECT OF LIGHT INTENSITY IN GREENHOUSE FARMING

Light is one of the most crucial environmental factors influencing the crop growth and development, which supplies energy for photosynthesis. However, in greenhouse environments, it is often difficult to meet the optimal light requirements of crops due to factors such as the optical properties of covering materials, the angle of sunlight incidence, and structural shading. During certain seasons, particularly during the winter, early spring, and rainy seasons, natural light levels inside the greenhouses are typically low (Gislerod *et al.*, 1989).

In addition to reducing dry matter accumulation and stem diameter growth, this low light condition also lowers the maximal RuBP regeneration rate, carboxylation efficiency, and net photosynthetic rate because of nonstomatal restriction. These occurrences cause crops to grow and develop more slowly, become more susceptible to pests, and produce fewer fruits and flowers. Crop quality and output are significantly impacted (Xin *et al.*, 2019).

Reduced productivity in greenhouses in northern nations during the winter months is mostly caused by a lack of light. Artificial illumination is widely employed in greenhouse production during times when natural light levels are low. It has been discovered that artificial light benefits a wide variety of ornamentals as well as horticultural crops, increasing yield and improving product quality (Xin *et al.*, 2019).

By using artificial light, the producers are able to have consistent output schedules throughout the year (Gislerod *et al.*, 1989). Altering the spectral distribution of natural radiation to influence plant growth was once considered impractical. However, the advent of double-layer greenhouse covering has allowed for variable light quality adjustment (Mortensen and Strømme, 1987).

Light influences plant growth by activating photoreceptors such as phytochromes, cryptochromes, and phototropins, which respond to its intensity and wavelength to regulate gene expression and developmental processes. Typically, red light makes up the base of lighting spectrums, and photosynthesis and normal plant growth require red light (Olle and Viršile, 2013).

Light intensity must be sufficient for plant growth, free from any distractions or environmental factors. In order to support a structure for growing plants that is transparent to light, a greenhouse should be sufficiently enclosed to reduce convective heat loss, or the exchange of air between the interior and exterior (Olle and Viršile, 2013).

Greenhouse lighting is primarily influenced by solar radiation, though artificial lighting (e.g., fluorescent or high-intensity discharge lamps) is often used to supplement light on cloudy days. Effective supplemental lighting requires careful planning, including consideration of light intensity, distribution, duration, and system maintenance. Monitoring plant-available light also depends on proper sensors and placement (Khot and Gaikwad, 2016).

The greenhouse structure is the first obstacle that solar radiation must overcome once it reaches the earth's surface. Typically dense, glazing bars and framing members absorb or reflect all of the light that strikes them. This also applies to gutters. Electric conduits, water lines, heating tools and pipes, horizontal airflow fans, shade curtains, and additional lighting are all positioned towards the top of the greenhouse, obstructing the light from reaching the plants within. Evaporative cooling pads and drying fans are often installed in the sidewalls to reduce the amount of sun radiation (Khot and Gaikwad, 2016).

Photosynthetically Active Radiation (PAR) refers to the light energy within the 400-700 nm wavelength range, which is the part of the spectrum that plants use for photosynthesis. This is often called the "photosynthesis band," and its intensity is measured in watts per square meter per second ($\text{W/m}^2\text{s}$) (McCree, 1971). However, photosynthesis is a quantum process, which depends more on the number of photons a plant receives rather than the energy carried by each photon (Barnes *et al.*, 1993). When it comes to plant growth and development, PAR is measured as the number of photons

reaching a given area, known as Photosynthetic Photon Flux Density (PPFD), and is expressed in $\mu\text{mol}/\text{m}^2\text{s}$. Traditionally, horticultural lighting has focused on factors like yield quality, quantity, and optimizing light conditions for specific crops, including light intensity, spectrum, and photoperiod. Recently, there has been growing interest in intelligent lighting systems that can precisely deliver the required light while minimizing energy consumption (Mohagheghi and Moallem, 2023). Light intensity can be measured in terms of the photosynthetic photon flux density (PPFD) for plant physiological studies because photosynthesis is a photon-driven activity (Mosharafian *et al.*, 2021).

Light plays a crucial role in plant growth, shaping their development, structure, distribution of dry matter, and even water content. While it's often assumed that more light directly leads to higher production, the relationship between light and photosynthesis is not that straightforward. Leaf photosynthesis follows a non-linear pattern in response to light, meaning that at a certain point, more light doesn't necessarily mean more photosynthesis. Additionally, the impact of light on plants is influenced by various other factors, such as CO_2 levels, temperature, and the density of leaves in a given area (leaf area index). For over 20 years, Dutch growers have followed a simple rule of thumb: a 1% increase in light leads to a 1% increase in plant growth and production. However, this effect isn't the same for all crops. While vegetable crops generally show a strong response to additional light, the impact is often weaker for cut flowers and potted plants. In these cases, a 1% increase in light is typically expected to result in only about a 0.5% increase in growth and production. For most crops, a 1% increase in light typically leads to a 0.5% to 1% increase in the final harvestable yield. The effect of light on plant growth is influenced by various factors. Plants tend to benefit more from additional light when light levels are low or when CO_2 concentration and temperature are higher. As a result, the impact of extra light is generally greater in winter than in summer, with winter values slightly above and summer values slightly below the yearly average.

The growth response to light also depends on when and for how long the light level changes. In greenhouses, adjusting light intensity affects other environmental conditions. One key factor is the inverse relationship between CO_2 levels and sunlight—

when light increases, CO₂ often decreases, which can limit the positive effects of extra light. Because of these interactions, greenhouse lighting should not be viewed in isolation but as a crucial part of overall farm management (Marcelis *et al.*, 2005).

2.4 EFFECT OF RELATIVE HUMIDITY ON GREENHOUSE CULTIVATION

The importance of air humidity for designing greenhouse for crop production is frequently underestimated. Both the humidity of air outside and inside of a greenhouse shall be meticulously evaluated and considered while planning a greenhouse. Furthermore, both absolute humidity and relative humidity has to be properly measured and shall be considered with due importance. Plant growth and production will slow down or stop when the humidity in air is lower than 30% or higher than 90%.

The following two reasons, in general, may be decisive for a deviation of relative humidity in the greenhouse:

- i. The varying exchange condition of air volume in respect of water vapour at an equal rate of water vapour supply by way of evapotranspiration.
- ii. The varying inside temperature condition of the greenhouse influences the relative humidity considerably. The high inside temperature reduces the relative humidity of inside air of the greenhouse, but due to high transpiration the absolute humidity increases accordingly.

Humidity: Humidity is the water vapour present in the air. Status of humidity is generally considered and measured in different ways in relation to temperature viz. relative humidity (RH), absolute humidity, vapour pressure deficit (VPD) and dew point.

Relative humidity: It is the water vapour present in percentage of maximum water vapour that can be retained by air at a given temperature. It is expressed as the ratio of water vapour actually present in the air and maximum water vapour that can be retained by that air at a given temperature. For example, per cubic meter of air at 20°C can hold 17.3g water vapour in maximum (100%). So, if it holds 13g/m³, then the relative humidity is 75%. The relative humidity falls with increase in temperature and rises with decrease in temperature. Now, the most problematic situation is higher relative humidity at higher temperature.

Absolute Humidity: It is the actual weight of water vapour per cubic meter of air and expressed as g/m^3 . Conversion of absolute humidity to relative humidity can be done only when the temperature is known. For example, 15 g/m^3 at 17.5°C equals to 100% relative humidity while with same absolute humidity at 25°C the relative humidity equals to 65% and at 30°C it equals to 50%. Thus, under greenhouse, when absolute humidity is very high at higher temperature, it is really difficult to control.

Vapour Pressure Deficit: VPD indicates 'drying effect' of the air. It is the relation between vapour pressure of a particular gas, here the water vapour, and the normal air pressure (pressure of all gases in the air together) that is expressed as millibar or kilopascal (KPa). It normally ranges from 10 to 50 millibar or from 1 to 4 KPa.

Dew-point: It is a point of temperature and absolute humidity below which the excess water vapour in air condenses. For example, air with 10 g/m^3 and 20 g/m^3 has dew point of 11°C and 22.5°C respectively. That means, under greenhouse condition, when dew-point arrived, the relative humidity will reach 100%, and any further drop of temperature reduces the maximum holding capacity of water vapour of that air. The excess water vapour condenses and precipitates as dew on the crop, which can invite or spread the fungal infection.

Effect of Relative Humidity: We understand that RH 95% at 20°C means 16.5 g/m^3 absolute humidity. In theory RH below 100% means that there is no condensation, but the temperature throughout the greenhouse may not be equal and in few corner spots the RH may be 100%. As a result, condensation takes place on the leaves. Thus, the spores of Botrytis or other fungal disease starts growing. So, any greenhouse owner should know the RH reading and its variation inside, and monitor it regularly.

The temperature increase in the poly house could be the cause of the shift in relative humidity over time. The poly house's humidity levels were higher in the morning and progressively dropped in the afternoon as the temperature rose. The poly house was packed with vegetation, and the plants were properly irrigated, so the ground surface of the greenhouse was constantly moist. This could be the cause of this. A specific amount of water in the soil evaporates at night. Water vapor escaped from the poly house to the exterior relatively less at night since it was covered with an ultraviolet stabilized sheet and there was no sunlight. Additionally, increased transpiration from

the leaves will occur in the early morning when the sun first rises. The polyhouse's interior relative humidity increased as a result of both of these causes working together (Umesha B., 2011).

2.5 EFFECT OF SOIL TEMPERATURE IN POLYHOUSE FARMING

Physical and chemical forms within the soil are influenced by spatial/temporal changes as well as by soil temperature. The last mentioned could be an exceptionally critical meteorological parameter for exchanging warm vitality from soil to the air and vice versa. It is, as well, an essential parameter in agrarian applications like depth determination, plant development, fertilizer degradation, potential evaporation and control of microbiological exercises. Numerous of these applications require information on the thermal administration of the upper layers to the more profound layers. Within the case of agrarian soils, information on soil temperature is essential for plant improvement and inducing the state of the roots of developed crops, which is for the most plants distributed from 0 to 50 cm of development. Vitality trades and temperature dispersion at the surface and within the upper layers of the soil are imperative, both within the field of horticulture and in their connection to the perspectives of nursery warming. This guideline has been the subject of several studies. Most nursery climates consider, which take into consideration warm trades with the soil, streamline the issue by considering that the soil is of homogeneous and isotropic composition (Benzari *et al.*, 2022).

Generally, the soil temperature inside a polyhouse is higher than the soil temperature outside because the polyhouse microclimate retains more heat from the sunlight and so produces a warmer soil environment within its walls. The exact difference depends on the type of plastic, weather and shading or ventilation systems.

2.5.1 Impacts of soil temperature on soil processes

The biological, chemical, and physical characteristics of soils that support plant growth and productivity are all influenced by soil temperature. With most soil microbes working best between 10°C and 35.6°C and soil macro-organisms thriving between 10°C and 24°C but dying at extremes like 58°C, optimal soil temperatures (roughly 10°C to 28°C) stimulate extracellular enzymes that drive the decomposition of organic

matter, enhance microbial activity and nutrient mineralization, and promote root respiration. In contrast, temperatures below freezing inhibit these processes and result in the accumulation of organic matter.

Chemically, higher soil temperatures enhance the availability of water-soluble phosphorus by improving diffusion, decrease the cation exchange capacity by burning organic matter and reducing clay fractions, and raise soil pH by denaturing organic acids. Additionally, warmer soils have lower water viscosity, which speeds up water percolation and evaporation, lowering soil moisture. Finally, changed thermal regimes affect soil aeration through increased CO₂ production from microbial respiration.

Physically, higher temperatures cause dehydration of clay minerals and cracking of sand particles, resulting in a decrease in sand content and an increase in silt, while also improving aggregate stability above 30°C. By promoting or impeding water and nutrient uptake and root development, these interrelated effects on soil properties directly affect plant growth. While suboptimal or excessively high temperatures hinder these processes, ultimately affecting overall plant performance and yield, optimal temperatures encourage vigorous root elongation and lateral branching, which support efficient nutrient uptake and robust plant growth (Onwuka, 2018).

2.5.2 Effect of soil temperature on plant growth

Soil temperature is very important in greenhouse crop production and affects plant growth, root growth, nutrient uptake, and general plant vigor. Soil temperature, unlike air temperature, exerts a more immediate effect on plant physiology, especially in heat-loving fruit and vegetable crops. Such crops typically grow well if the soil temperature is kept within the range of 18°C to 23°C. When soil temperature falls below 10°C, it seriously inhibits root metabolic processes and nutrient uptake, causing plant health to decline and yields to decrease. Conversely, when soil temperature is above 25°C, it may result in the acceleration of root aging, with detrimental effects on plant growth. Hence, it is crucial to have optimal soil temperatures to guarantee healthy root systems, effective nutrient uptake, and maximum crop yields in greenhouse conditions (Jiao *et al.*, 2024).

Soil in a greenhouse also serves as a major heat reservoir due to its high thermal inertia. During the day, it takes up any radiant heat and releases it during the night slowly, which helps to stabilize the greenhouse climate and provide favourable conditions for plant growth (Trudel and Gosselin, 1982).

Research has shown that controlling the soil temperature is so critical for optimizing the plant's physiological processes, as it assures energy/mass transfer efficiency between the soil and the atmosphere. Clear understanding of these heat transfer dynamics can elevate the crop yield, thus improving general productivity of greenhouses (Jiao *et al.*, 2024).

Plant growth and development are influenced by the temperature of the soil. Warming of the soil results in decreased root system development and increased shoot growth as shown by plant height and shoot dry weight. More effective root systems were thought to be responsible for the higher mineral content of the plants kept at higher root temperatures and the higher water content of the shoots (Trudel and Gosselin, 1982).

Here are some important things to know about soil temperature in a greenhouse:

- a. **Root Growth:** When the soil is warm, but not too hot, plant roots grow better. This helps them soak up more water and nutrients. Strong roots mean stronger plants.
- b. **Nutrient Absorption:** Warmer soil gets more microbes buzzing around. These tiny helpers break down nutrients and make them easier for plants to take in.
- c. **Seed Germination:** If the soil is warm enough, seeds germinate faster. This means seedlings pop up quicker. It helps get the plants started on the right foot.
- d. **Plant Health:** A comfy temperature for the soil helps plants do their jobs better. They can use energy more effectively, which leads to healthier plants and more growth.

Simply keeping an eye on soil temperature can really help plants thrive in a greenhouse. Warm soil can lead to strong roots, better nutrient access, quicker seed growth, and overall healthier plants.

2.6 CLIMATE CONTROL STRATEGIES IN A GREENHOUSE

Planning and development of mechanization system for a tropical greenhouse includes different stages, including considering of natural variables, control algorithm, instrumentation and software or hardware interface. In difference to cold arid climates, a tropical greenhouse not only provide a warm and wet environment for the crops but also have to provide a climatic condition in which plants can be protected against excessive rainfall, direct sunlight, diseases, insects and birds. High relative humidity and ambient temperature climate in a tropical greenhouse forms a complex energy system influenced by changes in outside condition. So, it is not an easy natural control assignment (Shamshiri and Ismail., 2013). Greenhouse cultivation is much more expensive than traditional field cultivation. So, a vigilant monitoring and automation control of various parameters like air temperature, relative humidity, light radiation, CO₂ concentration, etc are very significant for achieving high yield (Bailey, 2002).

2.6.1 Climate control systems

Climate control systems in greenhouses are essential for modern agricultural practices, allowing farmers to create and maintain an environment tailored to the specific needs of their plants. These systems ensure precise regulation of temperature, humidity, light, and CO₂ levels, facilitating optimal growth conditions throughout the year. Additionally, climate control systems support the cultivation of a diverse range of crops, irrespective of their native climate, enabling the production of high-value, off-season, and exotic varieties. By effectively managing environmental factors, these systems enhance plant physiology, potentially accelerating growth rates and reducing the time to harvest. Consequently, this leads to increased overall crop yields and improved efficiency in resource utilization, such as water and energy.

Some of the important microclimatic parameters inside a greenhouse are:

- Temperature
- Solar radiation and light intensity
- RH
- CO₂ concentration

Table 2.1 Various greenhouse parameters on microclimatic conditions (Santhosh *et al.*, 2017)

| Parameters | Micro climatic parameters | | |
|--|---|---|---|
| | Temperature | Relative humidity | Solar radiation |
| Shape of greenhouse (Quonset & saw tooth) | 3°C lesser temperature in sawtooth in comparison to Quonset shape | 13% lesser RH in Quonset shape in comparison to saw tooth shape | 5 – 10% greater radiation in sawtooth shape |
| Size of greenhouse | Higher greenhouse height lesser temperature at plant level up to 2°C. Greater length more 20 m without adequate ventilation increases temperature. | 10 – 20% Higher humidity at lower height. | Higher solar radiation at upper 25% height as compared to lower levels |
| Cladding material (Diffused & UV Stabilized) | UV stabilized clear film maintained a slightly higher temperature than diffused film in both summer and winter months. Maximum temperature reduction found in diffused film (2°C) and UV stabilized (1°C) in comparison to outside temperature. | Higher humidity in UV film cladded greenhouse. | The percentage of solar energy reduction due to cladding films during summer was observed as 82% and 76% for the UV and diffused covers respectively. |

| | | | |
|---------------------|--|-------------------------|-----------------|
| Shading and Fogging | 3 - 4°C temperature reduction during peak summer months. | 15 – 20% increase in RH | No effect found |
|---------------------|--|-------------------------|-----------------|

2.6.2 Methods of controlling the greenhouse climate

There are numerous ways for controlling the microclimate inside a greenhouse depending upon the external climatic conditions of the area (Mahesh *et al.*, 2018). Some of them are:

i. Natural Ventilation

Effective ventilation plays a crucial role in regulating the temperature within a greenhouse, particularly during periods of intense solar radiation. To mitigate excess heat, it is essential to ensure a uniform circulation of air from the outside to the inside of the greenhouse. Inadequate ventilation can adversely affect the composition of indoor air, primarily by lowering the concentration of CO₂.

Natural ventilation plays a crucial role in removing excess moisture and preventing its buildup in the air surrounding the leaves, which can lead to condensation and the development of diseases. This process is driven by pressure differences caused by wind and temperature variations between the interior and exterior of a greenhouse. It occurs through various openings in the greenhouse structure, effectively managing humidity and temperature levels while facilitating adequate air exchange. Effective ventilation in a greenhouse can be achieved through a combination of roof vents, front doors, and fans. When the greenhouse is fitted with ventilation openings both at ground level and near the roof, this system facilitates the replacement of warm internal air with cooler external air on hot, sunny days with minimal wind. The cooler air enters through the lower openings, while the warmer air escapes through the roof vents, driven by the density differences between the varying air temperatures, which helps to lower the overall temperature inside the greenhouse. To analyze the factors influencing greenhouse air temperature and to determine the necessary actions for temperature regulation, a simplified model of the greenhouse energy balance is proposed. As noted by Kittas *et al.* (2005), this energy balance can be streamlined for practical application,

$$V_a = (0.0003\tau R_{s,o-max}) / (\Delta T)$$

where,

V_a = ratio of Q/A_g ,

Q = ventilation flow rate, $\text{m}^3[\text{air}] \text{ s}^{-1}$

A_g = greenhouse ground surface area, m^2

τ = greenhouse transmission coefficient to solar radiation

$R_{s,o-\max}$ = maximum outside solar radiation, W m^{-2}

ΔT = temperature difference between greenhouse and outside air, $^{\circ}\text{C}$.

The required ventilation rate can be achieved through either natural or mechanical means. It is suggested that the total ventilator area should be equivalent to 15-30% of the floor area. Beyond 30%, the impact of increasing the ventilation area on the temperature difference becomes minimal (Santhosh *et al.*, 2017).

ii. Forced Ventilation

The concept of forced ventilation involves generating an airflow throughout the house. Fans expel air from one side while openings on the opposite side allow fresh air to enter. Utilizing fans for forced ventilation is the most efficient method for ventilating a greenhouse, although it does require electricity. These fans are essential for maintaining consistent temperature and humidity levels within the greenhouse. Fresh air is drawn in from one side, effectively displacing the hot, stale air that exits from the other side. It is recommended that ventilation fans be positioned on the side facing the wind, with a maximum distance of 8-10 meters between each fan. Additionally, the inlet opening on the side opposite the fan should be at least 1.25 times larger than the fan's area. The speed of the incoming air should be carefully regulated, not exceeding 0.5 m/s in greenhouses containing crops. Furthermore, the openings should automatically close when the fans are not in use (Santhosh *et al.*, 2017).

iii. Shade Covers

The management of air temperature is a critical objective for greenhouses in India, particularly due to the high temperatures experienced for nearly eight months of the year. The primary contributor to heat accumulation in these structures is direct solar radiation. This heat can be mitigated through the use of shading or reflective materials.

When appropriately selected and installed, shade nets can enhance crop production during periods or in regions where temperature and solar radiation levels are unfavorable. Additionally, shade nets positioned within the greenhouse can reduce wind speed, which in turn diminishes the leaf boundary layer and lowers the concentration of CO₂ available near the leaf surface. The way plants respond to light intensity and quality is significant in greenhouse settings where shade nets are employed to decrease the radiation load. A substantial reduction in solar radiation is anticipated to decrease the rate of leaf transpiration, consequently raising the temperature of the canopy (Jakson *et al.*, 1981).

iv. Evaporative Cooling Systems

Evaporative cooling systems are frequently employed in greenhouses to manage temperature and humidity. These coolers operate on the principle of water evaporation, which cools the incoming air, resulting in a decrease in temperature and an increase in humidity (Franco *et al.*, 2014; Hegazy *et al.*, 2022).

The most frequent form of evaporative cooling is the fogging system, where water is sprayed directly inside a naturally ventilated greenhouse. Another variety is the pad-fan cooling method. In this case, the incoming air is channeled through damp evaporative pads, with fans located on the opposite side of the pads aiding in greenhouse ventilation. To improve the cooling efficiency of the evaporative cooling system, a liquid desiccant (dehumidifier) has been integrated into the system to lower the humidity of the surrounding air. This system achieves significantly lower reductions in air temperature, enabling the establishment and maintenance of favorable growing conditions for vegetable crops throughout all seasons in greenhouses. Studies have shown that the cooling system equipped with the dehumidifier resulted in a reduction of the mean daily maximum temperatures by 5.5 - 7.5 °C during the warm season, particularly in hot and humid climates. Another method for enhancing evaporative cooling is the implementation of passive downdraft evaporative cooling wind catchers, which will gather wind from higher altitudes while expelling contaminated air, using a mechanism akin to that of a mechanical ventilation system. Nonetheless, there is a scarcity of research regarding the use of wind catchers in greenhouses, and additional

studies are necessary to verify their effect on mechanical ventilation performance and the impact of adjacent structures (Akpenpuun *et al.*, 2023).

v. Greenhouse Heaters

Heaters are frequently utilized as an active method for temperature control in greenhouses, especially in northern regions where additional heating is required to sustain appropriate growing conditions (Ahamed *et al.*, 2018). Two categories of heating systems are employed in the greenhouse setting—active and passive heating systems. Active heating systems are primarily classified into three types: hot water-pipe heating systems, hot air heating systems, and IR heating systems. Generally, the water heating system is widely used in large commercial greenhouses, whereas hot air and IR heating systems are primarily utilized in smaller greenhouses. The passive method of greenhouse heating leverages solar energy for warmth by incorporating various heat storage materials like water, rock bed, and phase change materials (Akpenpuun *et al.*, 2023).

ASAE (2000) suggested the greenhouse heating (Hg) requirement can be calculated by:

$$H_g = UA (T_i - T_o)$$

where,

U = heat loss coefficient ($W\ m^2 / K$)

A = exposed greenhouse surface area (m^2)

T_i = inside air temperature (K)

T_o = outside air temperature (K)

The heating system must supply heat to the greenhouse at the same speed at which it is dissipated. There are various well-known heating systems for greenhouses. The most frequent and least costly is the unit heater system (Santhosh *et al.*, 2017).

vi. Control Of Carbon Dioxide Enrichment

Effective management of carbon dioxide (CO_2) level is crucial for enhancing both the yield and quality of crops while simultaneously minimizing the carbon footprint of greenhouse operations. However, regulating CO_2 enrichment within greenhouses presents challenges due to its dynamic, interactive nature and inherent time

delays. Maintaining ideal CO₂ levels is complicated by the interplay with other environmental factors such as temperature, humidity, and light intensity, often resulting in suboptimal or excessive CO₂ concentrations. The ideal CO₂ level for optimal plant growth is around 1000 ppm (Chen, 2010; Jin *et al.*, 2009), yet typical ambient CO₂ levels hover around 350 ppm and can drop below 150 ppm during daylight hours in greenhouses, which is inadequate for optimal crop development. Furthermore, elevated CO₂ levels can hinder plant growth, lead to leaf damage, and increase CO₂ loss through leakage (Panwar *et al.*, 2011). So maintaining the desired CO₂ level is crucial for the optimum growing environment of plants inside a greenhouse.

The primary elements that influence the variations of CO₂ in greenhouses include photosynthesis, crop and soil respiration, and ventilation. Typically, the intensity of photosynthesis in plants gradually rises to its peak at noon when the light and temperature settings are most favorable. Following this peak, it gradually decreases. The intensity of respiration similarly fluctuates with a single peak curve in alignment with photosynthesis intensity. As photosynthesis and respiration fluctuate, the CO₂ concentration in greenhouses generally exhibits an erratic “U” shape throughout the day. When utilizing perforated plastic tubes instead of relying on natural diffusion, CO₂ distribution in the greenhouse becomes more uniform. Circulation fans further enhance the uniformity of CO₂ distribution due to the effectiveness of free convection. Certain control strategies, such as classical methods and some robust control techniques, manage CO₂ by eliminating the deviation between desired variable set points and actual measured values. Additionally, other optimal control methods that take into account greenhouse behavior, actuator performances, energy consumption, and that foresee environmental parameter changes are gaining more interest. Maximizing economic advantages is favored by growers and is also beneficial for advancing precision greenhouse techniques and sophisticated control methods. Furthermore, most research has primarily concentrated on optimizing the financial benefits of managing CO₂ enrichment (Yongwei *et al.*, 2018).

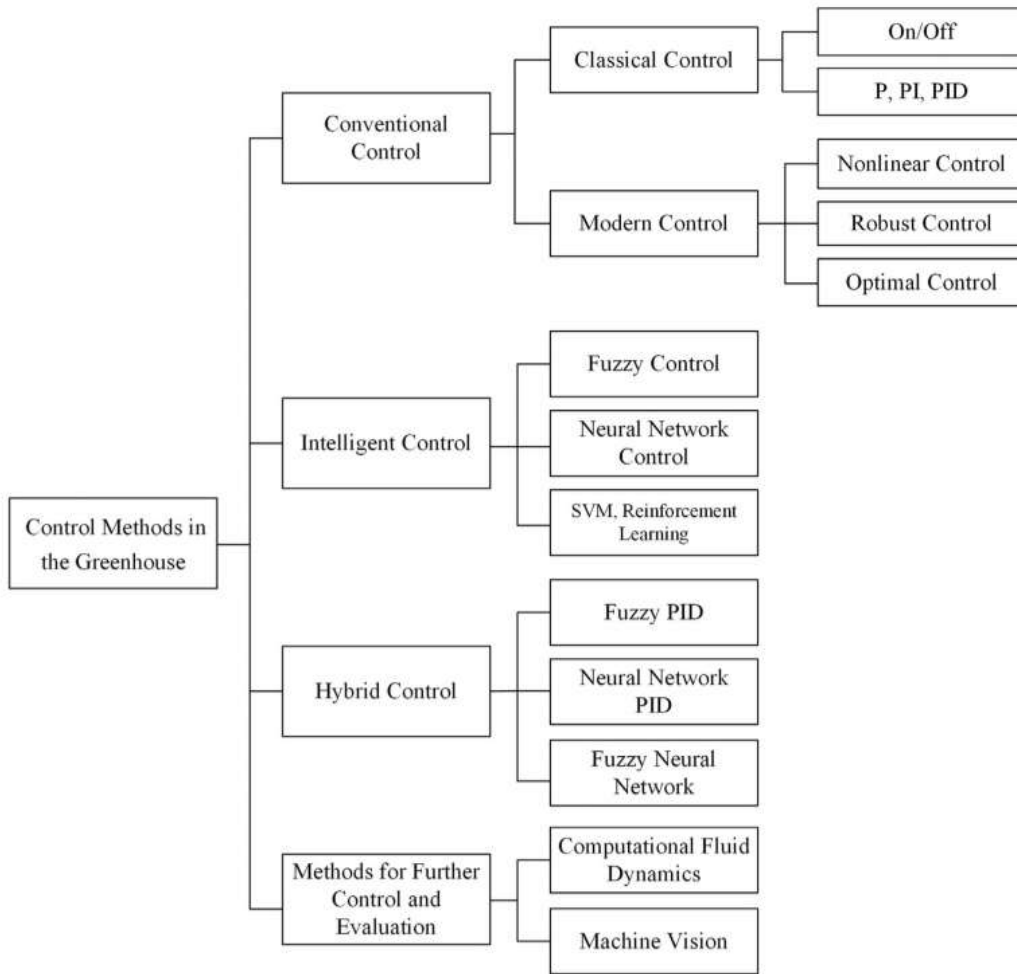


Fig.2.1 Classification of CO₂ control methods in the greenhouse

vii. Smart Greenhouse and IoT Technology

Global attention has been drawn to the greenhouse industry as a result of the agriculture sector's increased and, eventually, industrialized attempts to meet the expanding demand for food, which encompasses both quantity and quality. Nevertheless, energy consumption and greenhouse operating costs are relatively substantial, accounting for almost half of greenhouse production costs. This calls for intelligent farming systems that automate tasks and processes to guarantee that the greenhouse's conditions are met in order to maximize plant yield while utilizing resources as efficiently as possible (Ullah *et al.*, 2022). A smart farm is a system that integrates agricultural technology, the Internet of Things (IoT), and information and communication technologies to allow a farm to run and autonomously regulate a

greenhouse environment with little human intervention. The Internet of Things is a very fortunate collection of technologies that could offer a wide range of solutions for the development of agriculture. The United Nations Food and Agricultural Organization projects that there will be 8.6 billion people on the planet by 2025 and 9.6 billion by 2050 (Tzounis *et al.*, 2017). As a result, by 2050, there will need to be a startling 70% increase in global food production. The need to modernize and enhance agricultural techniques is highlighted by the world's population growth and the rising demand for premium goods. At the same time, there is an increasing need to use resources, especially water, as efficiently as possible (Ihoume *et al.*, 2023).

The idea of the smart greenhouse and the usage of IoT in agriculture were inspired by the realities of population growth. A network of devices having electronics, sensors, actuators, software, and connection are all part of the Internet of Things. The physical or perception layer, network layer, middleware layer, service layer, and application layer are the five main layers into which the Internet of Things is generally divided. Together, these tiers are essential for data chores like gathering, sending, storing, analyzing, and presenting data, as well as for supporting related applications. By providing previously unheard-of control and optimization of environmental conditions to support optimal plant growth and productivity, the use of IoT applications in microclimate management has completely transformed the greenhouse productivity, quality, and profitability (Othmane *et al.*, 2021; Jaliyagoda *et al.*, 2023).

In agriculturally developed countries, the adoption of precision agricultural systems is especially noticeable (Jaliyagoda *et al.*, 2023). As a result, numerous models that make use of certain trained artificial intelligence algorithms have been published. The inability of these models to adjust to the intricate and changing microclimate of the greenhouse, however, restricts their applicability to prediction, optimization, and control. In order to monitor and regulate the greenhouse environment on their own, application of learning modules based on artificial neural networks were investigated to integrate prediction, optimization, and control. According to reports, their suggested methodology reduced production costs by 67.96% and energy expenditures by 61.97% (Ullah *et al.*, 2022).

The ability of smart agriculture to maximize resource use and improve production efficiency makes its widespread integration crucial and is particularly important in developing or undeveloped economies. To ensure ideal circumstances for plant growth, the IoT system can, for example, automatically turn on cooling systems and open vents to remove excess heat when temperature levels rise above the acceptable range. This intelligent and smooth reaction to shifting environmental conditions lowers the chance of crop stress and lessens the need for human intervention. IoT devices' remote accessibility gives producers flexibility and convenience by enabling them to utilize computers or cellphones to monitor and manage the greenhouse microclimate from any location. For example, Ihoume *et al.*, (2023) used strawberries (*Fragaria vulgaris*) as the test crop and integrated IoT into a low-cost, active, and sustainable autonomous system for heating agricultural greenhouses. They found that the integration of IoT into the system allowed for real-time data visualization and analysis, which improved efficiency and quick response. This is a crucial step in the development of automated and intelligent smart agriculture methods in regulated growing conditions (Akpenpuun *et al.*, 2023).

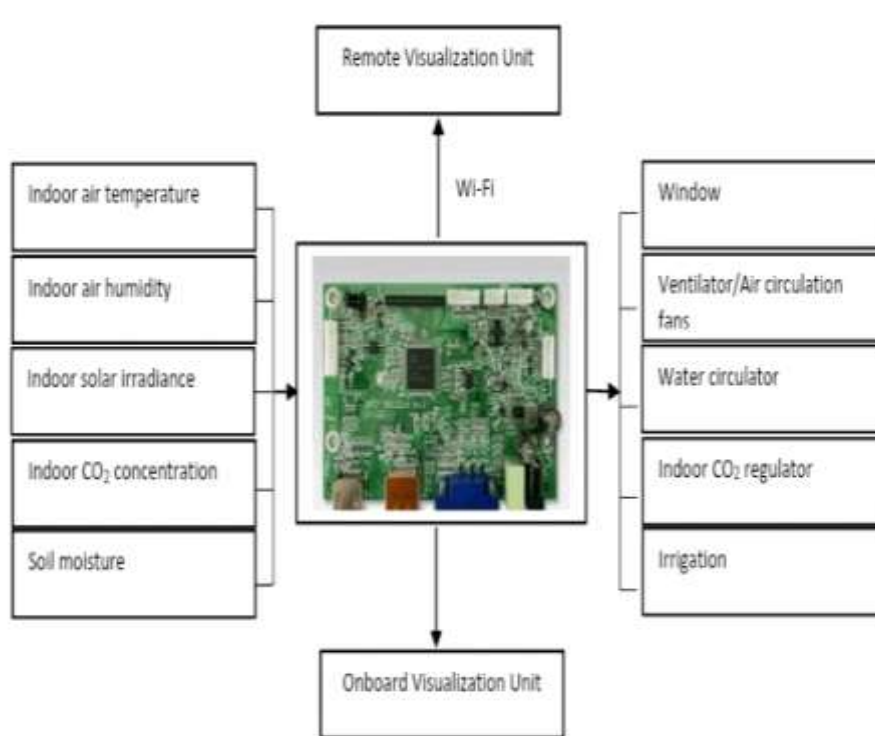


Fig.2.2 Smart IoT controller for greenhouse automation

2.7 CARBON DIOXIDE (CO₂) CONCENTRATION, AIR CIRCULATION AND VENTILATION EFFECTS

The net photosynthetic rate typically rises between 0 and 1000 mol mol⁻¹ as the CO₂ concentration rises (Allen and Amthor, 1995). Thus, to encourage photosynthesis and plant growth in greenhouses with the vents covered, the CO₂ concentration is frequently raised throughout the day to roughly 1000 mol mol⁻¹ (also known as "CO₂ enrichment") (Hand *et al.*, 1993; Nederhoff and Vegter, 1994; Aikman, 1996; Ceulemans *et al.*, 1997). However, during the day, when solar radiation and/or air temperature are high, fans must be turned on (also known as "forced ventilation") or roof and/or side vents must be opened (also known as "natural ventilation") to maintain the greenhouse's air temperature or water vapor pressure deficit (VPD) at ideal levels. But recently, there have been reports of using descending fog technology to control the greenhouse's air temperature and VPD. This is helpful since it lessens the need for natural ventilation, allowing the greenhouse to sustain higher CO₂ concentrations (Ohshima *et al.*, 2008; Stanghellini and Kempkes, 2008).

However, it is impractical to employ CO₂ enrichment to keep the concentration of CO₂ inside the greenhouse greater than that outside while it is ventilated. This is because a significant amount of CO₂ would be emitted outdoors, resulting in both high CO₂ costs and the emission of CO₂, a gas that warms the planet. As a result, CO₂ is often only enhanced when there is no ventilation in the early morning and late afternoon (Hand, 1984; Sanchez-Guerrero *et al.*, 2005). However, in a ventilated greenhouse with fully grown plants, the noon CO₂ concentration is around 50–60 mol mol⁻¹ lower than outside (Sanchez-Guerrero *et al.*, 2005), even if the greenhouse vents allow CO₂ gas from the outside to enter the interior. It suggests that the plants' net photosynthetic rate is constrained by the CO₂ depletion in vented greenhouses. The vented greenhouse should therefore be supplied with CO₂ gas and kept at a concentration of 350–450 mol mol⁻¹ (also known as "zero or null balance CO₂ enrichment"). When ventilation is required in the greenhouse, this method works well.

When the stomata are kept open, the net photosynthetic rate also rises as air circulation over the leaves increases, ranging from 0 to 0.8 m s⁻¹ (Kitaya *et al.*, 2004; Yabuki, 2004). Additionally, as air circulation increases between 0 and 1.0 m s⁻¹, the

transpiration rate rises as well (Kitaya *et al.*, 2003). This is due to the fact that air movement lowers the resistance of CO₂ and H₂O (water vapor) fluxes at the leaf border layer. As air circulation increases, the net photosynthetic and transpiration rates might rise until they reach their optimal level (Shibuya and Kozai, 1998; Kitaya *et al.*, 2003).

The species of plants, the community structure, the depth of the plant canopy, the wind direction, the location of the plants in the greenhouses, etc. all affect the ideal air circulation for the net photosynthetic and transpiration rates (Wadsworth, 1959; Morse and Evans, 1962; Shibuya and Kozai, 1998; Kitaya *et al.*, 2000; Sase, 2006). Conversely, reduced gas exchange results from inadequate air circulation above the plant canopy due to increased resistance of the leaf boundary layer (Kim *et al.*, 1996; Kitaya *et al.*, 1998).

There are two types of ventilation: natural (due to wind pressure and/or thermal buoyancy) and forced (mechanical, such fans). Generally speaking, mechanical ventilation is made to offer the highest air exchange rate appropriate for the local climate. The fans are staged to offer possibly 10%, 30%, and 100% of full capacity, and the divergence of the indoor air temperature above the desired set point controls the ventilation capacity, which is typically one complete air exchange per minute. Wind-driven ventilation can be strong and is linearly related to wind speed. Although thermal buoyant ventilation is dependent on the temperature differential between the air and the elevation difference between the inlets and exits, it is unlikely to be very effective in real-world settings. However, with the right design and management, it can be sufficient for greenhouse ventilation.

Over the past ten years, a far deeper comprehension of the nuances of natural ventilation has emerged. Adequate side and roof ventilation is made possible by new greenhouse designs. The open roof greenhouse, which is the most extreme, works best in gutter-connected greenhouses that are vast in size and lack enough sidewall space to offer a suitable intake area.

An empirical approach to determining ventilation rates driven by the wind when inlet and outlet vents have the same areas is as follows (Albright, 1990).

$$V = EAV_w$$

V- Ventilation rate, $\text{m}^3 \text{s}^{-1}$

E- Ventilation opening effectiveness

A- Gross vent area opening, m^2

V_w - Wind speed, m s^{-1}

Regretfully, when ventilation is required, constant wind direction and speed are usually not guaranteed. Therefore, ventilation by thermal buoyancy alone must be taken into account when designing a natural ventilation system. For scenarios with equal inlet and output regions, ventilation can be empirically calculated using thermal buoyancy (Albright, 1990).

$$V=0.65A [g \Delta h (T_i-T_o)/T_t]^{0.5}$$

g- Acceleration of gravity on earth's surface, m s^{-2}

Δh - Elevation difference, m

T- Absolute temperature, K

2.8 MATHEMATICAL AND COMPUTATIONAL MODELLING FOR GREENHOUSE MICROCLIMATE

The mathematical model should be able to predict accurately the thermal behaviour of the greenhouse by considering all the involved parameters including geometrical specifications, orientation and shape and climatic conditions.

Several studies modelled the greenhouse by dividing it into zones. (Sharma *et al.*, 1999) examined the effects of numerous parameters: infiltration rate, plants thermal capacity and relative humidity on crops and air temperatures. They divided the greenhouse horizontally into four zones. The heat transfer between different zones is assumed to be unidirectional. It has been concluded from this study that the temperature difference between the different zones is negligible.

Computational Fluid Dynamics (CFD) is extensively applied to simulate greenhouse microclimates in greater detail. CFD captures spatial variations in

temperature, humidity, and air velocity, offering a more accurate understanding of the internal microclimate. These simulations are particularly useful for:

- a. Optimizing ventilation
- b. Studying airflow patterns
- c. Evaluating heating and cooling strategies

Various tools like MATLAB, COMSOL, TRNSYS, and Ansys Fluent are used for modelling and simulation (Choab *et al.*, 2019).

In general, the model equations are based on the energy balance method (Avissar and Mahrer, 1982) applied to four vertical layers in the greenhouse. This model is built using energy and mass balance equations, designed to capture how heat, moisture, and energy move through a greenhouse. To keep things organized, the greenhouse is divided into four main layers: soil (the ground where plants grow), air (the space inside the greenhouse), vegetation (the plants themselves), cover (the roof and walls of the greenhouse).

The model takes into account a variety of important processes including: solar radiation (sunlight coming in) and thermal radiation (heat given off by different surfaces), sensible heat flux (how heat moves between air, plants, soil, and the greenhouse cover), latent heat flux (energy used or released when water evaporates or condenses), heat and moisture transfer in the soil, ventilation (airflow created by fans or vents) and air exchange through leaks (air sneaking in or out through small openings).

The model focuses on predicting hourly air and leaf temperatures, relative humidity (RH), and leaf wetness duration (LWD). These are critical parameters influencing crop health, productivity, and the potential spread of diseases like *Botrytis* (Zhang *et al.*, 1997).

➤ Mathematical Modelling of Greenhouse Microclimate Under Vertically Trained Soilless Cropped Conditions

Most greenhouse models treat the greenhouse air as uniform, assuming a well-mixed environment. This model improves accuracy by acknowledging that temperature and humidity vary significantly with height, especially in taller crop stands. This reflects

more realistic microclimatic conditions, which is crucial for vertical crop training systems.

Inside the greenhouse, the environment is divided into several layers, and the model tracks how heat and moisture move through each one.

- I. Heat transfer is modelled in two main ways: Sensible heat balance, which looks at how temperature changes between the layers and Latent heat balance, which focuses on how moisture (humidity) moves like water evaporating from the soil or plants releasing water through transpiration.
- II. Convective Heat Transfer Coefficient: To figure out how easily heat moves between the air and other surfaces (like leaves or soil), the model uses Bansal's formula, which has been adjusted to better fit greenhouse conditions where airflow can be quite different from the outdoors.
- III. Leaf Area Density (LAD): Another key input is Leaf Area Density, which basically measures how much leaf surface area there is within a given volume of greenhouse space. This is important because leaves play a huge role in vertical heat transfer, affecting how heat moves up and down between layers.

The model doesn't just focus on air temperature and humidity when predicting the greenhouse microclimate — it also connects to other important factors like:

- a. Leaf Area Index (LAI), which measures how much of the ground is covered by plant leaves
- b. Plant temperature (T_p), showing how warm the plants themselves are
- c. Growing media temperature (T_{gm}), tracking how heat moves through the soil or other materials the plants are growing in
- d. External weather conditions, like sunlight, wind, and outdoor temperature (Singh *et al.*, 2022)

The assemblage of climatological parameters forming around living plants inside a greenhouse is termed as greenhouse microclimate. Solar radiation, temperature distribution (Sauser *et al.*, 1998) and relative humidity are the main climatic parameters needed to evaluate the climate suitability in a region for crop growth under protected

cultivation. Modelling is a commonly used technique for quantification of greenhouse microclimate. The main objective of greenhouse microclimate modelling is to quantitatively describe the energy and mass transport processes by mechanism of convection within the medium, the exchange processes between air and plant elements and other surfaces, and the ways in which plants respond to the environmental factors. Energy balance equations have been used to construct a model which permits prediction of climatic conditions in a greenhouse based on outside weather conditions (Maher and Flaherty, 1973). For describing heat and mass transport processes in a greenhouse microclimate, mathematical models have been successfully developed (Chandra *et al.*, 1981; Yang *et al.*, 1990).

Kimball (1973) simulated the greenhouse energy balance using a digital computer program. He calculated the fluxes of solar radiation from sun angle equations and the optical properties of the greenhouse walls and vegetation. The thermal radiative, sensible, latent and conductive heat fluxes were modelled.

Seki *et al* (1995) developed a mathematical model on greenhouse microclimate for cucumber with the combination of plant growth sub-model i.e. population dynamics and the transport process sub-model. They considered the fact that the number of plant leaves is a function not only of time and space but also of the area of an individual leaf. The proposed model gives a good prediction of plant community growth process, energy and mass transfer processes in the community.

Wang and Boulard (2000) simulated the microclimate of a naturally ventilated plastic house using the Gembloux Greenhouse Dynamic Model (GGDM). Improved calculations of natural ventilation flux and stomatal resistance of vegetation were introduced, based on experimental equations from previous research. A linear non dimensional ventilation function was developed and compared with those obtained by other authors. While validating the model by comparing the predicted and observed data, a good agreement was obtained. The sensitivity analysis showed that the external wind speed and opening angle of the vents were the most important factors influencing the ventilation flux.

Zhang *et al* (2002) developed a dynamic one-dimensional model (PSCLIMATE) to simulate microclimate on and around leaf surface for greenhouse cucumbers. Based on

energy balance of plant leaves and heat and mass transfer among air strata and leaves, the model predicts climate profiles within a plant canopy and the microclimate within a leaf surface boundary layer. The model accurately predicted air temperature and relative humidity within the plant canopy.

Luo *et al* (2005) conducted a simulation study using the Greenhouse Process (KASPRO) model to explore alternatives to the existing Venlo-type greenhouse climate control policy under Chinese subtropical climate conditions. The results showed that using outside hourly weather data as inputs, the KASPRO model generally gives satisfactory predictions of greenhouse air temperature, humidity and canopy transpiration rate under both summer and winter climate conditions for subtropical China.

Yildiz and Stombaugh (2006) developed and validated a dynamic simulation model for accurate prediction of microclimate in a greenhouse as a function of dynamic environmental factors. Korner *et al* (2007) designed a simple deterministic microclimate model for dynamic greenhouse climate control. The model calculates crop temperature and latent heat of evaporation in different vertical levels of a dense canopy of potted plants.

Kavga *et al* (2009) developed a simple theoretical model that contains all the essential physics and subsequently used in parametric studies. Experimental and simulation results confirmed that, with infrared (IR) heating, inside air temperatures several degrees lower than the desired plant canopy temperature were sustained, and that this temperature difference increased proportionally to drop in outside night temperature (Singh *et al.*, 2016).

The statistical comparisons between the model predictions and the actual observed temperature data showed that the microclimatic model which simulates energy and mass transport processes through conduction, convection, and radiation was able to accurately predict the temperatures of air within the plant community, the plant leaves, the growing media, and the greenhouse cover in a naturally ventilated greenhouse with crops. The model can be integrated into a broader greenhouse climate model to assess how different parameters interact and affect the greenhouse microclimate. This makes it a valuable tool for designing more energy efficient systems. It can also serve as a

design aid, helping to fine-tune ventilation system characteristics and optimize control settings ultimately leading to significant savings in both energy and time (Singh *et al.*, 2018).

➤ A Numerical Simulation of The Greenhouse Microclimate

The potential use of a numerical model lies in the possibility to estimate heating and cooling requirements during different climatological conditions and at different sites. Thus, when planning decisions are made concerning the various aspects of greenhouse siting, the usage of a numerical model may be of help (Mahrer and Avissar, 1984).

➤ Microclimate Modelling Approaches

There are various approaches to modelling greenhouse microclimates, ranging from physical (thermodynamic) models to data-driven, empirical models like those based on machine learning. Some of the most common techniques include:

- a. Energy balance models, which simulate heat and mass transfer within the greenhouse
- b. Neural networks (such as ANN, RBF, and ARMAX), which learn patterns from historical data to predict future conditions
- c. Hybrid models, which combine physical process modelling with optimization techniques like Genetic Algorithms (GA) or Particle Swarm Optimization (PSO)
- d. AI-based controllers, including fuzzy logic systems and Adaptive Neuro-Fuzzy Inference Systems (ANFIS), which can make real-time decisions to maintain optimal conditions (Gupta *et al.*, 2020)

2.9 SENSORS AND DATA COLLECTION FOR MICROCLIMATE ANALYSIS

Sensors play a crucial role in monitoring and controlling greenhouse environments. Keeping track of microclimatic conditions is essential to protecting crops from harsh weather and ensuring optimal growth. However, the greenhouse environment is influenced by many factors, making manual monitoring and control challenging especially in large-scale facilities that require multiple sensors and actuators to function efficiently. Relying on manual supervision in such a complex system is not only time-consuming but also impractical. That's why automated

monitoring and control systems have become a necessity. These systems help regulate key microclimatic factors like temperature, humidity, and solar radiation, which are all interconnected in a non-linear way. To manage these variables effectively, a well-designed sensor system is essential for maintaining the ideal growing conditions inside the greenhouse (Bhujel *et al.*,2020). Sensors have been around for a long time, but their widespread use across different industries really took off with the development of wireless sensor networks (WSNs). This, combined with advancements in semiconductor technology, networking, and material science, has made sensors more efficient, reliable, and versatile than ever before. These innovations have paved the way for their extensive application in fields ranging from agriculture and healthcare to industrial automation and environmental monitoring (Labs, 2013). Before the development of communication standards and Internet Protocol (IP)-based sensing devices, one of the biggest challenges in various systems was managing multiple sensors and integrating their data effectively. Without a standardized way for sensors to communicate, coordinating and making sense of the collected information was complex and inefficient (Mainetti *et al.*,2011). Advancements in sensors and sensing technologies have transformed greenhouse management into a smart, real-time, and remotely accessible system.

The progress in semiconductor technology has played a key role in this evolution, making sensors smaller while enhancing their performance. These improvements have contributed to the widespread adoption of sensor technology across various fields. One of the most important areas where sensors are making a significant impact is agriculture, offering numerous benefits such as improved efficiency, better resource management, and enhanced crop productivity (Aqeel-Ur-Rehman *et al.*,2014). Wireless Sensor Networks (WSNs) have emerged as one of the most influential technologies of the 21st century, especially in sensor applications (Rodríguez *et al.*,2017) developed a WSN system capable of transmitting data from individual sensor nodes to the cloud using ZigBee communication. By applying data mining techniques, they were able to predict environmental patterns for Rose crops grown in the field. The system also incorporated cloud-based big data storage and web-based client monitoring for real-time observation and control. Today, the use of WSNs in agriculture is expanding rapidly due to their flexibility, scalability, cost-effectiveness, and ease of

implementation. One of the key benefits of an IoT-based system is its ability to stay connected and accessible from anywhere in the world, making remote monitoring and control effortless. Unlike traditional systems, IoT-enabled sensors can send data directly to the cloud in digital form, eliminating the hassle of merging information from different types of sensors. This not only simplifies data management but also ensures a more efficient and reliable system. Efficient greenhouse climate control not only enhances crop yield but also minimizes costs and optimizes resource usage. Automated greenhouse systems are designed to monitor and regulate environmental conditions without the need for constant human supervision.

To achieve this level of automation, a variety of sensors and actuators are utilized. Commonly used sensors include those for temperature, humidity, light, and CO₂, which help maintain optimal internal conditions. Meanwhile, meteorological sensors provide insights into external weather conditions. Additionally, modern greenhouse systems incorporate specialized sensors for soil moisture, pH levels, pressure, power failures, smoke detection, and even cameras for real-time monitoring. Advanced greenhouse facilities today rely on a combination of smart sensors, intelligent controllers, and efficient actuators to create and maintain ideal growing conditions. Beyond traditional sensors, virtual sensing technologies driven by mathematical models, machine learning, and computational fluid dynamics (CFD) are also being employed to improve accuracy and decision-making in greenhouse management (Pawlowski *et al.*,2016; Guzmán *et al.*,2019; Muñoz *et al.*,2019).

2.9.1 Sensor Devices

A sensor device is a type of transducer that detects environmental parameters such as temperature, humidity, and light, converting one form of energy into another. In greenhouse environments, where conditions are highly dynamic, intricate, and non-linear, a range of sensors is necessary to effectively monitor and regulate the microclimate. The signals generated by these sensors can be either linear or non-linear, depending on their design and operational characteristics. Sensors are broadly classified into active sensors, which require an external power source, and passive sensors, which function without any external power input. As highlighted earlier, sensors serve as the core component of any monitoring and control system, and their seamless integration

into a Greenhouse Microclimate Monitoring and Control (GMMC) system is essential to achieving both accuracy and efficiency.

Since these sensors are positioned directly within the environment where measurements are taken, they must be robust, resilient to environmental factors, and capable of delivering precise and noise-free data over extended periods. Among the most commonly used sensors in GMMC systems are those that measure temperature, humidity, CO₂ concentration, light intensity, and soil moisture, all of which are critical in maintaining optimal conditions for plant growth.

2.9.1.1 Temperature Sensors

Greenhouses are designed to create a warm and controlled environment by trapping heat energy. Their translucent coverings allow sunlight to enter while preventing heat from escaping. Since temperature regulation accounts for 70–85% of a greenhouse's total energy consumption (Ahamed *et al.*,2019), maintaining the right temperature is essential for plant growth and energy efficiency. However, achieving a uniform temperature inside a greenhouse can be challenging. Research by (Ferentinos *et al.*,2017) found that temperature variations inside a greenhouse can reach 3.3°C, with the most significant fluctuations occurring during summer daylight hours. One of the key concerns in greenhouse management is ensuring that plants are exposed to optimal temperature conditions. To achieve this, temperature sensors should be strategically placed above the plants. According to (Nelson, 2003), in pot-plant greenhouse systems, sensors should ideally be installed 15 to 30 cm above the rim of the pots to provide accurate temperature readings.

In modern Greenhouse Microclimate Monitoring and Control (GMMC) systems, temperature and humidity sensors are often combined into a single module for efficiency. Since different greenhouse locations and climates experience varying temperature patterns, choosing the right sensors and positioning them correctly is crucial. In addition to monitoring air temperature, many greenhouse systems also use soil temperature sensors, which provide insights into soil conditions, and leaf temperature sensors, which help assess plant health (Liang-Ying *et al.*,2015; Aiello *et al.*,2018). For certain applications, thermal sensors are preferred as they can measure temperature without direct contact, making them ideal for environments where non-

contact readings are necessary. There are various types of temperature sensors, each designed for different conditions and needs. To ensure accurate temperature measurements, sensors should be placed close to the plant canopy, as this helps capture the actual temperature that plants experience. Additionally, sensors should be protected from direct sunlight, heating systems, ventilation, cooling units, and sources of electromagnetic radiation to avoid inaccurate readings. The choice of a temperature sensor also depends on the greenhouse environment. For instance, if the greenhouse is located near an area with high electromagnetic interference, thermocouple sensors may not be the best option. Instead, resistance temperature detectors (RTDs) or infrared (IR) sensors would be more suitable.

2.9.1.2 Humidity Sensor

Humidity, or the amount of water vapor present in a greenhouse, is influenced by several factors, including condensation on the covering, moisture exchange through ventilation, soil evaporation, and plant transpiration (Shamshiri *et al.*,2018). Additionally, humidity and temperature share an inverse relationship, meaning both must be managed together to maintain an optimal greenhouse environment. From a plant physiology perspective, humidity plays a key role in determining the vapor pressure deficit (VPD) the difference between the actual moisture content in the air and the moisture content when the air is fully saturated (Mukazhanov *et al.*,2017). In most greenhouse systems, relative humidity is commonly measured to regulate the microclimate. Depending on the sensor type and design, humidity sensors work by detecting changes in resistance or capacitance, which are then used to calculate moisture levels in the air.

Types of Humidity Sensors

Based on their working principles, humidity sensors are classified into three main categories (Wilson, 2005):

- Capacitive Humidity Sensor (CHS): Measures humidity by detecting changes in the dielectric constant, which varies proportionally with relative humidity.

- Resistive Humidity Sensor (RHS): Determines humidity based on changes in resistance, which follows a logarithmic inverse relationship with moisture levels.
- Thermal Humidity Sensor (THS): Uses thermal conductivity to measure absolute humidity in the air, as humidity levels directly impact how heat is transferred.

Since humidity and temperature inside a greenhouse are closely linked, it is recommended to position both temperature and humidity sensors together for more accurate climate monitoring. Nowadays, integrated temperature and humidity sensor modules are widely used, simplifying system design by reducing the number of sensor devices, thereby lowering power consumption, data transmission load, and memory usage. However, some greenhouse systems opt for compact data loggers that record temperature, humidity, and CO₂ levels (Basak *et al.*, 2019). These devices only store environmental data but do not provide real-time feedback or automatic climate control.

2.9.1.3 Light Sensor

Solar energy is the primary natural energy source in greenhouse technology, providing both light and heat essential for plant growth. The amount of light entering a greenhouse depends on factors such as the materials used for covering, the structure, and its orientation (Panwar *et al.*, 2011). Similarly, the way light is diffused inside the greenhouse often unevenly also depends on these structural elements and covering materials. Interestingly, plant photosynthesis is more efficient under diffused light than direct sunlight, as it creates a more uniform light distribution around the plant canopy (Li and Yang, 2015). Additionally, since different plant species have varying light requirements, the ideal light intensity depends on the type of crops being cultivated. While most greenhouses rely solely on solar energy for lighting, supplementary artificial lighting at specific wavelengths can significantly enhance yield (Kaiser *et al.*, 2019).

Modern greenhouses increasingly use LED lighting, favoured for its energy efficiency, durability, and adaptability. Conversely, curtains and shading materials are employed to prevent excessive light exposure. Among light sensors, light-dependent

resistors (LDRs) are commonly used in small-scale greenhouses, whereas photosynthetically active radiation (PAR) quantum sensors are more effective for assessing the actual light available to plants. Since plants are highly sensitive to the 400–700 nm wavelength range, quantum light sensors measure the intensity of light within this spectrum and express it in terms of photosynthetic photon flux density (PPFD), providing a more precise indication of light conditions for plant growth.

2.9.1.4 CO₂ Sensor

Carbon dioxide (CO₂) is a vital component of plant photosynthesis, playing a crucial role in plant growth. During this process, plant leaves absorb CO₂ from the atmosphere, roots uptake water and nutrients from the soil, and chlorophyll captures light energy all essential for completing photosynthesis. The CO₂ concentration inside a greenhouse is influenced by several factors, including temperature, humidity, solar radiation, and plant transpiration. In an open environment, CO₂ levels are typically around 400 ppm, but higher concentrations (400–1000 ppm) can enhance plant growth and yield (Bao *et al.*,2018). At night, CO₂ levels inside a greenhouse tend to increase due to plant respiration and, in some cases, fuel combustion from biofuel-based heating systems. However, during the daytime, CO₂ becomes scarce as plants actively consume it for photosynthesis. The stomata in plant leaves regulate CO₂ intake, but their opening and closing are highly dependent on environmental factors like temperature and humidity. To optimize CO₂ absorption, these factors must be carefully managed. Additionally, ventilation and window openings can significantly lower CO₂ concentrations inside the greenhouse (Takeya *et al.*,2017).

The choice of CO₂ sensors depends on factors such as measurement range, cost, size, type, and reliability. While small-scale and home-based greenhouses often rely on natural CO₂ levels, large-scale commercial greenhouses implement supplementary CO₂ systems to maintain optimal levels, typically around 1000 ppm.

CO₂ sensors can be broadly classified into three types based on their working principles (Neethirajan *et al.*,2009).

- Optical-based CO₂ sensors
- Electrochemical-based CO₂ sensors

➤ Metal oxide-based CO₂ sensors

Selecting the right CO₂ sensor ensures precise monitoring and regulation, contributing to healthier plant growth and improved yields.

2.9.1.5 Soil Moisture Sensor

In soil-based cultivation, plants absorb essential nutrients through their roots, making it crucial to maintain an optimal moisture level in the soil. While inadequate water supply can hinder plant growth, excessive water can increase the risk of plant diseases. Hence, precise water management is essential for healthy crop production. Traditionally, irrigation methods did not rely on soil moisture sensors but instead followed a fixed schedule-based approach. This method, commonly used in earlier greenhouse systems, involved watering plants based on previous evapotranspiration data or farmers' experience (Bonachela *et al.*, 2006). However, such an approach often failed to meet the plant's actual water requirements, leading to either overwatering or underwatering.

In contrast, modern sensor-based irrigation systems provide water only when needed, optimizing water usage and improving both crop quality and yield (Henderson *et al.*, 2018). The soil's field capacity (FC) and wilting point (WP) which depend on factors like soil texture and crop type serve as critical thresholds for determining water availability for plants (Datta *et al.*, 2018).

Various soil moisture sensors help measure water levels in the soil, ensuring precise irrigation control. These sensors generally operate based on two primary principles (Bogena *et al.*, 2007; Garg *et al.*, 2016):

- a. Water Tension–Based Sensors (Measure the force required for plant roots to extract water)
 - Tensiometer
 - Granular Matrix Sensor (GMS)
- b. Soil Water Content–Based Sensors (Measure the actual moisture content in the soil)
 - Time Domain Reflectometry (TDR)

- Capacitive Sensor

By utilizing appropriate soil moisture sensors, greenhouse irrigation can be better regulated, ensuring efficient water use while promoting optimal plant growth and sustainability.

MATERIALS & METHODS

CHAPTER-III

MATERIALS AND METHODS

This chapter describes the components, tools, and techniques used in the design and implementation of an Internet of Things (IoT)-based sensor system intended for real-time monitoring of environmental parameter inside polyhouse.

3.1 DETAILS OF STUDY AREA

3.1.1 Experimental location

The experiment was conducted at the Precision Farming Development Centre (PFDC) of Kelappaji College of Agricultural Engineering and Food Technology (KCAEFT), Tavanur, Kerala. The experimental site is geographically situated at 10° 51' 8" North latitude and 75° 59' 12" East longitude, with an elevation of 22 m above mean sea level. The region experiences a tropical monsoon climate.

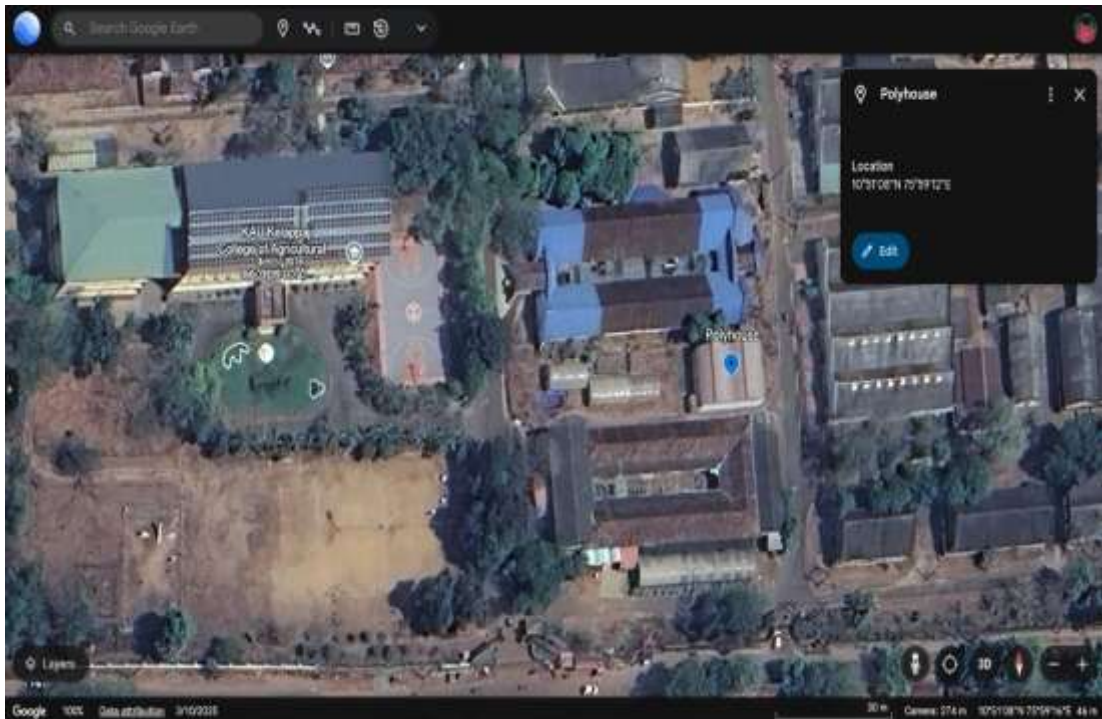


Fig. 3.1 Location of study area

Table 3.1 Details of study area

| | |
|---------------------------------|--|
| Location | Precision Farming Development Centre (PFDC) of KCAEFT, Tavanur, Kerala. |
| Latitude & Longitude | 10°51'08"N & 75°59'12"E |
| Average annual rainfall | 2500 mm to 2900 mm |
| Geography | Area falls in the border line of northern hemisphere and central zone of Kerala. |

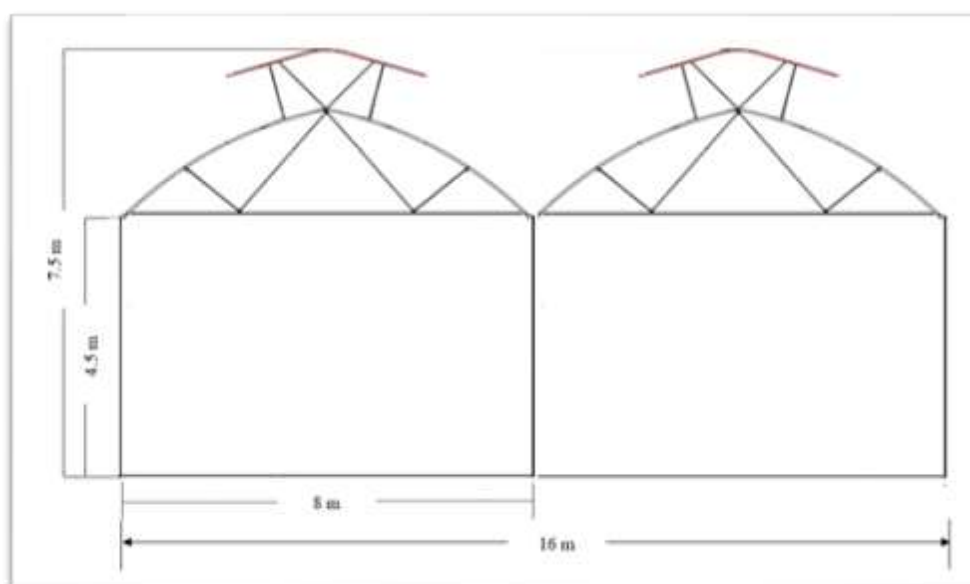


Fig 3.2 Experimental plot



Plate 3.1 Polyhouse

Table 3.2 Specifications of the polyhouse

| | |
|----------------------|--|
| Location | Eastern end of the PFDC office building |
| Size | 12 x 16 m, multi span with double door entry |
| Centre Height | 7.5 m |
| Total Width | 16 m (2 x 8 m span) |
| Gutter Height | 4.5 m |
| Span Width | 8 m |
| Bay Length | 3 m |
| Double Door | 2.5 m x 2 m |

3.2 INTEGRATION OF IOT AND EMBEDDED SENSOR TECHNOLOGIES FOR REAL-TIME MONITORING IN POLYHOUSE

This section covers the concept of the Internet of Things (IoT) and describes the design and deployment of an IoT based real-time microclimate monitoring and control system for greenhouse cultivations.

3.2.1 Description and concept of Internet of Things (IoT)

The Internet of Things (IoT) refers to a network of interconnected devices—ranging from computing systems and sensors to mechanical and digital machines—capable of communicating and exchanging data without direct human intervention (Gillis, 2021). These devices, often equipped with unique identifiers (UIDs), collectively form a digital ecosystem that facilitates automated monitoring and control across various domains, including agriculture.

One of the key advantages of IoT is that it allows data to be monitored from virtually anywhere in the world. Devices can be controlled and observed remotely in real-time, significantly reducing the need for manual labour and minimizing the risks associated with accessing remote or hazardous locations.

In the context of greenhouse automation, an IoT-based system typically includes a variety of sensors to monitor critical environmental parameters, a control unit to process and analyse the sensor data and triggers actuators accordingly through relays to maintain optimal growing conditions (Mohanty and Patil, 2013). These sensors usually measure factors like air temperature, humidity, wind speed and light intensity. The type of microcontroller used in the system can vary depending on the specific parameters that need to be monitored and controlled.

Actuators, which are crucial for adjusting the greenhouse environment, may include devices like foggers, exhaust fans, and artificial lighting systems. These components work together to maintain optimal growing conditions inside the greenhouse (Riahi *et al.*, 2020).

3.2.2 Hardware and Software Components Used in the IoT System

In an IoT setup, hardware refers to the physical devices that collect, process, and transmit data. These devices not only gather information but can also act on commands based on the data analysis. On the other hand, IoT software includes the programs and platforms that manage tasks such as data acquisition, processing, storage, and automation. This includes operating systems, firmware, applications, and middleware. The components used in this study are detailed in the sections below.

3.2.2.1 Hardware components

- Sensors
 - a) DHT22 temperature and humidity sensor
 - b) BH1750 light sensor
 - c) SHT10 Soil Temperature and Humidity Sensor
 - d) Wind Speed Sensor
- Microcontroller: Node MCU ESP32-S
- Wi-Fi modem
- Extension board

3.2.2.2 Software components

- Arduino IDE (Integrated Development Environment)
- ThingSpeak

3.2.3 Details of Hardware components used

The hardware components employed in this study, along with their descriptions and technical specifications, are detailed in the following section.

3.2.3.1 Sensors

A sensor is an electronic device that is designed to detect and measure physical phenomena or environmental conditions such as temperature, humidity, pressure, light etc and convert this information into a signal that can be interpreted by other devices, such as microcontrollers, computers, or control systems. This signal is typically electrical in nature, either analog or digital, and is used for monitoring, analysing, or automating processes.

a) DHT22 Temperature & Humidity Sensor

The DHT22 temperature & humidity sensor was used in this study to measure temperature and RH. The sensor uses a thermistor and a capacitive humidity sensor to measure the surrounding air temperature and RH respectively (Plate 3.3). The humidity sensing capacitor has two electrodes separated by a moisture-sensitive dielectric substrate. Variations in humidity alter the dielectric constant, leading to measurable changes in capacitance. For temperature measurement, the sensor employs a Negative Temperature Coefficient (NTC) thermistor, where resistance decreases with increasing temperature. Specifications of the sensor are shown in Table 3.3.



Plate 3.2 DHT22 temperature & humidity Sensor

Table 3.3 Specifications of DHT22 temperature & humidity Sensor

| | |
|--------------------------------|---|
| Temperature range | -40-80°C |
| Relative Humidity range | 0-100% RH |
| Resolution | Temperature: 0.1°C Humidity: 0.1% RH |
| Operating voltage | 3-5.5 V DC |
| Current supply | 1-1.5 mA |

b) BH1750 Light sensor

BH1750 light sensor was used in the study to measure light intensity. It is a small and low-cost sensor that uses a photodiode. It absorbs energy from light and changes into electricity with the help of the photoelectric effect. The electricity produced is proportional to the intensity of light that falls on the sensor and sensor material. The BH1750 sensor is commonly used in applications that require automatic adjustment of the light level, such as in streetlights, backlight control for LCD displays, and indoor lighting systems. Overall, the BH1750 sensor is a reliable and accurate option for measuring light intensity and is widely used in various applications due to its low cost, high accuracy, and ease of use. A view of the BH1750 light sensor and its specifications are shown in Plate 3.4 and Table 3.4 respectively.



Plate 3.3 BH1750 Light sensor

Table 3.4 Specifications of BH1750 Light sensor

| | |
|------------------------------|--------|
| Operating Voltage (V) | 3 to 5 |
| Interface | I2C |
| Length (mm) | 18 |
| Width (mm) | 13 |
| Height (mm) | 3 |
| Weight (g) | 5 |

c) SHT10 Soil Temperature and Moisture Sensor

The SHT10 is a digital sensor used to measure both temperature and humidity accurately. It works using CMOSens® technology, which combines a humidity sensor, a temperature sensor, and a 14-bit converter in one small device. This makes the sensor reliable and gives accurate digital readings.

To measure humidity, the sensor uses a capacitive element made of a special material placed between two tiny electrodes. When the humidity in the air changes, the material's electrical property (called capacitance) changes. The sensor detects this change and converts it into a digital signal.

For temperature, the sensor uses a band-gap sensor, which measures temperature based on how certain materials behave with heat. This method gives stable and precise temperature readings, which are also converted into digital form.

The SHT10 sends these readings to a microcontroller (like an Arduino or ESP32) using a simple two-wire connection. Although it's similar to I2C communication, it uses its own timing method. Since the sensor outputs data in digital form, there's no need for extra circuitry to convert signals. Its specifications are given in Table 3.5



Fig 3.3 SHT10 Soil Temperature and Humidity Sensor

Table 3.5 Specifications of SHT10 Soil Temperature and Humidity Sensor

| | |
|-----------------------------|--------|
| Item Type | Sensor |
| Model No. | SHT10 |
| Voltage Rating (VDC) | 3 to 5 |

d) Wind Speed Sensor

A wind speed sensor (anemometer) works by using three or four cups attached to horizontal arms that rotate around a vertical shaft. When wind blows, it pushes the cups, causing them to spin faster as the wind gets stronger (Plate 3.5) Inside the sensor, a magnetic or optical sensor counts the number of rotations per unit time. This count is then used to calculate the wind speed, since the speed of rotation is directly related to how fast the wind is moving. Some models generate an analog voltage signal (e.g. 0–5V) or pulses, which can be read by a microcontroller like Arduino or ESP32. The final output is often displayed in units such as m/s or km/h. This type of sensor is commonly used in weather stations, greenhouses, and outdoor environmental monitoring systems. Its specifications are given in Table 3.6.



Plate 3.4 Wind Speed Sensor

Table 3.6 Specifications of Wind Speed Sensor

| | |
|-------------------------------|-------------------------|
| Voltage Rating (VDC) | 12 to 24 |
| Power Consumption (W) | Voltage MAX $\leq 0.3W$ |
| Signal Range | 0 – 5 V |
| Operating Current (mA) | 4-20 mA |
| Resolution | 0.1 m/s |
| Measurement Range | 0-30 m/s |
| System error | $\pm 3\%$ |

3.2.3.2 Microcontroller *NODE MCU ESP 32S*

NodeMCU ESP32-S is a Wi-Fi and Bluetooth-enabled microcontroller that reads input from sensors (like DHT22), processes the data, and sends it wirelessly to the internet or controls devices like fans or lights (plate 3.6). It has a powerful dual-core processor, built-in ADC/DAC, and multiple communication interfaces (I²C, SPI, UART) for real-time automation and IoT applications. Its specifications are shown in Table 3.7



Plate 3.5 NodeMCU ESP32-S microcontroller

Table 3.7 Specifications of Microcontroller

| | |
|---------------------------------|---|
| Flash Memory (MB): | 4 MB |
| Processor | Single or Dual core Tensilica Xtensa 32-bit LX6 |
| Operating Voltage (VDC): | 2.3 ~ 3.6 |
| Operating Current (mA): | 80 |

3.2.3.3 WI-FI Modem

In this study, a Jio Wi-Fi modem was used to provide internet connectivity to the NodeMCU ESP32 microcontroller. The Jio Wi-Fi modem, commonly known as JioFi, is a portable hotspot device offered by Jio, a leading telecom provider in India. It allows users to wirelessly connect multiple devices to the internet using Jio's 4G network, ensuring a stable and high-speed connection.



Plate 3.6 Jio WI-FI Modem

The JioFi device is compact and user-friendly. To set it up, a Jio SIM card is inserted into the device, which is then powered on. Nearby devices can connect to the Wi-Fi network it creates using the provided password. The Jio Wi-Fi modem used in this project, along with its specifications, is shown in Plate 3.7 and Table 3.8 respectively.

Table 3.8 Specifications of Jio WI-FI Modem

| | |
|-----------------------------------|---|
| Model Name | M2s 4G hotspot support jio sim voice and data (device, battery, data cable) |
| Device Throughput | Up to 21 Mbps |
| Voice Support | Call Support only for Android Smartphones |
| Expandable Memory Capacity | Expandable Memory Capacity 32 GB |

3.2.4 Details of software used

Details of the different software used for the development of the system is described in the following sections.

3.2.4.1 Arduino IDE software

The Arduino Integrated Development Environment (IDE) is an open-source software platform used for writing, compiling, and uploading code to Arduino-compatible microcontroller boards. It is the primary tool used to create embedded systems and IoT applications. IDE offers a simplified programming experience tailored

for beginners while being robust enough for advanced users and supports C and C++ programming languages usually divided into two main functions:

- `void setup()`: Runs once at the beginning
- `void loop()`: Continuously runs after setup completes

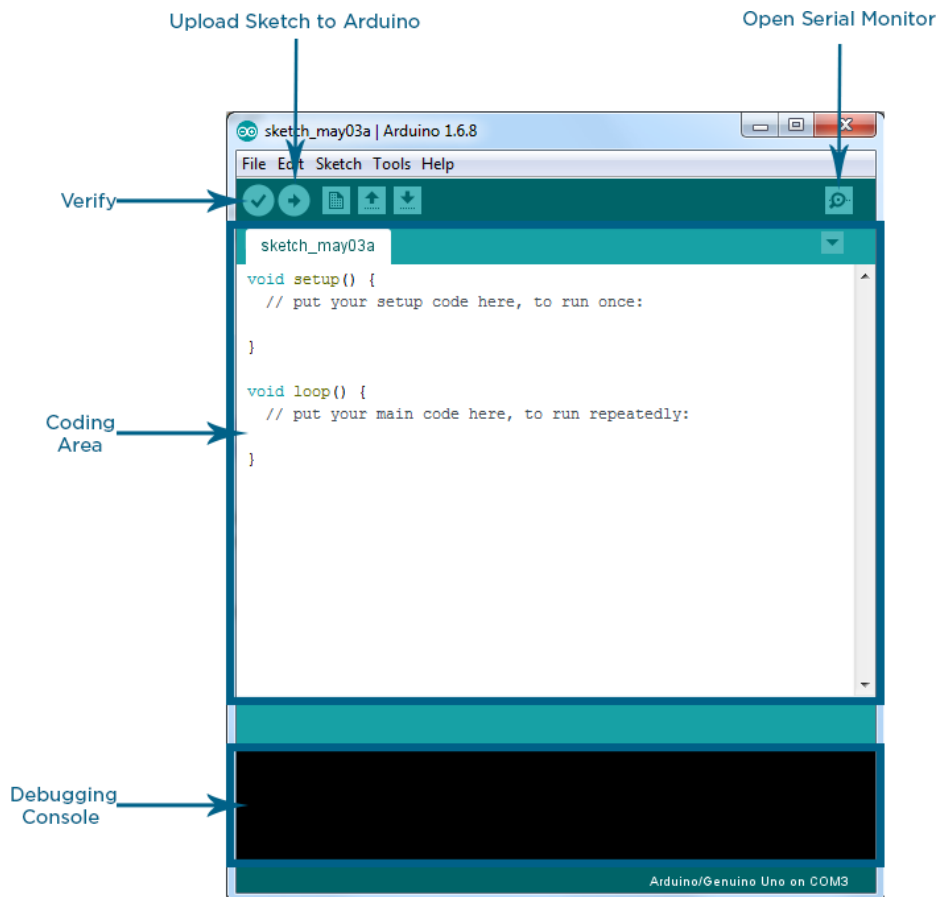


Fig.3.4 Arduino IDE windows interface

Key Features

- **Cross-Platform Compatibility:** Arduino IDE is available for Windows, Mac OS, and Linux.
- **Open Source:** Freely available under the GNU General Public License (GPL).
- **Board Support:** Built-in support for a wide range of Arduino boards, with additional board support (e.g., ESP32, STM32) via Board Manager.

- Extensive Libraries: Includes a vast number of libraries for sensors, actuators, communication protocols, and IoT platforms.
- Serial Monitor & Plotter: Useful tools for debugging and real-time data visualization.
- Sketch System: Projects are organized as "sketches" (.ino files), which are easy to manage and deploy.
- Auto-formatting and Syntax Highlighting: Improves readability and debugging.
- Simple Upload Process: One-click compiling and uploading to the microcontroller via USB or serial interface.

Steps to Upload Code

- Connect the Arduino or compatible board via USB
- Select the board from Tools > Board
- Select the correct COM port from Tools > Port
- Click the Upload button (right arrow icon)

The IDE will compile the code, convert it to machine instructions, and upload it to the microcontroller's flash memory.

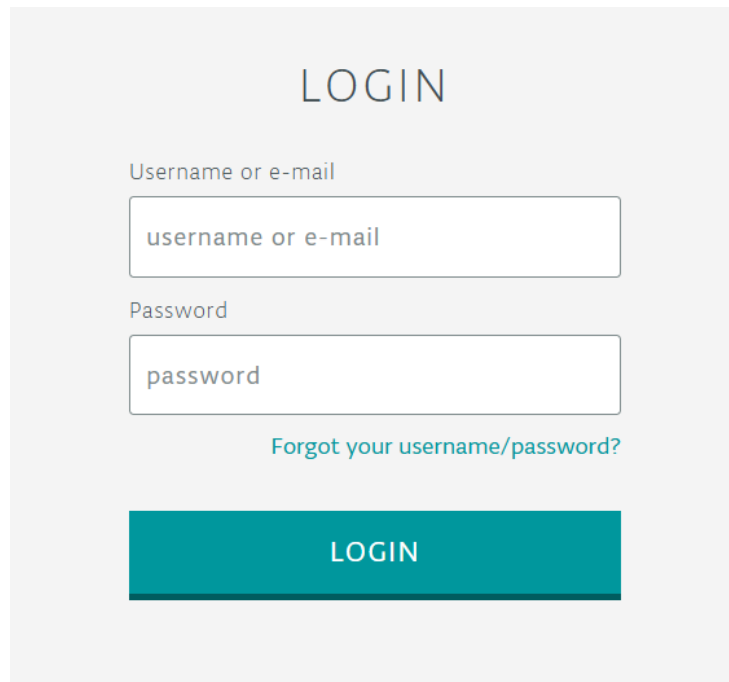
Setting Up of Arduino IDE

Various steps followed are:

- a. Install & create account in Arduino IDE
- b. Connect the Arduino board Using USB cable
- c. Open the Arduino IDE
- d. Select Board and Port
- e. Write or open a sketch
- f. Upload the sketch
- g. Check the output data

a. Creating an Arduino account

In order to start an Arduino account, log in/sign up in the Arduino site as shown in fig.3.6



A login form titled "LOGIN" on a light gray background. It contains two input fields: "Username or e-mail" with the placeholder text "username or e-mail", and "Password" with the placeholder text "password". Below the password field is a link that says "Forgot your username/password?". At the bottom is a teal button with the text "LOGIN" in white capital letters.

Fig.3.5 Arduino account creation

b. Connect the Arduino Board

Connect the Arduino board to the computer using a USB cable to power it and enable communication for uploading code.

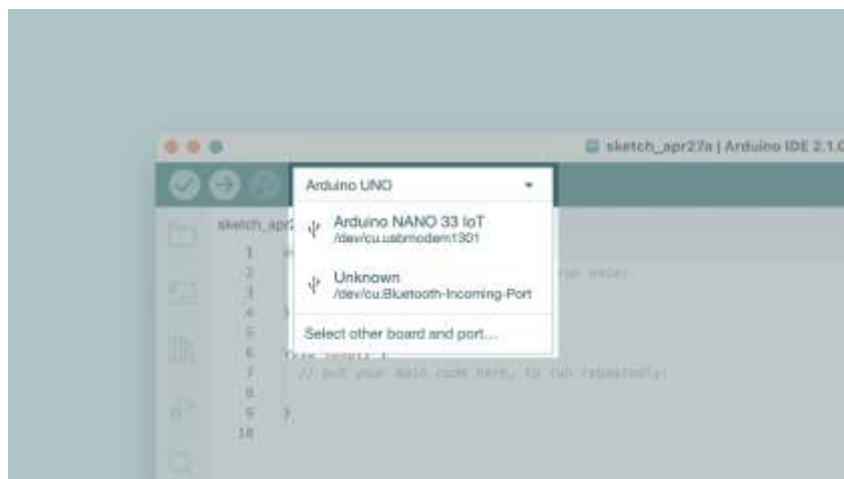


Fig.3.6 ESP 32S board connection with USB cable

c. Open the Arduino IDE

Open the Arduino IDE on your computer to write, compile, and upload code to the Arduino board.



Fig.3.7 Arduino dashboard

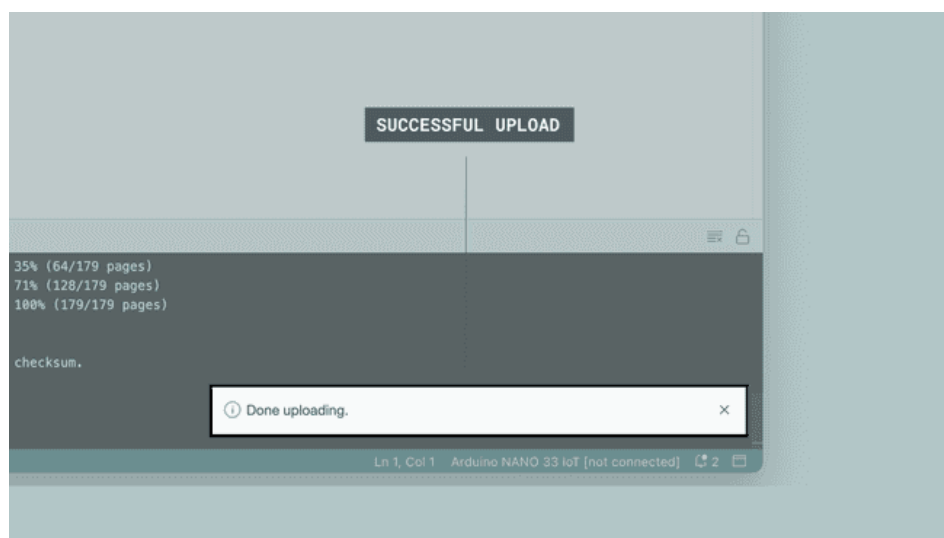
d. Select Board and Port

In the Arduino IDE, go to the "**Tools**" menu, select the appropriate **board model**, and then choose the correct **COM port** to establish communication with the connected Arduino board.

Click the Upload button in the Arduino IDE to compile the sketch and transfer it to the Arduino board. Once uploaded, the board will automatically start running the program.



(a)



(b)

Fig.3.10 Successful upload printed in the console

g. Check the output data

Open the Serial Monitor from the Tools menu in the Arduino IDE to view and verify the output data being sent from the Arduino board. This helps in monitoring sensor readings and debugging the code if needed.

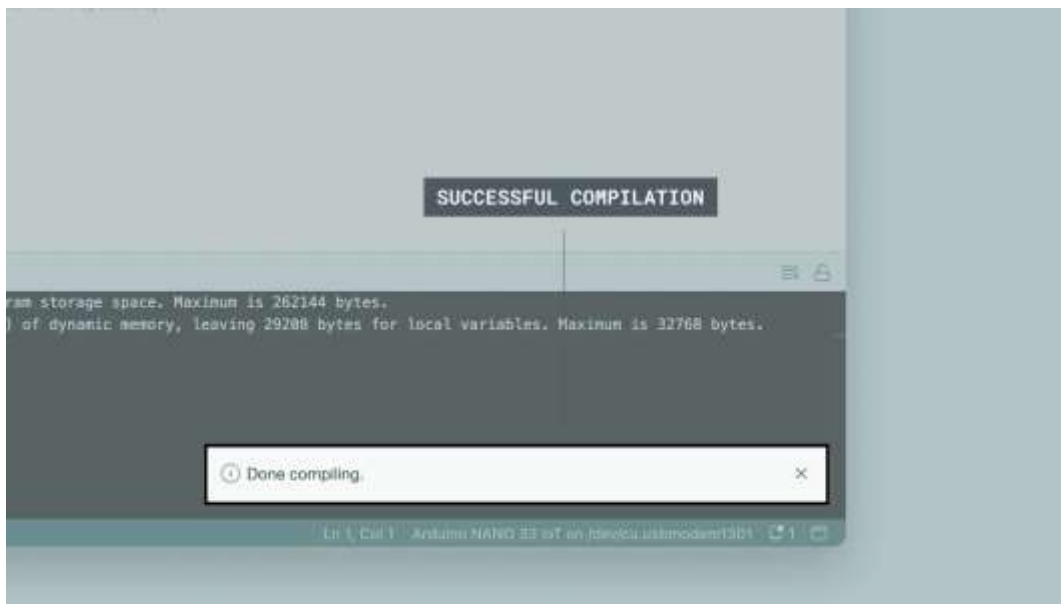


Fig.3.11 Successful compilation printed in the console



Fig.3.12 Serial monitoring of data

3.2.4.2 Thingspeak

ThingSpeak is an open-source Internet of Things (IoT) analytics platform that enables users to collect, store, analyze, visualize, and act on data from sensors or devices over the internet. It is cloud-based and is widely used for real-time monitoring and data logging applications.

Developed by MathWorks, ThingSpeak offers seamless integration with MATLAB, enabling advanced data analysis and visualization capabilities. It operates through a client-server model i.e., data is collected from sensors or devices (clients), sent via Wi-Fi or cellular network to the ThingSpeak cloud (server), and then visualized or analyzed in real time. Devices such as Arduino, ESP32, Raspberry Pi, and other microcontrollers can be easily connected to ThingSpeak. In ThingSpeak, a channel is a virtual container where data from a device or sensor is stored. Each channel can hold up to 8 data fields, plus metadata like location, status messages, and timestamps.

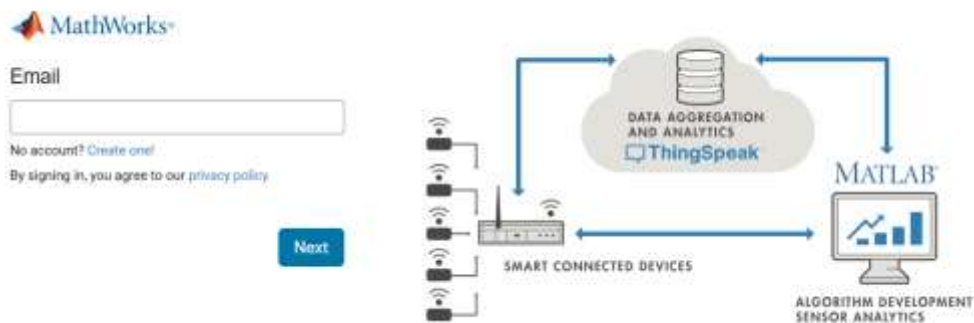


Fig 3.13 ThingSpeak windows interface

ThingSpeak offers built-in visualization tools including:

- Line charts
- Bar graphs
- Numeric displays
- Gauge meters
- Histograms and scatter plots

Users can view live or historical data trends, compare multiple fields, and configure chart settings (color, range, axis labels).

ThingSpeak can be used in a wide variety of fields including:

- Environmental monitoring (temperature, humidity, air quality)
- Home automation (smart devices, lighting, HVAC control)
- Industrial IoT (machine telemetry, predictive maintenance)
- Agriculture (soil moisture, weather tracking)
- Smart cities (traffic, pollution, public utilities)

Setting Up ThingSpeak

- Account Creation
- Channel Configuration
- API Keys
- Data Uploading

➤ Account Creation

- Create an account or log in using a MathWorks ID
- Confirm the email and access the dashboard

➤ Channel Configuration

- Click on "Channels" > "New Channel"
- Configure channel name and up to 8 data fields (e.g., Field 1, Field 2...)
- Add optional metadata: location, description, tags
- Save the channel

ThingSpeak Channels Apps Support Commercial Use How to Buy

New Channel

Name:

Description:

Field 1:
 Field 2:
 Field 3:
 Field 4:
 Field 5:
 Field 6:
 Field 7:
 Field 8:

Metadata:

Tag:

Link to External Site:

Link to GitHub:

Help

Channels store all the data that a ThingSpeak application collects. Each channel includes eight fields that can hold any type of data, plus three fields for location data and one for status data. Once you collect data in a channel, you can use ThingSpeak apps to analyze and visualize it.

Channel Settings

- Percentage complete:** Calculated based on data entered into the various fields of a channel. Enter the name, description, location, URL, video, and tag to complete your channel.
- Channel Name:** Enter a unique name for the ThingSpeak channel.
- Description:** Enter a description of the ThingSpeak channel.
- Fields:** Check the box to enable the field, and enter a field name. Each ThingSpeak channel can have up to 8 fields.
- Metadata:** Enter information about channel data, including JSON, XML, or CSV data.
- Tags:** Enter keywords that identify the channel. Separate tags with commas.
- Link to External Site:** If you have a website that contains information about your ThingSpeak channel, specify the URL.
- Show Channel Location:**
 - Latitude:** Specify the latitude position in decimal degrees. For example, the latitude of the city of London is 51.5072.
 - Longitude:** Specify the longitude position in decimal degrees. For example, the longitude of the city of London is 0.1278.
 - Elevation:** Specify the elevation position in meters. For example, the elevation of the city of London is 32.033.
- Video URL:** If you have a YouTube™ or other video that displays your channel information, specify the full path of the video URL.
- Link to GitHub:** If you store your ThingSpeak code on GitHub®, specify the GitHub repository URL.

Using the Channel

Fig.3.14 Channels

➤ API Keys

Each channel is assigned:

- Write API Key: Required for uploading data
- Read API Key: Used for data access from applications or dashboards

These keys are unique and used to ensure secure data transmission.

ThingSpeak Channels Apps Support Commercial Use How to Buy

example-channel

Channel ID: 123456
 Author: myusername@domain.com
 Location: Private

Private View Public View Channel Settings Channel API Keys Data Import Export

Write API Key

Key:

[Generate New API Key](#)

Read API Keys

Key:
 Note:

[Generate New API Key](#) [Delete API Key](#)

[Generate New API Key](#)

Help

API keys enable you to use the data in a channel to read data from a private channel. API keys are also generated when you create a new channel.

API Keys Settings

- Write API Key:** Use this key to write data to a channel. If you lost your key, this key is deprecated. Visit Generate New API Key.
- Read API Key:** Use this key to allow other people to read your channel's data and charts. Click Generate Read API Key to generate an additional read key for the channel.
- Note:** Use this link to enter information about channel read keys. For example, attributes to help track all users with access to your channel.

API Requests

Write a Channel Feed

```
curl -XPOST https://api.thingspeak.com/channels/123456/feed.json
```

Read a Channel Feed

```
curl -XGET https://api.thingspeak.com/channels/123456/feed.json?key=100506
```

Read a Channel Feed

```
curl -XGET https://api.thingspeak.com/channels/123456/feed.json?key=100506
```

[Read a Channel Feed](#)

Fig.3.15 API Key interface

➤ Data Uploading

Data can be uploaded using:

- HTTP GET/POST requests
- MQTT/MQTT over TLS
- MATLAB scripts

ThingSpeak is therefore such a powerful and flexible IoT cloud platform for storing, visualizing, and analyzing time-stamped data from connected devices. With its ease of use, built-in visualization tools, and MATLAB integration, it serves as an ideal platform for both academic projects and industrial IoT deployments. Its support for multiple communication protocols and automation features makes it a highly adaptable solution for real-time remote monitoring systems across various domains.

3.3 OVERALL SYSTEM DESIGN AND BLOCK DIAGRAM

The system is designed to monitor microclimatic conditions inside a polyhouse using a network of integrated environmental sensors. These sensors are responsible for collecting real-time data on key microclimatic parameters such as:

- Temperature (°C)
- Relative humidity (%)
- Light intensity (Lux)
- Wind speed (air velocity, m/s)
- Soil moisture/temperature (optional/if included)

Maintaining the optimal combination of these parameters is crucial for the healthy growth and productivity of crops cultivated inside the polyhouse. The data is sent to the ThingSpeak cloud platform, allowing for real-time and historical analysis. By deploying this system, farmers and greenhouse managers can make data-driven decisions to control ventilation, irrigation, and shading mechanisms.

At the core of the system is the ESP32-S NodeMCU, a low-power, Wi-Fi-enabled microcontroller capable of handling multiple sensor inputs and transmitting data over the internet. ESP32 Development board is based on the ESP WROOM32 WIFI Module. It's a low-footprint, minimal system development board powered by the latest ESP-WROOM-32 module and can be easily inserted into a solderless breadboard.

It contains the entire basic support circuitry for the ESP-WROOM-32, including the USB-UART bridge, reset- and boot-mode buttons, LDO regulator and a micro-USB connector. Every important GPIO is available to the developer. Its key roles include:

I. Sensor Interface And Data Acquisition

The ESP-32S reads analog and digital signals from connected sensors like:

- DHT22 – for ambient temperature and humidity
- BH1750 – for light intensity in lux
- Anemometer – for wind speed/airflow
- SHT10 (Optional: Soil sensors) – to monitor root-zone environment

II. Data Processing

The raw signals from each sensor are processed and formatted by the ESP-32S for further transmission. Minimal local computation may include averaging, filtering noise, and timestamping.

III. Wireless Communication

The ESP-32S sends the collected data wirelessly to a cloud platform (e.g., Thingspeak, Blynk, Firebase, or MQTT-based server). This wireless transmission enables remote access to the environmental data via internet-connected devices.

➤ Cloud connectivity – ThingSpeak integration

Cloud connectivity plays a central role in transforming the polyhouse monitoring data from a basic sensor network into a real-time, remotely accessible smart cloud interface. The ThingSpeak IoT platform is used to collect, store, analyse, and visualize environmental data gathered by the ESP-32S NodeMCU microcontroller from various sensors.

a. Internet Connectivity via JioFi

The JioFi device acts as a mobile hotspot, providing 4G LTE-based Wi-Fi connectivity inside the polyhouse. The ESP-32S is configured to connect to the JioFi network using its SSID and password. This ensures portable and reliable internet access, especially in rural or agricultural areas where broadband may not be available.

b. Data Transmission Workflow

The ESP-32S connects to a Wi-Fi network and transmits sensor data to the ThingSpeak server at predefined time intervals (e.g., every 2 minutes). Each environmental parameter (e.g., temperature, humidity, light, wind speed) is assigned a

separate field/channel in ThingSpeak. The data is formatted as HTTP GET or POST requests using the ThingSpeak API, with an API key for authentication.

- ThingSpeak Channel Setup

On ThingSpeak a channel is created to receive and visualize sensor data. Up to 8 fields per channel can be used to accommodate multiple sensors. Maximum of 4 channels can be made in a single account. Each field represents one parameter (e.g., Field 1 – Temperature, Field 2 – Humidity, etc.).

- Real-Time Data Visualization

Thingspeak provides built-in real-time graphs and widgets that automatically update as new data is received, allow users to customize time ranges and graph types and display data on dashboards accessible via any device with a browser (mobile or desktop). This allows farm managers or researchers to continuously monitor polyhouse conditions without being physically present.

- Historical Data Logging and Export

All transmitted data is stored permanently in the cloud (For a maximum period of approximately 14 days in ThingSpeak). Users can view historical trends, enabling seasonal and long-term analysis. Data can be exported in CSV format for use in Excel or other analytics software.

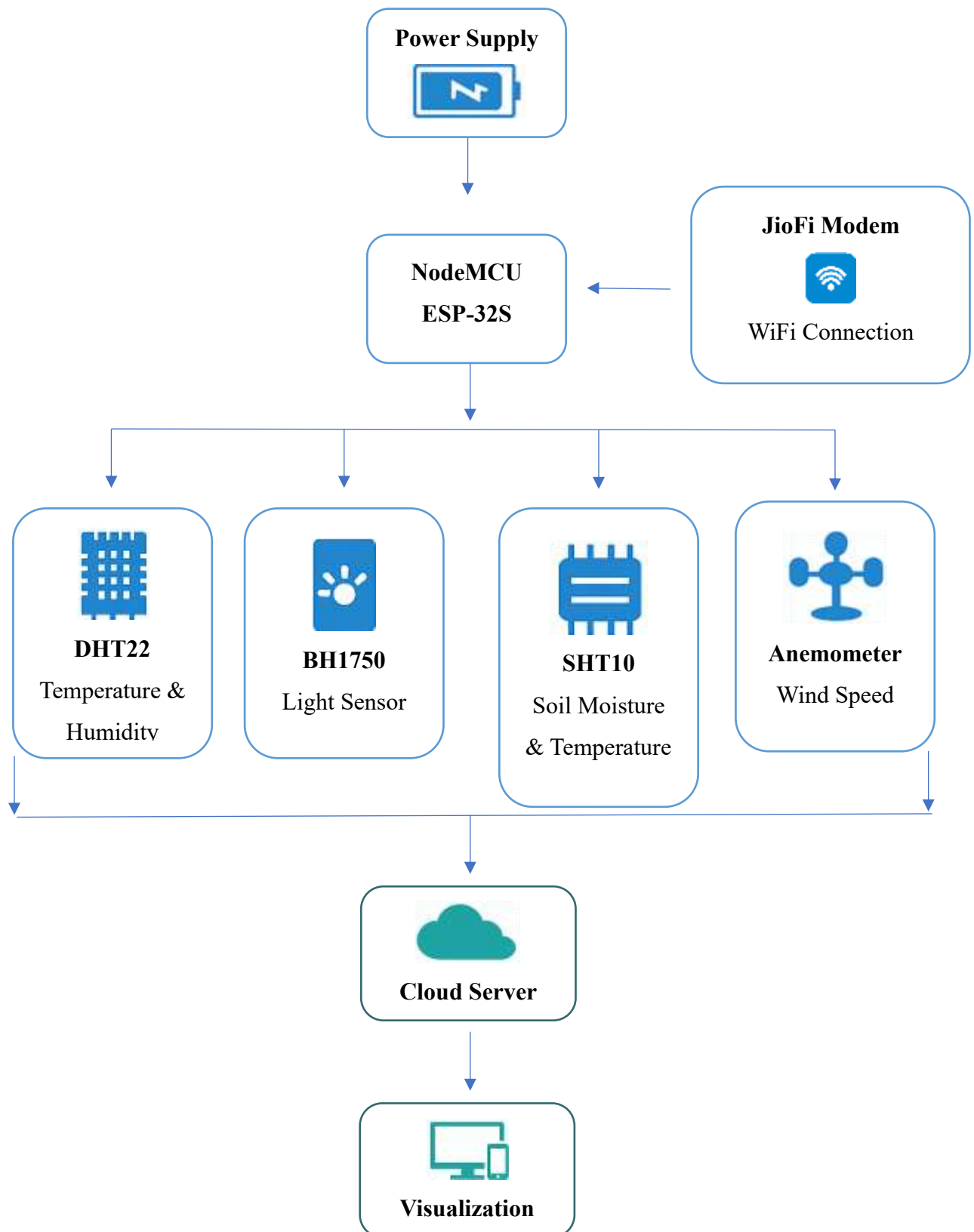


Fig.3.16 System overview

3.4 INTEGRATING SEVERAL COMPONENTS WITH THE ESP32-S

The ESP 32S microcontroller was used as the system's central processing unit, connected to several environmental sensors to monitor real-time data. The DHT22 sensor was used to sense temperature and humidity, the BH1750 light intensity sensor was employed to sense the ambient light level, and an anemometer was connected to sense wind speed. This interfacing with various components is explained in the following section.

3.4.1 Integrating ESP32-S and DHT22 Temperature & Humidity Sensor

Various pins of esp32s and DHT22 sensor are shown in fig.3.18 The DHT22 sensor module features three pins: VCC for power supply, Data for serial communication, and GND for ground connection. Esp32 Pins and its corresponding connection with DHT22 pins is shown in Table 3.10

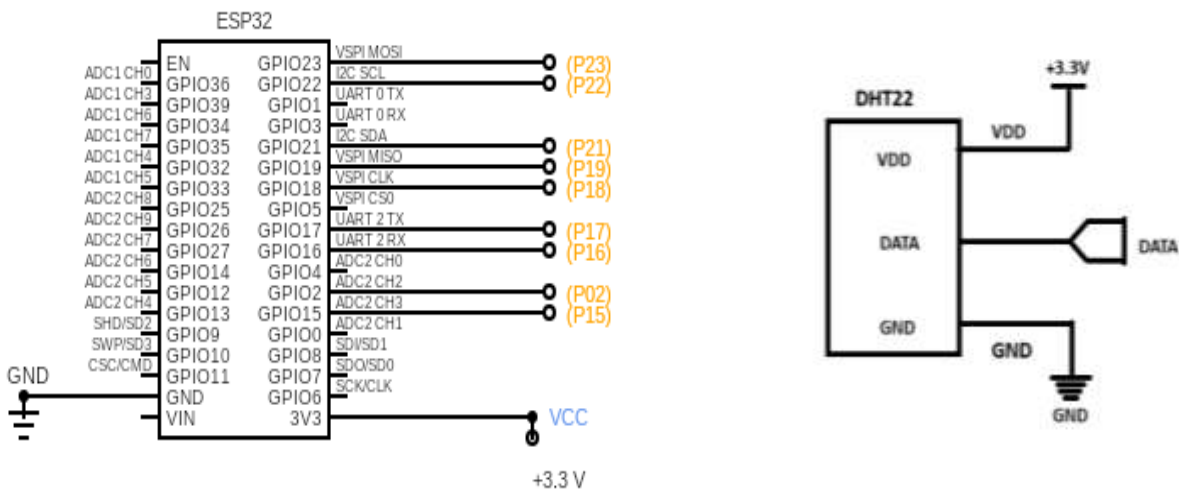


Fig.3.17 pins of ESP32, DHT22 sensor and their interfacing

Table 3.9 ESP32 pins and its connection with DHT22 temperature & humidity sensor pins

| ESP32 Pins | DHT22 Temperature & Humidity Sensor Pins |
|------------|--|
| 3.3V or 5V | VCC/VDD (all 9 sensors) |
| GND | GND (all 9 sensors) |
| GPIO18 | DATA (Sensor 1) |
| GPIO19 | DATA (Sensor 2) |
| GPIO21 | DATA (Sensor 3) |
| GPIO22 | DATA (Sensor 4) |
| GPIO23 | DATA (Sensor 5) |
| GPIO17 | DATA (Sensor 6) |
| GPIO15 | DATA (Sensor 7) |
| GPIO2 | DATA (Sensor 8) |
| GPIO16 | DATA (Sensor 9) |

3.4.2 Integrating Esp 32 pins and Light Intensity Sensor

The BH1750 light sensor has four pins: VCC, serial clock pin (SCL), serial data pin (SDA), and GND (as shown in Fig.3.19). In this study, the VCC pin of the sensor was connected to the 5V pin of the ESP32-S. The SCL pin of the sensor was connected to GPIO22 of the ESP32-S, while the SDA pin was connected to GPIO21. The GND pin of the sensor was connected to one of the GND pins on the ESP32-S. The connections between the ESP32-S pins and the BH1750 light sensor pins are summarized in Table .3.11

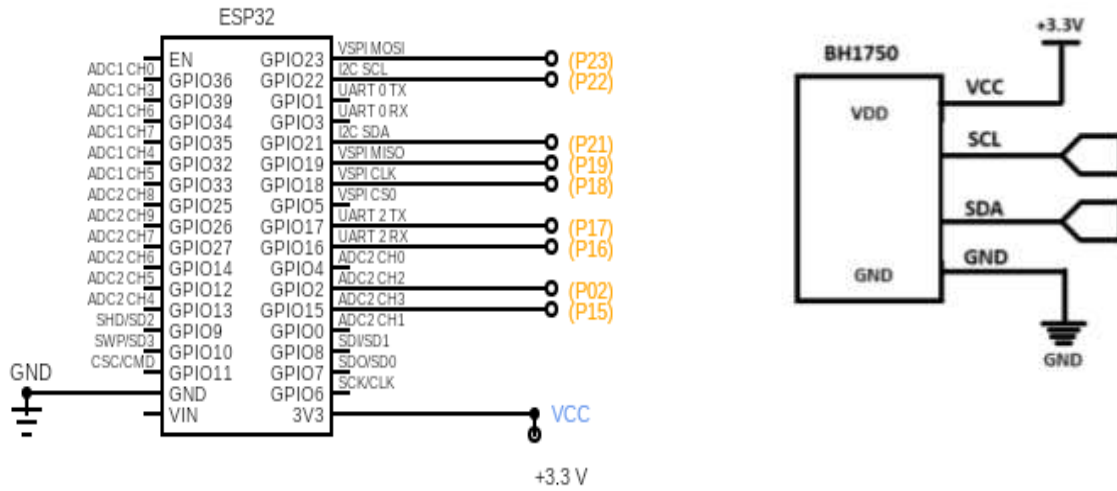


Fig.3.18 pins of ESP32, BH1750 light Intensity sensor and their interfacing

Table 3.10 ESP32 pins and its connection with BH1750 light Intensity sensor pins

| ESP32 Pins | BH1750 LIGHT Intensity Sensor Pins |
|------------|------------------------------------|
| 3.3V or 5V | VCC/VDD (all 9 sensors) |
| GPIO18 | GND (all 9 sensors) |
| GPIO19 | DATA (Sensor 1) |
| GPIO21 | DATA (Sensor 2) |
| GPIO22 | DATA (Sensor 3) |
| GPIO23 | DATA (Sensor 4) |
| GPIO17 | DATA (Sensor 5) |
| GPIO15 | DATA (Sensor 6) |
| GPIO2 | DATA (Sensor 7) |
| GPIO16 | DATA (Sensor 8) |

3.5 OVERALL CIRCUIT DIAGRAM OF IOT BASED SYSTEM

➤ Microcontroller

NodeMCU ESP32-S is used which has built in wifi.

➤ Sensors

DHT22 and BH1750 nine of each are connected to the one microcontroller. SHT10 and three anemometers are connected to another microcontroller. The data pins of different sensors are connected to the different GPIOs on the ESP32.

➤ Power Supply

All the sensors and microcontrollers are given a power supply of 5V or 3.5V by connecting the adapter end to the breadboard. All sensors are connected to VCC (Red wires) and GND (white wires) in the polyhouse. The figure shows rough circuit diagram for the whole connection in the polyhouse.

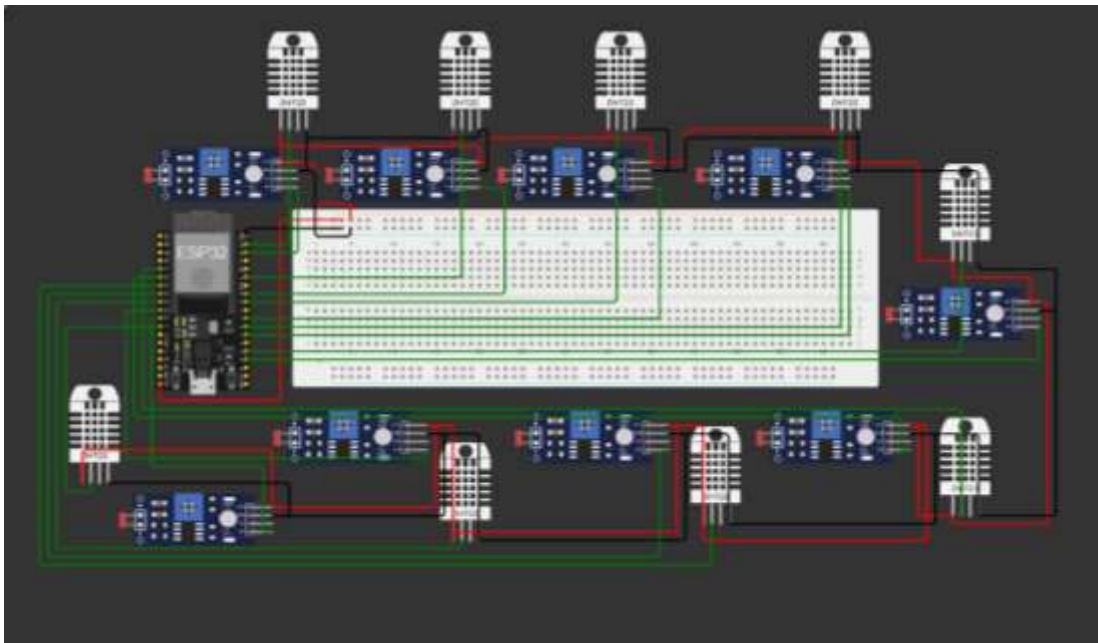


Fig.3.19 Schematic circuit diagram of sensors connected to microcontroller

➤ Connections

white wires are again used as data lines from each sensor to the ESP32. Data lines have individual pull-up resistors (standard 10k Ω) in some cases.

➤ Breadboard Layout

Efficient use of two large breadboard to distribute power. One is used to give power supply to the DHT22 and BH1750 and the other is used to give power to the SHT10 and anemometer which require higher voltage.

3.6 SOURCE CODE FOR READING TEMPERATURE, HUMIDITY, AND LIGHT INTENSITY

```
#include <DHT.h>
#include <WiFi.h>
#include <HTTPClient.h>

// Define DHT sensor pins
#define DHTPIN1 18
#define DHTPIN2 19
#define DHTPIN3 21
#define DHTPIN4 22
#define DHTPIN5 23
#define DHTPIN6 17
#define DHTPIN7 15
#define DHTPIN8 2
#define DHTPIN9 16

// Define DHT type
#define DHTTYPE DHT22

// Create DHT sensor objects
DHT dht1(DHTPIN1, DHTTYPE);
DHT dht2(DHTPIN2, DHTTYPE);
DHT dht3(DHTPIN3, DHTTYPE);
DHT dht4(DHTPIN4, DHTTYPE);
DHT dht5(DHTPIN5, DHTTYPE);
DHT dht6(DHTPIN6, DHTTYPE);
DHT dht7(DHTPIN7, DHTTYPE);
DHT dht8(DHTPIN8, DHTTYPE);
DHT dht9(DHTPIN9, DHTTYPE);

// Wi-Fi credentials
const char* ssid = "JioFi_2149165"; // Replace with your Wi-Fi SSID
const char* password = "cq7yi4qeqq"; // Replace with your Wi-Fi password

// ThingSpeak credentials
const char* server = "http://api.thingspeak.com/update"; // Use the update endpoint
const char* mywriteAPIKey1 = "1NP1KXHIBBR9WZ4S"; // Replace with your first Write API Key
const char* mywriteAPIKey2 = "47N7X84UKBWJW8AV"; // Replace with your second Write API Key
const char* mywriteAPIKey3 = "DH7MLHC3N0BUWG9R"; // Replace with your second Write API Key
const long channelID1 = 2965098; // Replace with your first ThingSpeak Channel ID
const long channelID2 = 2965099; // Replace with your second ThingSpeak Channel ID
const long channelID3 = 2965101; // Replace with your second ThingSpeak Channel ID
```

(a)


```

void setup() {
  Serial.begin(115200);

  // Initialize DHT sensors
  dht1.begin();
  dht2.begin();
  dht3.begin();
  dht4.begin();
  dht5.begin();
  dht6.begin();
  dht7.begin();
  dht8.begin();
  dht9.begin();

  // Connect to Wi-Fi
  WiFi.begin(ssid, password);
  while (WiFi.status() != WL_CONNECTED) {
    delay(1000);
    Serial.println("Connecting to WiFi...");
  }
  Serial.println("Connected to WiFi");
}

void loop() {
  // Read DHT sensors
  float humidity[9];
  float temperature[9];

  humidity[0] = dht1.readHumidity();
  temperature[0] = dht1.readTemperature();

  humidity[1] = dht2.readHumidity();
  temperature[1] = dht2.readTemperature();

  humidity[2] = dht3.readHumidity();
  temperature[2] = dht3.readTemperature();

  humidity[3] = dht4.readHumidity();
  temperature[3] = dht4.readTemperature();

  humidity[4] = dht5.readHumidity();

```

(b)

```

humidity[3] = dht4.readHumidity();
temperature[3] = dht4.readTemperature();

humidity[4] = dht5.readHumidity();
temperature[4] = dht5.readTemperature();

humidity[5] = dht6.readHumidity();
temperature[5] = dht6.readTemperature();

humidity[6] = dht7.readHumidity();
temperature[6] = dht7.readTemperature();

humidity[7] = dht8.readHumidity();
temperature[7] = dht8.readTemperature();

humidity[8] = dht9.readHumidity();
temperature[8] = dht9.readTemperature();

// Print DHT sensor readings
for (int i = 0; i < 9; i++) {
    Serial.print("DHT");
    Serial.print(i + 1);
    Serial.print(" - Humidity: ");
    Serial.print(humidity[i]);
    Serial.print("%, Temperature: ");
    Serial.print(temperature[i]);
    Serial.println("°C");
}

// Send data to ThingSpeak for the first channel
if (WiFi.status() == WL_CONNECTED) {
    HTTPClient http;

    // Construct the URL for the first POST request
    String url1 = String(server) + "?api_key=" + myWriteAPIKey1 +
        "&field1=" + String(temperature[0]) +
        "&field2=" + String(humidity[0]) +
        "&field3=" + String(temperature[1]) +
        "&field4=" + String(humidity[1]) +
        "&field5=" + String(temperature[2]) +

```

(c)

```

        "&field6=" + String(humidity[2]) +
        "&field7=" + String(temperature[3]) +
        "&field8=" + String(humidity[3]));
    http.begin(url1); // Specify the URL
    httpResponseCode = http.GET(); // Send the request

    // Check the response code
    if (httpResponseCode > 0) {
        String response = http.getString(); // Get the response payload
        Serial.println(httpResponseCode); // Print return code
        Serial.println(response); // Print response payload
    } else {
        Serial.print("Error on sending POST: ");
        Serial.println(httpResponseCode);
    }

    http.end(); // Free resources
} else {
    Serial.println("WiFi Disconnected");
}
if (WiFi.status() == WL_CONNECTED) {
    HTTPClient http;
    // Construct the URL for the second POST request
    String url2 = String(server) + "?api_key=" + myWriteAPIKey2 +
        "&field1=" + String(temperature[4]) +
        "&field2=" + String(humidity[4]) +
        "&field3=" + String(temperature[5]) +
        "&field4=" + String(humidity[5]) +
        "&field5=" + String(temperature[6]) +
        "&field6=" + String(humidity[6]) +
        "&field7=" + String(temperature[7]) +
        "&field8=" + String(humidity[7]));
    http.begin(url2); // Specify the URL
    httpResponseCode = http.GET(); // Send the request

    // Check the response code
    if (httpResponseCode > 0) {
        String response = http.getString(); // Get the response payload
        Serial.println(httpResponseCode); // Print return code
        Serial.println(response); // Print response payload
    } else {

```

(d)

```

// Check the response code
if (httpResponseCode > 0) {
    String response = http.getString(); // Get the response payload
    Serial.println(httpResponseCode); // Print return code
    Serial.println(response); // Print response payload
} else {
    Serial.print("Error on sending POST: ");
    Serial.println(httpResponseCode);
}
String url3 = String(server) + "?api_key=" + myWriteAPIKey3 +
    "&field1=" + String(temperature[8]) +
    "&field2=" + String(humidity[8]);

http.begin(url3); // Specify the URL

httpResponseCode = http.GET(); // Correct

// Check the response code
if (httpResponseCode > 0) {
    String response = http.getString(); // Get the response payload
    Serial.println(httpResponseCode); // Print return code
    Serial.println(response); // Print response payload
} else {
    Serial.print("Error on sending POST: ");
    Serial.println(httpResponseCode);
}

http.end(); // Free resources
} else {
    Serial.println("WiFi Disconnected");
}
if (WiFi.status() == WL_CONNECTED) {
    HTTPClient http;

    http.end(); // Free resources
} else {
    Serial.println("WiFi Disconnected");
}
// Wait for a while before the next reading
delay(300000); // Delay for 120 seconds
}

```

(e)

Fig.3.20 (a-e) Source Code for Reading Temperature and Relative Humidity

3.7 COST ESTIMATION FOR ECONOMICAL IMPLEMENTATION

Cost estimation is carried out to ensure an economical implementation by calculating the total expenses involved in wiring, components, and installation, helping to choose the most cost-effective design.

Table 3.11 Estimated cost of wire required at different microcontroller position

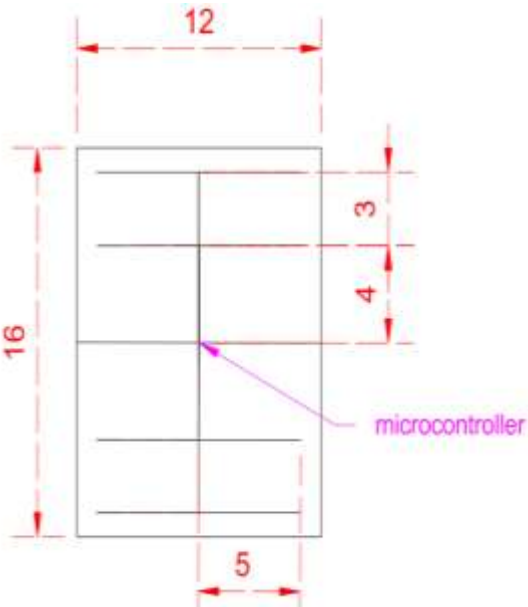
| Position of microcontroller | Power Supply (m) | Data Connection (m) | Pole Connection (Power + Data) (m) | Total Wire Required (m) | Total Amount (Rs.) (11/- per m) |
|---|-------------------------|----------------------------|---|--------------------------------|--|
| Microcontroller at centre | 128 | 564 | 150 | 842 | 9262 |
| Microcontroller at centre and connected diagonally | 140 | 420 | 150 | 710 | 7810 |
| Microcontroller at one end | 128 | 720 | 150 | 998 | 10978 |
| Microcontroller at one end and connected diagonally | 92.76 | 556.56 | 150 | 799.32 | 8572.52 |

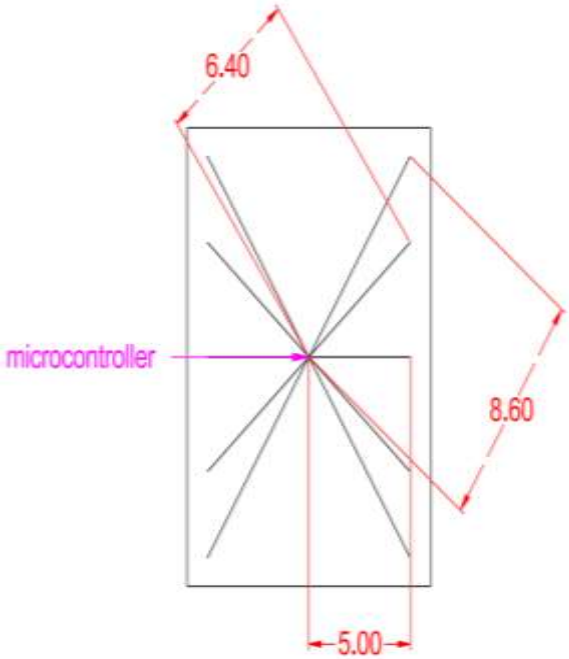
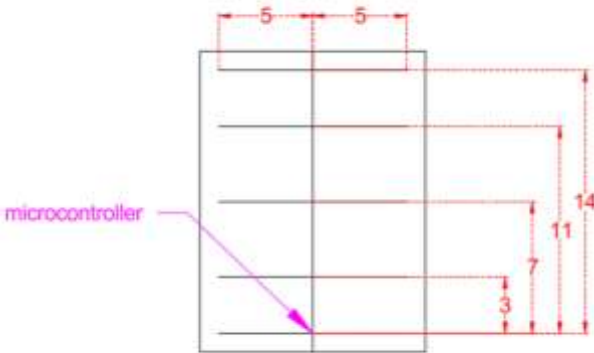
Table 3.12 Estimated cost of components

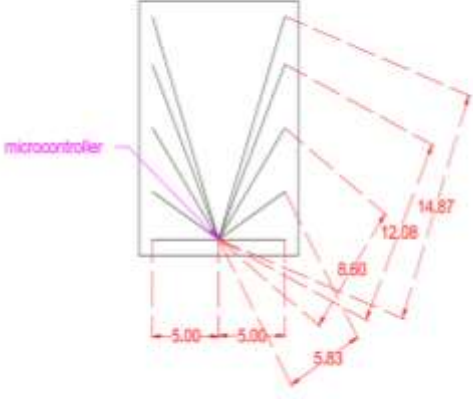
| Components | Quantity | Unit Price (Rs.) | Amount (Rs.) |
|----------------------------------|-----------------|-------------------------|---------------------|
| Node MCU ESP32S Microcontroller | 5 no. | 355 | 1775 |
| DHT22Temperature-humidity sensor | 34 no. | 115 | 3910 |
| Light intensity sensor | 34 no. | 79 | 2686 |

| | | | |
|-------------------------|---------|------|---------|
| Soil temperature sensor | 4 no. | 1720 | 6880 |
| Anemometer | 3 no. | 3000 | 9000 |
| Jumper wire | 150 no. | 2 | 300 |
| Jio WiFi modem | 1 no. | 2200 | 2200 |
| Bread board | 2 no. | 80 | 160 |
| Extension board | 1 no. | 380 | 380 |
| Total | | | 27291/- |

Table 3.13 Overall cost estimation of the system

| Position of microcontroller | Total Amount of wire (Rs.) | Total Amount of components (Rs.) | Overall cost of system (Rs.) |
|--|----------------------------|----------------------------------|------------------------------|
| <p>Microcontroller at centre</p>  | 9262 | 27291 | 36553 |

| | | | |
|--|-------|-------|-------|
| <p>Microcontroller at centre and connected diagonally</p>  | 7810 | 27291 | 35101 |
| <p>Microcontroller at one end</p>  | 10978 | 27291 | 38269 |

| | | | |
|--|---------|-------|----------|
| <p>Microcontroller at one end and connected diagonally</p>  | 8572.52 | 27291 | 35863.52 |
|--|---------|-------|----------|

From the estimated cost, the position of microcontroller at centre and connected diagonally is found to be economical. But, this way of connection will hinder the movement of workers inside the polyhouse. So, the position of microcontroller at centre is selected by replacing the cable wire with twin wire with a cost of Rs. 3 per meter. Therefore, the cost of wire is reduced to Rs. 2526 and the overall cost becomes Rs. 29817.

3.8 GROUND PREPARATION ACTIVITIES IN THE POLYHOUSE

The following steps outline the preparatory activities undertaken prior to conducting the experiment in the polyhouse:

- **Initial Ground Leveling Using Auto Level**
 - Conducted a detailed ground survey inside the polyhouse using an auto level to identify high and low points.
 - Created a leveling plan based on the readings to ensure uniform surface grading.
- **Earthwork and Volume Calculation**
 - Calculated the volume of earth to be cut or filled based on the leveling data.
 - Executed earthwork operations to achieve a consistent and even ground level throughout the polyhouse.

- **Final Level Check with Water Level Pipe**
 - Rechecked the entire ground level by water level using water tube to confirm precision and uniformity.
 - Made minor adjustments wherever necessary to finalize the level
- **Application of Weedicide**
 - Applied a broad-spectrum weedicide uniformly over the leveled ground surface.
 - Allowed sufficient time for the chemical to act and suppress any existing or potential weed growth.
- **Installation of Weed Mat**
 - Spread a high-quality weed mat over the entire area to block sunlight and prevent weed emergence.
 - Ensured proper alignment and full coverage of the surface.
- **Securing Weed Mat with Nails**
 - Fixed the weed mat securely using nails or U-pins at regular intervals.
 - Ensured that the mat was tightly held in place without wrinkles or lifting, ready for further operations.



(a)



(b)



(c)



(d)

Plate 3.7 Preparations for the experiment (a) Ground level checking with water level pipe (b) Application of weedicide (c) Fixing of weedmat (d) Final prepared polyhouse

RESULT & DISCUSSION

CHAPTER IV

RESULTS AND DISCUSSION

An IoT-based real-time microclimate monitoring system for a polyhouse was installed and tested. In this study, key microclimate parameters such as temperature, relative humidity, and light intensity were continuously monitored. The system was evaluated under polyhouse conditions without the presence of crops. Observations related to the microclimate behaviour were recorded and analysed. The results of the development and testing of the IoT-based microclimate monitoring system for the polyhouse are discussed in this chapter under the following subheads.

4.1 CALIBRATION OF SENSORS

In this study, three sensors were used: the DHT22 temperature and humidity sensor, the BH1750 light intensity sensor, and an anemometer for wind speed measurement. All sensors were calibrated by comparing the data acquired from the sensors with the corresponding values measured using standard reference instruments. Calibration curves were plotted in Microsoft Excel to derive calibration equations for each sensor. These equations were incorporated into the Arduino code to ensure more accurate sensor readings. The calibration process improved the reliability of the measured microclimate parameters. The results of the sensor calibrations are detailed below.

4.1.1 Results of calibration of DHT22 Temperature-Humidity sensor for temperature

Temperature readings from the DHT22 sensor and a dry bulb thermometer were recorded simultaneously. The collected values are presented in the table 4.1. A calibration curve was plotted using the dry bulb thermometer readings against the corresponding DHT22 sensor readings, as shown in the figure 4.1. From this plot, a calibration equation was derived to improve the accuracy of the temperature measurements obtained from the DHT22 sensor and the obtained equation was:

$$y=0.9155x+3.4837 \quad \text{(Eq.4.1)}$$

Table 4.1 DHT22 sensor reading and dry bulb temperature reading

| Time | Dry bulb temperature (°C) | DHT22 Sensor readings (°C) |
|-------------|--------------------------------------|---------------------------------------|
| 09:15 | 27 | 27.9 |
| 09:53 | 27.5 | 28.6 |
| 10:30 | 29.5 | 30.5 |
| 11:00 | 28 | 29.6 |
| 11:30 | 30 | 30.9 |
| 14:45 | 30 | 30.9 |
| 15:15 | 31 | 31.9 |
| 15:45 | 32 | 32.9 |
| 16:15 | 32 | 32.6 |
| 16:45 | 31 | 31.8 |
| 17:15 | 30.9 | 31.8 |
| 17:45 | 31 | 31.9 |

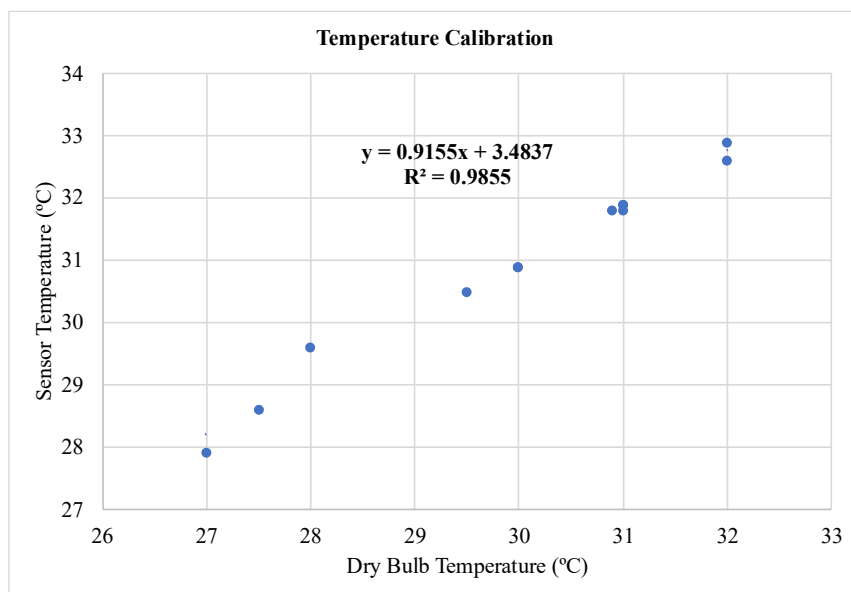


Fig 4.1 DHT22 sensor temperature calibration curve

4.1.2 Results of calibration of DHT22 sensor for Relative Humidity (RH)

Calibration of the relative humidity readings from the DHT22 sensor was carried out using the standard psychrometric equation (Eq. 4.2) from the obtained dry and wet bulb temperatures and the collected values are presented in the table 4.2.

$$RH = 100 * \left[\frac{6.122 * e^{\left(\frac{17.62T_d}{243.12+T_d}\right)} - 0.67 * (T_d - T_w)}{6.112 * e^{\left(\frac{17.62T_w}{243.12+T_w}\right)}} \right] \quad (\text{Eq. 4.2})$$

Where,

- RH= Relative Humidity (%)
- T_d = Dry bulb temperature (°C)
- T_w = Wet bulb temperature (°C)
- The term $6.122 * e^{\left(\frac{17.62T}{243.12+T}\right)}$ estimates the saturation vapor pressure in hPa at a given temperature T
- The subtraction of $0.67 * (T_d - T_w)$ approximates the actual vapor pressure, accounting for the cooling effect of evaporation
- The ratio then gives the relative humidity as a percentage

The obtained calibrated equation was:

$$Y=0.8019x+18.152 \quad (\text{Eq. 4.3})$$

Table 4.2 DHT22 Sensor reading and calculated reading for relative humidity

| Time | Wet Bulb (°C) | Dry Bulb (°C) | Relative Humidity (%) | Sensor RH (%) |
|-------|---------------|---------------|-----------------------|---------------|
| 09:15 | 26.5 | 27 | 96.16 | 94.2 |
| 09:53 | 26 | 27.5 | 88.81 | 90.8 |
| 10:30 | 27.5 | 29.5 | 85.78 | 88.4 |
| 11:30 | 27.5 | 30 | 82.55 | 84.6 |

| | | | | |
|-------|------|------|-------|------|
| 15:15 | 29 | 31 | 86.16 | 86.6 |
| 15:45 | 28.9 | 32 | 79.36 | 80 |
| 16:15 | 28.9 | 32 | 79.36 | 81.5 |
| 16:45 | 28 | 31 | 79.64 | 83.6 |
| 17:15 | 28.5 | 30.9 | 83.5 | 84.7 |
| 17:45 | 28 | 31 | 79.64 | 81.5 |

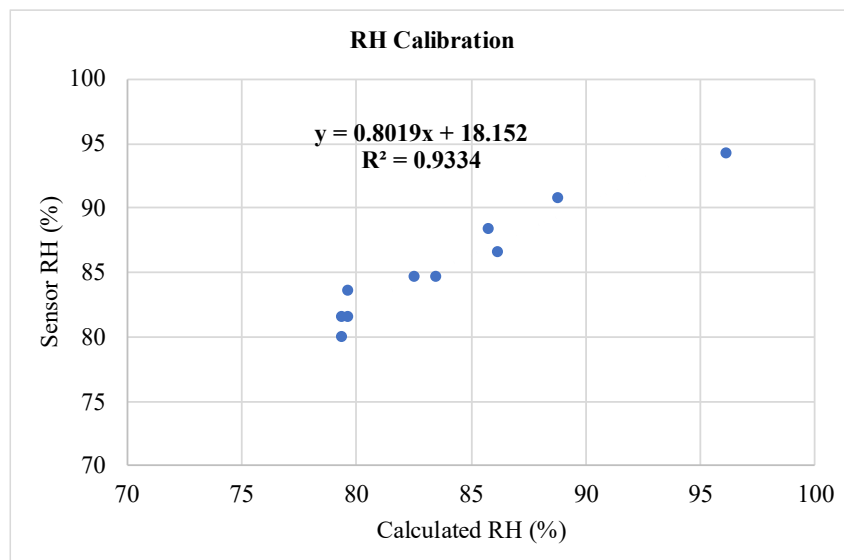


Fig 4.2 Calibration chart for DHT22 sensor for Relative Humidity

```

Serial.begin(115200);
dht.begin();
}
float calibrateTemperature(float rawTemp) {
    return 0.9155 * rawTemp + 3.4837;
}
float calibrateHumidity(float rawHum) {
    return 0.8019 * rawHum + 18.152;
}
void loop() {
    // Wait a few seconds between measurements
    delay(2000);
}

```

Fig 4.3 Incorporation of calibration equation into Arduino code

4.1.3 Results of calibration of BH1750 light intensity sensor

Light intensity readings from the BH1750 sensor and a standard lux meter were recorded simultaneously. To calibrate the BH1750 sensor, a calibration curve was plotted with the lux meter readings against the corresponding sensor output. Additionally, the sensor's voltage output and internal resistance characteristics were taken into account to understand its response under varying light conditions. Based on the calibration curve, a correction equation was derived to enhance the accuracy of light intensity measurements from the BH1750 sensor. This equation was incorporated into the Arduino code to ensure precise real-time monitoring of light levels.

4.1.3.1 Calibration of Lux Meter Reading Vs. Voltage

The sensor's voltage reading and the lux meter reading were taken simultaneously for obtaining the corresponding calibration chart (fig. 4.3) and the equation (Eq. 4.3) was then incorporated into Arduino code and the values obtained were presented in table 4.3.

$$Y=3E-05x-0.0363$$

(Eq. 4.3)

Table 4.3 Lux meter and voltage reading

| Time | Lux meter reading (Lux) | Voltage (V) |
|----------|-------------------------|-------------|
| 12:00 PM | 31820 | 1.744 |
| 12:30 PM | 46540 | 1.334 |
| 1:00 PM | 42430 | 1.503 |
| 2:00 PM | 51637 | 1.695 |
| 2:30 PM | 48590 | 1.346 |
| 3:00 PM | 37960 | 0.817 |
| 3:30 PM | 29040 | 0.705 |
| 4:00 PM | 38720 | 0.993 |
| 4:30 PM | 27760 | 0.845 |
| 5:00 PM | 18790 | 0.263 |
| 5:30 PM | 5224 | 0.155 |
| 6:00 PM | 1719 | 0.055 |

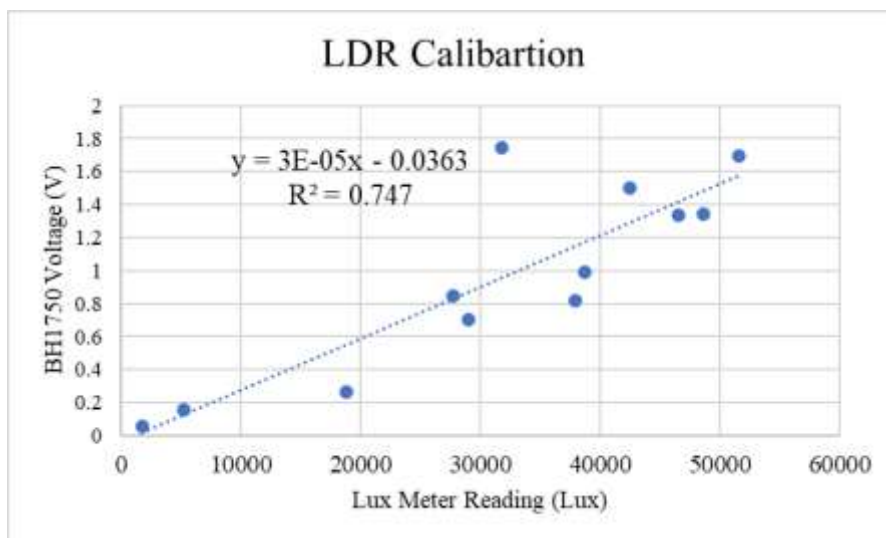


Fig 4.4 Calibration chart for BH1750 voltage vs. lux meter reading

```

    LDR sensor connected to GPIO34 (Analog Input)

const int ldrPin = 34;
void setup() {
    Serial.begin(115200);    // Start Serial Monitor
    analogReadResolution(12); // Set ADC resolution to 12 bits (0–4095)
}
void loop() {
    int ldrValue = analogRead(ldrPin); // Read LDR value
    float voltage = ldrValue * (3.3 / 4095.0); // Convert to voltage
    Serial.print("LDR Raw Value: ");
    Serial.print(ldrValue);
    Serial.print("Voltage:");
    Serial.print(voltage, 2);
    Serial.println("V");
}

```

Fig 4.5 Code used for the light intensity using lux meter reading and voltage

4.1.3.2 Calibration of Lux Meter Reading Vs. Sensor Reading

The sensor reading and the lux meter reading were then taken simultaneously for obtaining the corresponding calibration chart and the equation.

Table 4.4 Lux meter reading and BH1750 sensor reading

| Lux meter reading (Lux) | BH1750 sensor reading (Lux) |
|------------------------------------|--|
| 43.6 | 32.66 |
| 43.7 | 118.6 |
| 44.1 | 219.5 |
| 43.2 | 219.5 |
| 42.6 | 214.64 |

| | |
|------|--------|
| 41.8 | 209.87 |
| 41.2 | 205.78 |
| 38.3 | 191.76 |

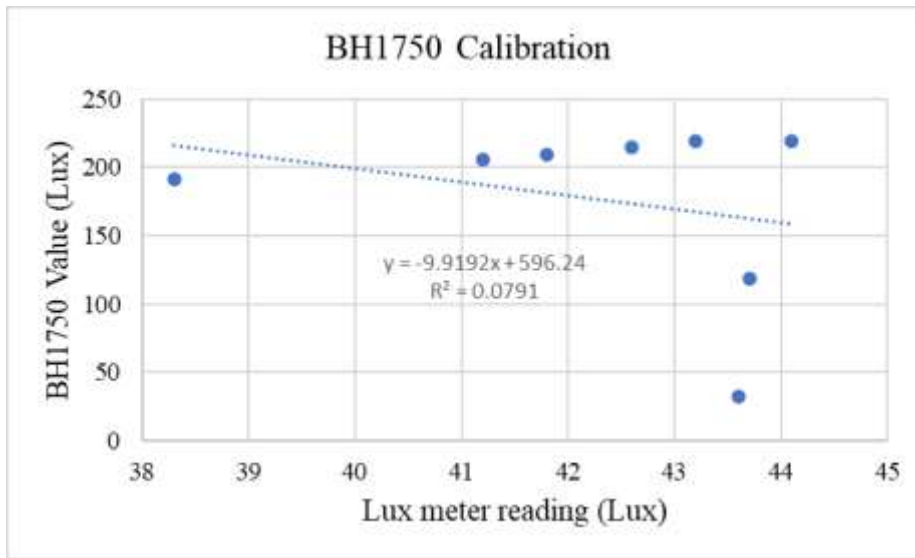


Fig 4.6 Calibration chart of lux meter reading vs. BH1750 sensor reading

4.1.3.3 Lux meter reading and Resistance

The sensor's resistance and the lux meter reading were then taken simultaneously for obtaining the corresponding calibration chart and the equation was incorporated into the code for the accurate reading.

Table 4.5 Lux meter reading and sensor resistance reading

| Lux meter reading (Lux) | Resistance (Kohms) |
|------------------------------------|-------------------------------|
| 5910 | 1.52 |
| 5990 | 1.51 |
| 6070 | 1.48 |
| 6230 | 1.44 |
| 6320 | 1.43 |
| 6260 | 1.43 |
| 6150 | 1.46 |

| | |
|------|------|
| 6180 | 1.44 |
| 6230 | 1.44 |
| 6260 | 1.43 |
| 6240 | 1.44 |
| 6160 | 1.44 |
| 6050 | 1.47 |
| 5970 | 1.47 |
| 5870 | 1.48 |
| 5720 | 1.52 |
| 5690 | 1.56 |
| 5580 | 1.59 |
| 5470 | 1.59 |

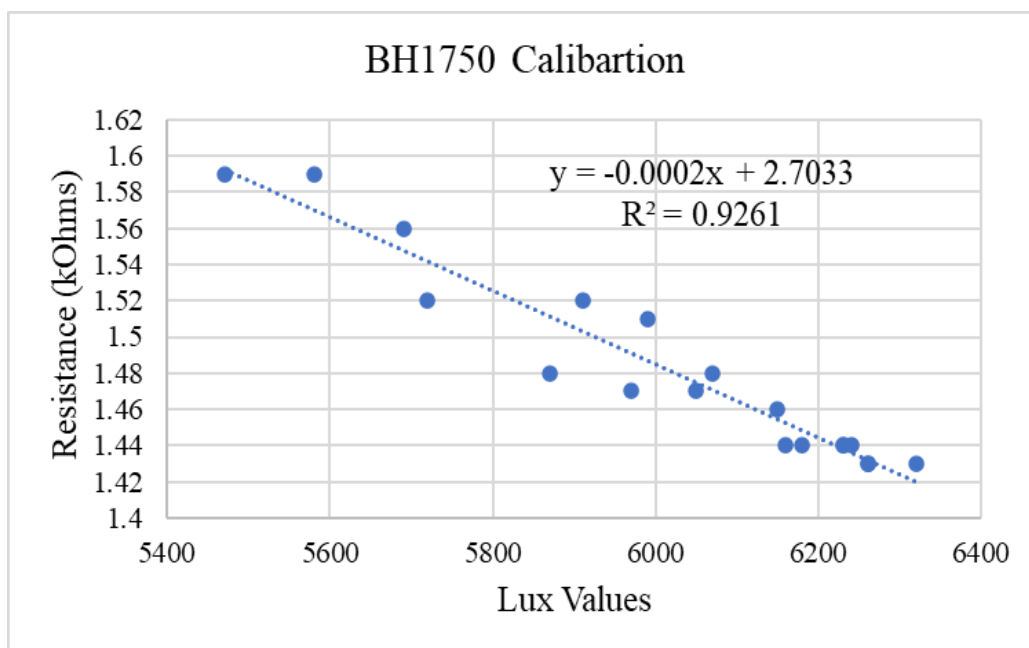


Fig 4.7 Calibration chart for lux meter reading vs. BH1750 sensor's resistance reading

```

// Constants for lux conversion

const float GAMMA = 0.7;    // This gamma value depends on your specific
                             photoresistor

const float RL10 = 30.16;    // Resistance at 10 lux (in kOhms)

void setup() {

    // Initialize serial communication

    Serial.begin(115200);

    Serial.println("Arduino Photoresistor Lux Meter");

    Serial.println("-----");

    delay(1000);

}

void loop() {

    // Read the analog value from photoresistor

    int rawValue = analogRead(PHOTORESISTOR_PIN);

    // Convert analog reading to voltage (0-5V)

    float voltage = rawValue * (5.0 / 1023.0);

    // Using voltage divider principle:  $R_{\text{photoresistor}} = R_{\text{known}} * (V_{\text{cc}}/V_{\text{out}} - 1)$ 

```

Fig 4.8 Code used for the light intensity using lux meter reading and resistance

In the above code, a resistance equation is used to convert the sensor output into lux reading using gamma and RL10 and how to obtain these values from the calibration chart is explained below:

Resistance equation

$$L = 10 * \left(\frac{R_{L10}}{R}\right)^{\frac{1}{\gamma}}$$
$$\left(\frac{L}{10}\right)^{\gamma} = \frac{R_{L10}}{R}$$
$$R = \frac{R_{L10}}{\left(\frac{L}{10}\right)^{\gamma}} = R_{L10} \left(\frac{10}{L}\right)^{\gamma}$$

Where,

R = Resistance of LDR at light intensity L Lux

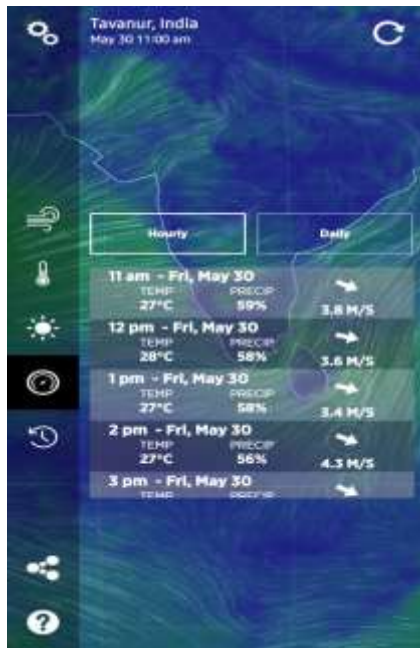
R_{L10} = Resistance at 10 Lux

γ = Slope of log-log curve

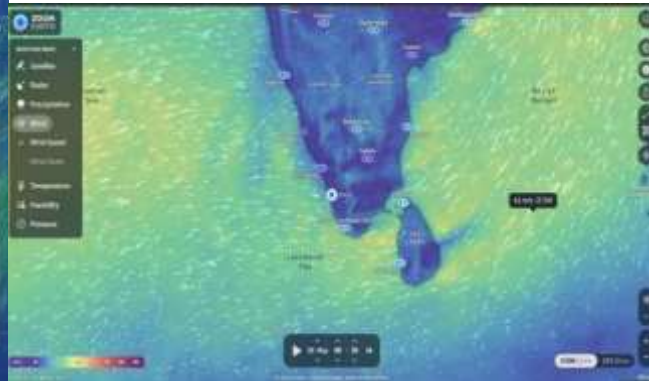
- $\text{Log } R = \text{Log } (R_{L10}) + \gamma \text{Log } (10/L)$
 $= \text{Log } (R_{L10}) + \gamma (\text{Log } (10) - \text{Log } (L))$
- $\text{Log } R = - \gamma \text{Log } L + \text{Constant}$
- $Y = mx + c$, so plot Log R Vs Log L
- Slope of the line $m = - \gamma$
- $C = \text{constant} = \text{Log } R_{L10} + \gamma \text{Log } 10$
- Compute R_{L10}

4.1.4 Results of calibration of wind speed sensor

To ensure accurate wind speed measurements, the anemometer used in this study was calibrated using reference data obtained from reliable weather data applications such as Wind Compass Pro and Zoom Earth. These applications provide real-time wind speed information based on location-specific meteorological data. Simultaneous readings from the anemometer and the weather apps were recorded under similar environmental conditions. The app-based wind speed values served as reference data, which were compared against the anemometer's output. A calibration curve was plotted to analyze the correlation, and a calibration equation was derived to correct any deviations. This improved the precision of wind speed monitoring within the system.



(a)



(b)

Fig 4.9 Weather data apps (a) Wind Compass Pro app (b) Zoom Earth app

The wind speed sensor is giving the output in terms of voltage and the corresponding m/s value can be obtained by referring the data sheet of the sensor (Fig.4.7). Then the readings from the sensor and the app was taken and the calibration chart (Fig.4.8) was drawn to get the relation between these readings to calibrate the sensor.

ROBU.IN

Relation between Speed and output Values:

| Wind Speed | Value | Wind Speed | Value | Wind Speed | Value |
|------------|-------|------------|-------|------------|-------|
| 1 | 0.17 | 11 | 1.83 | 21 | 3.6 |
| 2 | 0.33 | 12 | 2.0 | 22 | 3.67 |
| 3 | 0.5 | 13 | 2.17 | 23 | 3.83 |
| 4 | 0.67 | 14 | 2.33 | 24 | 4.0 |
| 5 | 0.83 | 15 | 2.5 | 25 | 4.17 |
| 6 | 1.0 | 16 | 2.67 | 26 | 4.33 |
| 7 | 1.17 | 17 | 2.83 | 27 | 4.5 |
| 8 | 1.33 | 18 | 3.0 | 28 | 4.67 |
| 9 | 1.5 | 19 | 3.17 | 29 | 4.83 |
| 10 | 1.67 | 20 | 3.33 | 30 | 5.0 |

Fig 4.10 Data Sheet of Wind Speed Sensor

Table 4.6 Readings from wind compass pro app and wind speed sensor

| Time | Wind Speed (m/s) | Wind Speed Sensor (m/s) |
|-------------|-------------------------|------------------------------------|
| 01:00 | 1 | 17.9 |
| 02:00 | 1 | 18.3 |
| 03:00 | 1 | 18.2 |
| 04:00 | 2 | 17.1 |
| 05:00 | 2 | 17 |
| 06:00 | 1 | 18.42 |
| 07:00 | 2 | 18.6 |
| 08:00 | 4 | 17.55 |
| 09:00 | 2 | 18.4 |
| 10:00 | 2 | 18.3 |
| 11:00 | 2 | 23.3 |
| 12:00 | 3 | 16 |
| 13:00 | 3 | 19.9 |
| 14:00 | 3 | 19.4 |
| 15:00 | 3 | 20.2 |
| 16:00 | 3 | 14.8 |
| 17:00 | 3 | 20.5 |
| 18:00 | 2 | 19.9 |
| 19:00 | 2 | 18.6 |
| 20:00 | 1 | 19.6 |
| 21:00 | 2 | 18.8 |

| | | |
|-------|---|------|
| 22:00 | 2 | 17.7 |
| 23:00 | 1 | 17.8 |

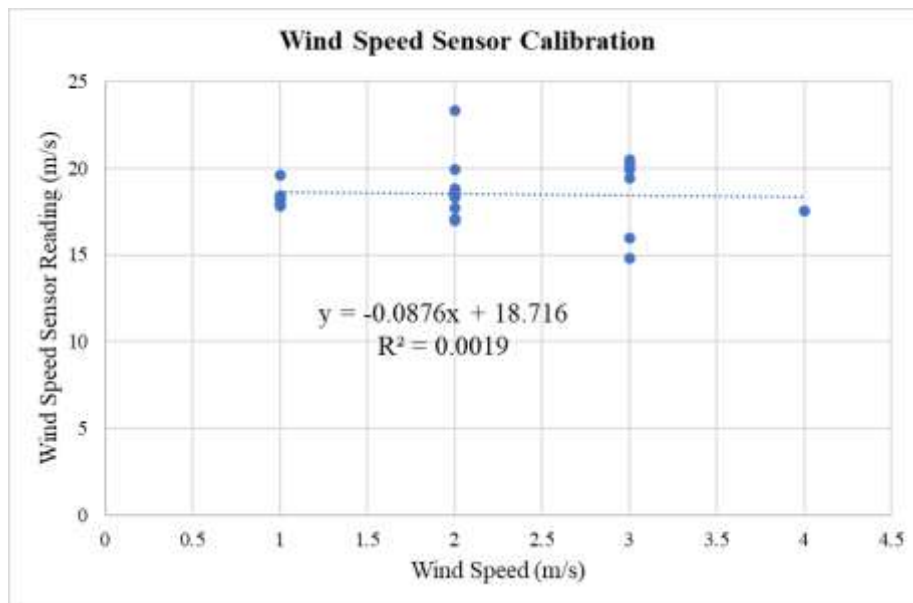


Fig 4.11 Wind Speed Sensor Calibration chart

```

{
  Serial.begin(9600);
}
void loop()
{
  int sensorValue = analogRead(A0);
  float outvoltage = sensorValue * (5.0 / 1023.0);
  Serial.print("outvoltage = ");
  Serial.print(outvoltage);
  Serial.println("V");
  int Level = 6*outvoltage;//The level of wind speed is proportional to the output
voltage.
  Serial.print("wind speed is ");
  Serial.print(Level);
  Serial.println(" level now");
}

```

```

Serial.println();
delay (500);
}

```

Fig 4.12 Code used for wind speed sensor

A reverse code with another set of sensor and app readings was then used to get the accurate sensor reading when the above code didn't give precise values.

Table 4.7 Readings from wind compass pro app and wind speed sensor

| Time | Wind Speed (m/s) | Wind Speed Sensor Reading (m/s) |
|-------------|-----------------------------|--|
| 01:00 | 1 | 12.1 |
| 02:00 | 1 | 11.7 |
| 03:00 | 1 | 11.8 |
| 04:00 | 1 | 11.58 |
| 05:00 | 2 | 11.4 |
| 06:00 | 2 | 11.6 |
| 07:00 | 2 | 11.7 |
| 08:00 | 3 | 10.1 |
| 09:00 | 3 | 10.6 |
| 10:00 | 2 | 11.4 |
| 11:00 | 2 | 11.2 |
| 12:00 | 1 | 12.2 |

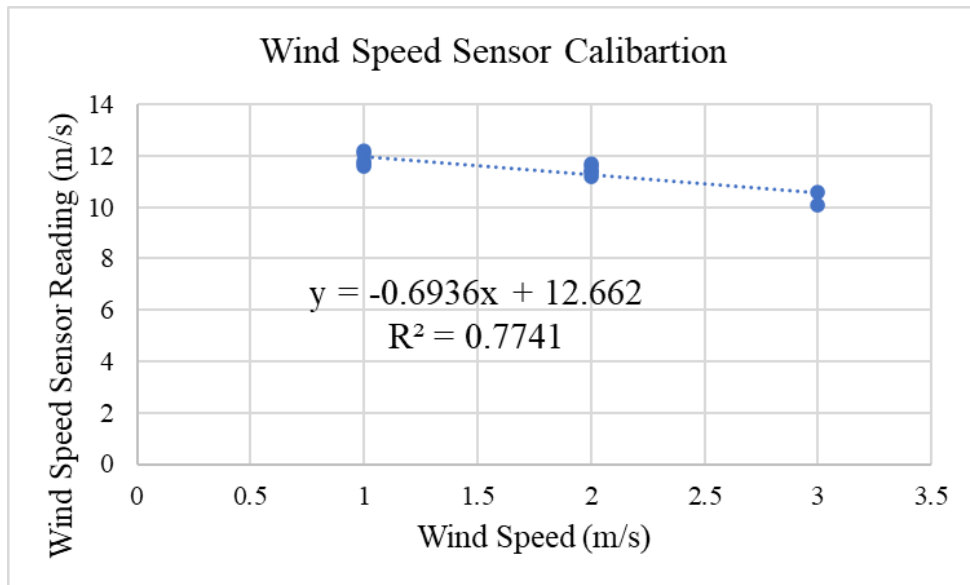


Fig 4.13 Wind Speed Sensor Calibration chart (Inverse code)

```
void setup() {
  Serial.begin(9600);
}

void loop() {
  int sensorValue = analogRead(A0); // Read analog input
  float voltage = sensorValue * (5.0 / 1023.0); // For Arduino UNO
  // Calculate wind speed using datasheet formula
  float windSpeed = voltage / 0.17; // From the datasheet: Speed = Voltage / 0.17
  // Optional: Clamp speed to 0–30 m/s
  if (windSpeed < 0) windSpeed = 0;
  if (windSpeed > 30) windSpeed = 30;
  // Display values
  Serial.print("Voltage: ");
  Serial.print(voltage, 2);
  Serial.print(" V, Wind Speed: ");
  Serial.print(windSpeed, 2);
}
```

```
Serial.println(" m/s");  
delay(500);  
}
```

Fig 4.14 Inverse code used for wind speed sensor

4.1.5 Results from SHT10 Soil temperature sensor

During the testing phase, the soil temperature sensor occasionally displayed negative readings, which were not in consistent with the actual environmental conditions inside the polyhouse. Such values are not acceptable in tropical settings and indicated potential issues in sensor calibration or code interpretation. The data and code used were reviewed, and corrective measures such as sensor rechecking and cross-validation with standard tools were initiated to ensure accurate and reliable temperature readings in future operation. The code used and the obtained data are shown in Fig 4.16 and Fig 4.17.

```
#include<SHT1x.h>  
// Define data and clock pins  
#define dataPin 21  
#define clockPin 22  
// Create an instance of the SHT1x sensor  
SHT1x sht(dataPin, clockPin);  
void setup() {  
  Serial.begin(115200);  
  Serial.println("SHT10 Sensor Reading Test");  
}  
void loop() {  
  float temperature = sht.readTemperatureC();  
  float humidity = sht.readHumidity();  
  Serial.print("Temperature: ");  
  Serial.print(temperature);  
  Serial.println(" °C");  
  Serial.print("Humidity: ");
```

```

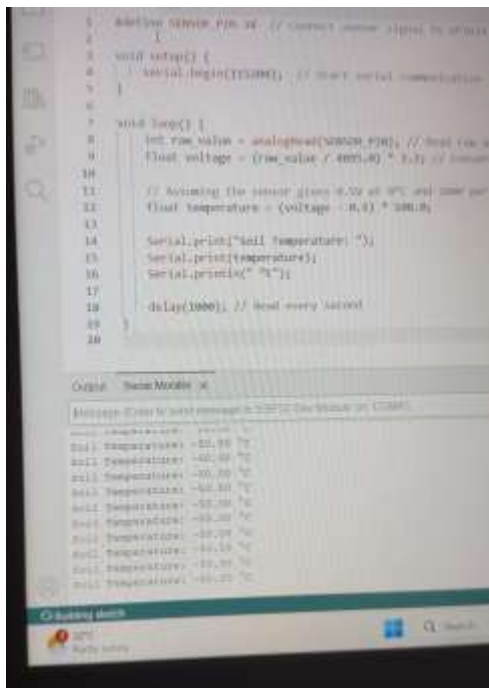
Serial.print(humidity);

Serial.println(" %");

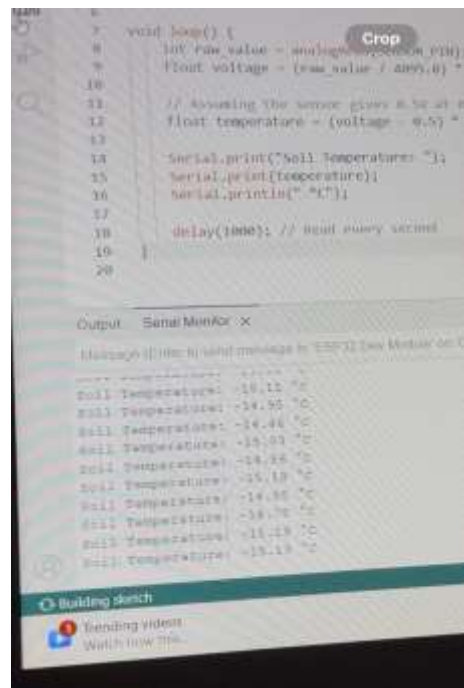
delay(2000); // Wait 2 seconds between readings
}

```

Fig 4.15 Code used for SHT10 Soil temperature sensor



(a)



(b)

Plate 4.1 Readings obtained from soil temperature sensor

4.2 OBTAINED READINGS AND GRAPHS OF TEMPERATURE AND HUMIDITY FROM THINGSPEAK

```
Output Serial Monitor X
Message (Enter to send message to 'NodeMCU-32S' on 'COM8')
Sensor A0 outvoltage = 1.37 V, wind speed = 21.77 m/s
Sensor A1 outvoltage = 1.75 V, wind speed = 10.52 m/s
Sensor A2 outvoltage = 0.00 V, wind speed = 0.00 m/s
Data sent to ThingSpeak.

Sensor A0 outvoltage = 1.79 V, wind speed = 19.25 m/s
Sensor A1 outvoltage = 1.28 V, wind speed = 7.69 m/s
Sensor A2 outvoltage = 0.00 V, wind speed = 0.00 m/s
Data sent to ThingSpeak.

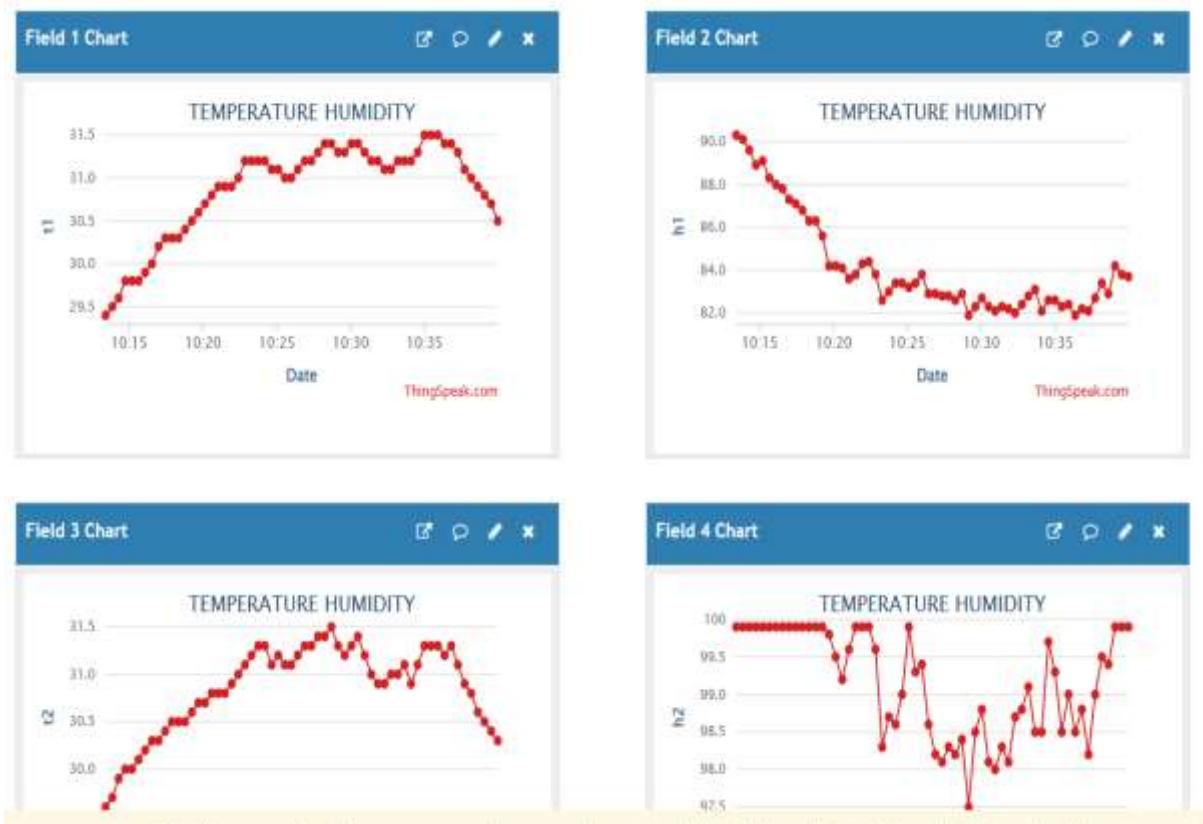
Sensor A0 outvoltage = 1.88 V, wind speed = 18.63 m/s
```

(a)

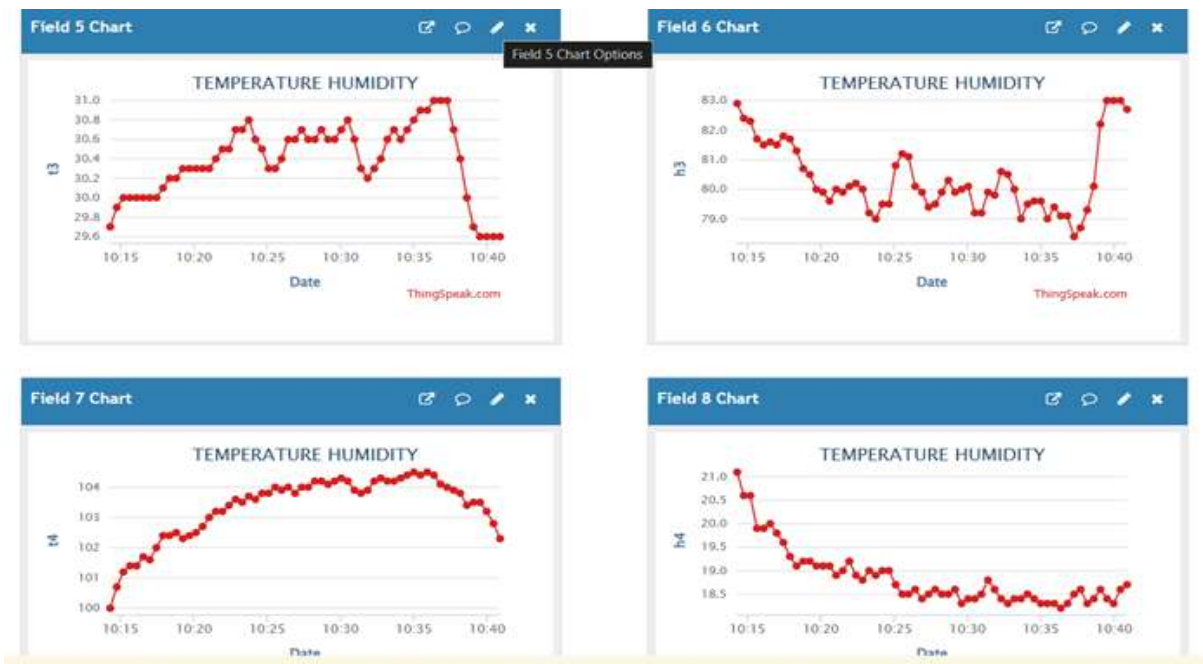
```
Message (Enter to send message to 'NodeMCU-32S' on 'COM8')
DHT1 - Humidity: 91.10%, Temperature: 28.70°C
DHT2 - Humidity: 99.90%, Temperature: 28.70°C
DHT3 - Humidity: 86.00%, Temperature: 28.70°C
DHT4 - Humidity: 21.80%, Temperature: 97.80°C
DHT5 - Humidity: nan%, Temperature: nan°C
DHT6 - Humidity: 90.30%, Temperature: 28.50°C
200
53
200
52
```

(b)

Plate 4.2 Sensor readings (a) Wind speed reading (b) Temperature-humidity reading



(a)



(b)



(c)

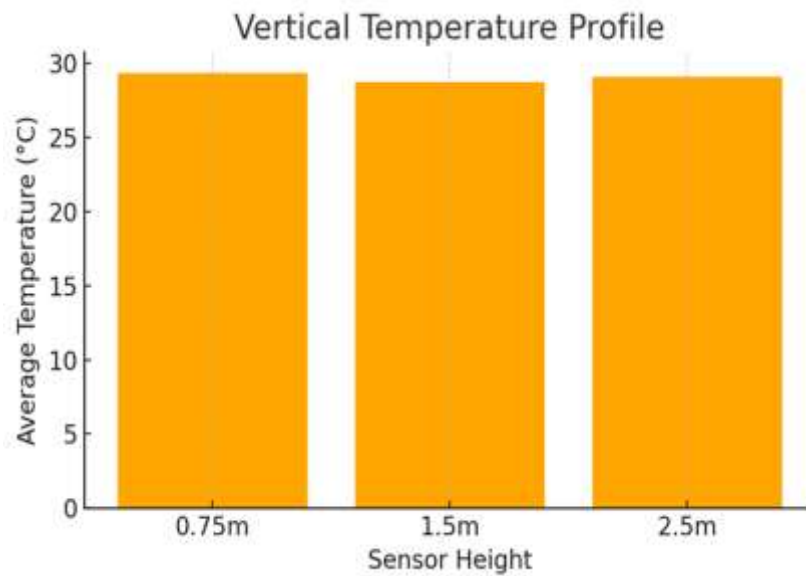
Fig.4.16 (a), (b) and (c) Obtained results of temperature and humidity from different poles

4.3 VERTICAL MICROCLIMATE VARIATION (HEIGHT-WISE COMPARISON)

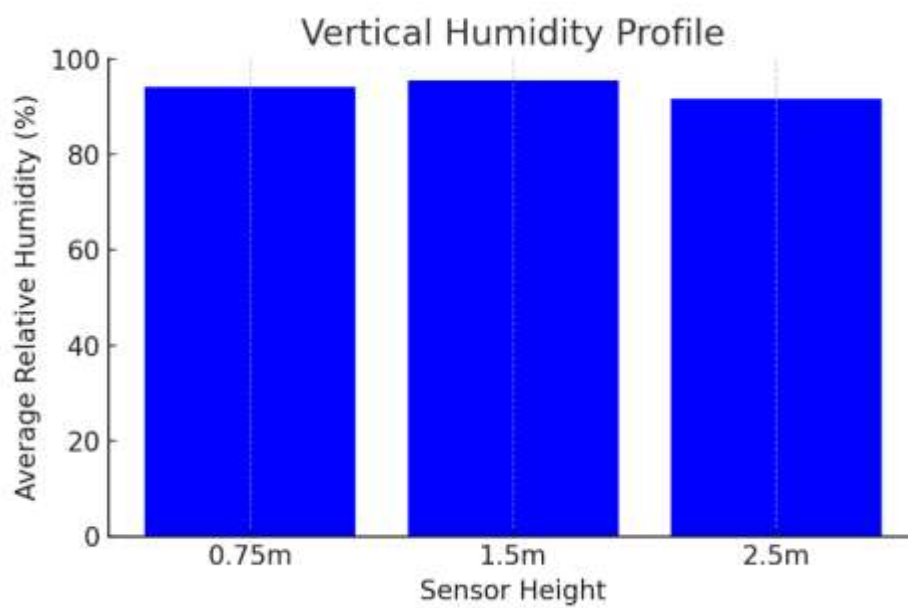
4.3.1 Temperature Gradient with Height

- During rainy days, temperature remains lower and more uniform, while humidity increases and stays consistently high throughout the polyhouse height.

| Relative Humidity (%) | Temperature (°C) |
|-----------------------|-----------------------|
| 0.75 m (H1): 94.06% | 0.75 m (T1): 29.34 °C |
| 1.5 m (H2): 95.37% | 1.5 m (T2): 28.76 °C |
| 2.5 m (H3): 91.65% | 2.5 m (T3): 29.10 °C |



(a)



(b)

Fig 4.17 Vertical variation (a) Temperature Profile (b) Humidity Profile

Reasons:

- **Reduced Temperature Gradient**
- Cloud cover and rainfall reduce incoming solar radiation

- As a result, less heat accumulates inside the polyhouse, especially at the top
- Temperature becomes more uniform across different heights
- The absence of strong sunlight reduces thermal convection, so the air is more evenly mixed

➤ **Increased and Uniform Humidity**

- External humidity increases significantly during rainfall
- Moisture enters the polyhouse through openings, ventilation, or seepage
- Relative humidity becomes high throughout the structure, not just near the ground
- The vertical difference in humidity levels diminishes

4.3.2 Time-Based Analysis – Rainy Day Conditions

- **Early Morning (00:00 – 06:00 hrs)**
 - a. Low temperature, relatively stable
 - b. High humidity, often nearing saturation (close to 100%)
- **Morning (06:00 – 12:00 hrs)**
 - a. Slight increase in temperature due to gradual light penetration
 - b. Humidity remains high, with little fluctuation
- **Afternoon (12:00 – 15:00 hrs)**
 - a. Temperature remains moderate, without sharp peaks due to cloud cover
 - b. Short sunny breaks may cause brief temperature spikes
 - c. Humidity slightly decreases, but stays relatively high
- **Evening (15:00 – 18:00 hrs)**
 - a. Temperature begins to decline steadily
 - b. Humidity starts increasing again as air cools

- **Night (18:00 – 24:00 hrs)**
 - a. Temperature stabilizes at lower levels
 - b. Humidity reaches peak levels, often close to saturation

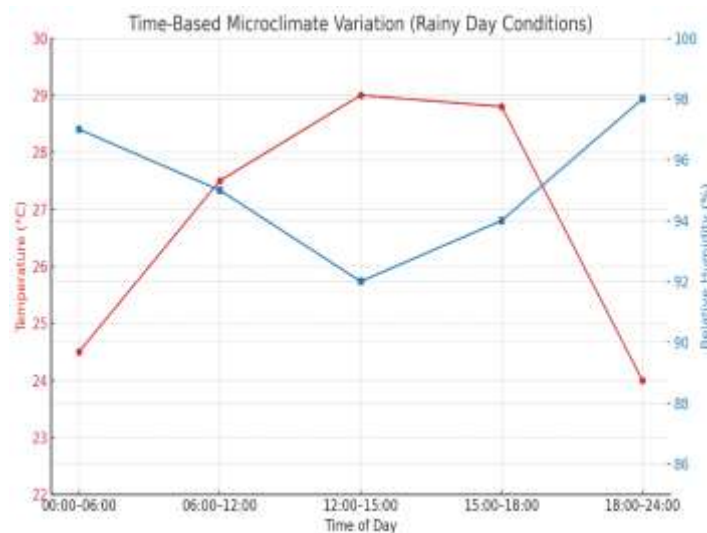


Fig 4.18 Time based microclimate variation

4.3.3 Temperature-Humidity Relationship (Combined Analysis)

Observed Correlation

- An inverse relationship was observed between temperature and relative humidity at all measured heights and times.
- As internal temperature increased, relative humidity decreased, which reflects the non-linear saturation capacity of warmer air.

4.4 CHALLENGES FACED DURING THE INSTALLATION OF DIFFERENT COMPONENTS IN POLYHOUSE

The different components that we used in polyhouse are Light intensity sensor, Temperature-Humidity sensor, Soil temperature sensor, Anemometer and Microcontroller. So, the challenges that we faced during installation of these are:

Table 4.8 Challenges Faced During the Installation of Different Components in Polyhouse

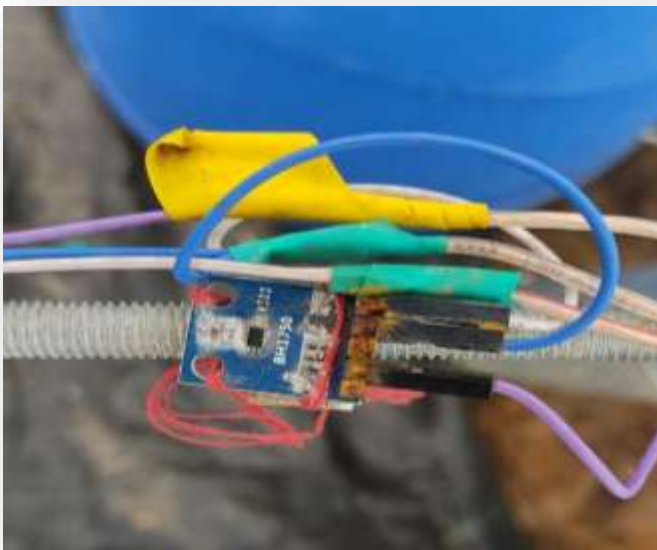
| Name of Sensors | Challenges Faced | Resolutions |
|---|--|--|
| Light intensity Sensor (GY-302 BH1750, Photoreceptor) (32 no) | Coding related problem | Depend on various AI tools for the appropriate code |
| | Unsoldered Sensor | Manual soldering |
| | Not getting reading in Lux | Used a code which converts ADC value into lux |
| | Large variation between Sensor and Lux meter reading | Calibration |
| | Calibration (Same reading after 3.3V) | Nil |
| | High intensity readings | Nil |
| | Readings are not getting (Showing as Overflow Lux) | Contacted resource persons |
| | Some of the Sensors are not at all working | Contacted resource persons |
| | Angle sensitivity | Nil |
| | Non linearity in response to light | Tried in various light intensities but the problem is not solved |
| | Shown a fixed range of 0-4095 lux | Purchased photoreceptor with 10Kohm resistor |

| | | |
|--|---|---|
| Soil Temperature Sensor (SHT10) (4 no) | Faulty Sensors | Approached the resource person but only 1 sensor is corrected |
| | Measurement of air temperature instead of soil temperature when buried not properly | Installed the sensor at proper depth |
| | Fixing of correct voltage supply | Purchased 5V adopter |
| | Not getting the appropriate code | Depend on various AI tools |
| Anemometer (3 no) | Low precision (0.4 -0.8 m/s) | Nil |
| | No sufficient wind velocity inside polyhouse to be detected by the anemometer | Nil |
| Temperature - Humidity sensor (DHT 22) (32 no) | Coding of multiple sensors was difficult | Depend on AI tools for getting code for multiple sensors |
| Microcontroller (Node MCU ESP32-S) (5 no) | Not compatible with Soil temperature sensor | Used ESP32 DEVKIT V1 microcontroller |
| | Among the 5, one is faulty | Nil |

4.4.1 General challenges:

- Using many sensors in a single system increases code complexity, makes fault detection harder, and complicates data collection and management

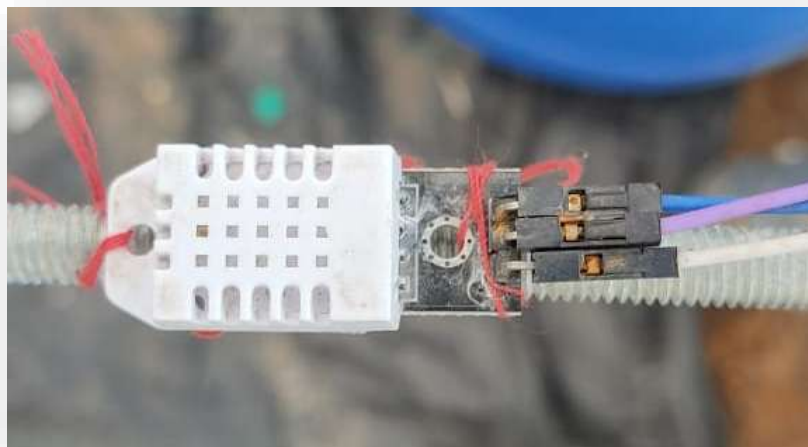
- Water leakage in the polyhouse caused sensor rusting
- Connecting sensors to the microcontroller took a lot of time
- JioFi modem battery lasted only 2 hours, so we added a relay for auto-charging
- ThingSpeak stores only 1 week of data, so we had to download it every week
- ThingSpeak allows only 4 channels and 8 sensors per channel, which was limiting
- Installing many sensors during the day was difficult due to heat
- Loose wire connections caused data issues so connected it properly
- Installing sensors outside the polyhouse needs extra care to protect them from rain and other environmental hazards
- Wiring the anemometer outside the polyhouse was challenging due to its distance from the power source
- Outside placed sensors are melted due to intense sunlight and didn't read the value
- Jumper wires are rusted within a short period of time
- Delay in receiving sensors affected the timeline
- Sensors were very sensitive and needed careful handling



(a)



(b)



(c)

Plate.4.3 Sensor damages (a) Rusty light intensity sensor (b) & (c) melted and rusty temperature -humidity sensor respectively

SUMMARY & CONCLUSION

CHAPTER V

SUMMARY AND CONCLUSION

The project titled “Real Time Monitoring of Microclimatic Parameters Inside Polyhouse Using IoT Embedded Sensor Systems” was undertaken with the objective of developing a functional, low-cost IoT-based solution for continuous monitoring of essential microclimatic parameters within a naturally ventilated polyhouse. The study conducted at the Department of Soil and Water Conservation Engineering, KCAEFT, Tavanur, spanned from January to May 2025 and focused on parameters such as air temperature, relative humidity, light intensity, soil temperature, and wind velocity each playing a vital role in influencing crop growth and physiological responses in protected cultivation environments.

An ESP32 microcontroller served as the core processing unit of the system, integrated with a suite of digital and analog sensors: DHT22 for temperature and humidity, BH1750 for light intensity, a thermistor-based probe for soil temperature, and a low-cost cup-type anemometer for wind velocity. The data was transmitted wirelessly in real time to the ThingSpeak cloud platform, enabling remote access, visualization, and storage.

During the calibration and testing phase, the BH1750 light sensor readings were compared against a standard lux meter. A calibration equation was derived from the plotted values, resulting in a high coefficient of determination ($R^2 = 0.986$), which indicates a strong correlation between sensor output and reference readings. This validated the light sensor’s potential for application in greenhouse environments under ideal conditions.

It was observed, however, that some of the low-cost sensors (specifically for wind velocity, light intensity, and soil temperature) exhibited limited precision under certain environmental conditions. This was attributed to factors such as sensor range constraints, mechanical sensitivity, and non-linear response at extreme values. While these sensors provided useful trend data, there is scope for enhancing system accuracy through the integration of more advanced, industrial-grade sensors in future applications.

Despite these limitations, the system effectively demonstrated diurnal trends in microclimatic variation. Temperature consistently increased from morning to noon, followed by a gradual decrease, while relative humidity displayed an inverse pattern. Soil temperature inside the polyhouse was slightly elevated compared to external soil, indicating the buffering effect of the polyhouse microclimate. Wind speed fluctuations were captured, albeit with some response delay due to the sensor's mechanical inertia.

The project successfully achieved its core objectives: the development, deployment, and real-time operation of a microcontroller-based embedded sensor system tailored for microclimatic monitoring in a greenhouse setting. The real-time data collection and remote access capabilities offered by the ESP32 and ThingSpeak integration make this system a scalable and cost-efficient alternative for small and medium-scale farmers practicing protected cultivation.

While the system performance was largely satisfactory, it also highlighted the importance of sensor calibration, environmental shielding, and periodic validation to ensure data reliability - especially in highly sensitive parameters such as soil temperature and wind speed. The trends observed across the monitored parameters underscore the dynamic nature of polyhouse microclimates, and the potential for using such data to guide decisions on ventilation, shading, irrigation, and fertigation.

In summary, this project lays a strong foundation for smart greenhouse monitoring systems using embedded IoT technology. It demonstrates how low-cost hardware, when combined with cloud-based platforms and practical engineering design, can empower modern agriculture with data-driven microclimate management tools.

5.1 SUGGESTIONS AND RECOMMENDATIONS

5.1.1 Future scopes

➤ **CO₂ Sensor Integration**

Incorporating CO₂ sensors will provide critical insights into the carbon dioxide levels within the polyhouse, enabling better control of plant respiration and growth.

➤ **Automated Controllers for Optimization**

The next phase should include the integration of smart controllers (e.g., for ventilation, irrigation, shading, and misting systems) that automatically adjust conditions based on real-time sensor data, thereby optimizing microclimatic factors for improved crop yield and health.

➤ **Machine Learning for Predictive Analysis**

Future systems can leverage machine learning algorithms to predict environmental changes and optimize responses accordingly, making the system more intelligent and adaptive.

➤ **Energy Efficiency and Renewable Integration**

The system can be enhanced by incorporating solar panels and energy-efficient devices to reduce operational costs and support sustainable farming practices.

5.1.2 Recommendations

➤ **Modular Sensor Architecture**

Adopt a modular and scalable sensor network that allows easy addition or removal of sensors without overcomplicating the system.

➤ **Wireless Communication Protocols**

Use efficient communication protocols like LoRa, Zigbee, or MQTT for reliable and long-range data transmission with minimal power consumption.

➤ **Data Logging and Analytics**

Implement continuous data logging and analytics for long-term tracking of environmental trends, which can help in making data-driven decisions.



Plate 5.1 Project Team

REFERENCE

CHAPTER VI

REFERENCES

- Ahamed, M.S., Guo, H. & Tanino, K. 2019, 'Energy saving techniques for reducing the heating cost of conventional greenhouses', *Biosyst. Eng.*, vol. 178, pp. 9–33.
- Aiello, G., Giovino, I., Vallone, M., Catania, P. & Argento, A. 2018, 'A decision support system based on multisensor data fusion for sustainable greenhouse management', *J. Clean. Prod.*, vol. 172, pp. 4057–4065.
- Aikman, D.P., 1996. A procedure for optimizing carbon dioxide enrichment of a glasshouse tomato crop. *J. Agric. Eng. Res.* 63, 171–184.
- Akpenpuun, T. D., Ogunlowo, Q. O., Na, W-H., Rabiou, A., Adesanya, M. A., Dutta, P., Zakir, E., Ogundele, O. M., Kim, H-T, and Lee, H-W. "Review of Temperature Management Strategies and Techniques in the Greenhouse Microenvironment." Adeleke University *J. of Engg. and Technology* 6, no. 2 (2023): 126-147. <https://www.aujet.adelekeuniversity.edu.ng>.
- Albright, L.D. 1990. Environment control for animals and plants. ASAE, St. Joseph, MI, USA. 453 pp.
- Allen Jr., L.H., Amthor, J.S., 1995. Plant physiological responses to elevated CO₂, temperature, air pollution, and UV-B radiation. In: Woodwell, G.M., Mackenzie, F.T. (Eds.), *Biotic Feedbacks in the Global Climatic System: Will the Warming Feed the Warming?* Oxford Univ. Press, Oxford, New York, pp. 51–84
- Aqeel-Ur-Rehman, Abbasi, A.Z., Islam, N. & Shaikh, Z.A. 2014, 'A review of wireless sensors and networks' applications in agriculture', *Comput. Stand. Interfaces*, vol. 36, no. 2, pp. 263–270.

- Bailey, B.J. 2002. Control and monitoring of glasshouses. Proceedings of the UK Controlled Environment Users' Group. Vol. 13, 2-5.
- Bao, J., Lu, W.-H., Zhao, J. & Bi, X.T. 2018, 'Greenhouses for CO₂ sequestration from atmosphere', *Carbon Resour. Convers.*, vol. 1, no. 2, pp. 183–190.
- Barnes, C., Tibbitts, T., Sager, J., Deitzer, G., Bubenheim, D., Koerner, G. and Bugbee, B. (1993) 'Accuracy of quantum sensors measuring yield photon flux and photosynthetic photon flux', *HortScience*, 28(12), pp. 1197–1200.
- Basak, J.K., Qasim, W., Okyere, F.G., Khan, F., Lee, J., Park, J. & Kim, H.T. 2019, 'Regression analysis to estimate morphology parameters of pepper plant in a controlled greenhouse system', *J. Biosyst. Eng.*, vol. 44, no. 2, pp. 57–68.
- Bezari, S., Metidji, N., Lebbi, M., Merabti, S., Tearnbucha, C., Sudsutad, W., Lorenzini, G., Ahmad, H., & Menni, Y. (2022). Investigation and analysis of soil temperature under solar greenhouse conditions in a semi-arid region. *International Journal of Design & Nature and Ecodynamics*, 17(3), 325–332.
- Bhujel, A., Basak, J.K., Khan, F., Arulmozhi, E., Jaihuni, M., Sihalath, T., Lee, D., Park, J. & Kim, H.T. 2020, 'Sensor systems for greenhouse microclimate monitoring and control: a review', *J. Biosyst. Eng.*, vol. 45, pp. 341–361.
- Bogena, H.R., Huisman, J.A., Oberdörster, C. & Vereecken, H. 2007, 'Evaluation of a low-cost soil water content sensor for wireless network applications', *J. Hydrol.*, vol. 344, no. 1–2, pp. 32–42.
- Bonachela, S., González, A.M. & Fernández, M.D. 2006, 'Irrigation scheduling of plastic greenhouse vegetable crops based on historical weather data', *Irrig. Sci.*, vol. 25, no. 1, pp. 53–62.

- Campen, J.B. and Bot, G.P.A. (2003) 'Determination of greenhouse-specific aspects of ventilation using three-dimensional computational fluid dynamics', *Biosystems Engineering*, 84(1), pp. 69-77.
- Ceulemans, R., Taylor, G., Bosac, C., Wilkins, D., Besford, R.T., 1997. Photosynthetic acclimation to elevated CO₂ in poplar grown in glasshouse cabinets or in open top chambers depends on duration of exposure. *J. Exp. Bot.* 48 (314), 1681–1689
- Chen S, Liu A, Tang F, Hou P, Lu Y, Yuan P. A Review of Environmental Control Strategies and Models for Modern Agricultural Greenhouses. *Sensors*. 2025; 25(5):1388. <https://doi.org/10.3390/s25051388>
- Chen, C., Shen, T. and Weng, Y. (2011) 'Simple model to study the effect of temperature on the greenhouse with shading nets', *African Journal of Biotechnology*, 10(25), pp. 5001-5014.
- Chen, S. (2010). Greenhouse environmental monitoring system with IPSO and BPNN. *Computer Measurement & Control*, 18(3), 601-604. <https://doi.org/10.16526/j.cnki.11-4762/tp.2010.03.063>, 610.
- Choab, N., Allouhi, A., El Maakoul, A., Kousksou, T., Saadeddine, S. and Jamil, A., 2019. Review on greenhouse microclimate and application: Design parameters, thermal modelling and simulation, climate controlling technologies. *Solar Energy*, 191, pp.109-137.
- Datta, S., Taghvaeian, S., Ochsner, T.E., Moriasi, D., Gowda, P. & Steiner, J.L. 2018, 'Performance assessment of five different soil moisture sensors under irrigated field conditions in Oklahoma', *Sensors (Switzerland)*, vol. 18, no. 11, pp. 1–17.

- Ferentinos, K.P., Katsoulas, N., Tzounis, A., Bartzanas, T. & Kittas, C. 2017, 'Wireless sensor networks for greenhouse climate and plant condition assessment', *Biosyst. Eng.*, vol. 153, pp. 70–81.
- Franco, A., Valera, D. L. and Peña, A. (2014). Energy efficiency in greenhouse evaporative cooling techniques: cooling boxes versus cellulose pads. *Energies*, 7(3), 1427-1447.
- Frausto, H.U., Pieters, J.G. and Deltour, J.M. (2003) 'Modelling greenhouse temperature by means of auto regressive models', *Biosystems Engineering*, 84(2), pp. 147-157.
- Garg, A., Munoth, P. & Goyal, R. 2016, 'Application of soil moisture sensors in agriculture: a review', *Proc. Int. Conf. Hydraul. Water Resour. Coast. Eng. (Hydro2016)*, CWPRS, Pune, India, pp. 1662–1672.
- Gislerød, H.R., Eidsten, I.M. and Mortensen, L.M. (1989) 'The interaction of daily lighting period and light intensity on growth of some greenhouse plants', *Sci. Hortic.*, 38(3–4), pp. 295–304.
- Grimstad, S.O. and Frimanslund, E. (1993) 'Effect of different day and night temperature regimes on greenhouse cucumber young plant production, flower bud formation and early yield', *Scientia horticultrae*, 53(3), pp. 191-204.
- Gupta, D., Santosh, D.T. and Debnath, S., 2020. Modelling and simulation application for greenhouse microclimatic studies and structural analysis. *Protected Cultivation and Smart Agriculture; Maitra, S., Gaikwad, DJ, Shankar, T., Eds*, pp.300-312.

- Guzmán, C.H., Carrera, J.L., Durán, H.A., Berumen, J., Ortiz, A.A. & Guirette, O.A. 2019, 'Implementation of virtual sensors for monitoring temperature in greenhouses using CFD and control', *Sensors*, vol. 19, no. 1, p. 60.
- Hand, D.W., 1984. Crop responses to winter and summer CO₂ enrichment. *Acta Hortic.* 162, 45–63.
- Hand, D.W., Warren Wilson, J., Acock, B., 1993. Effects of light and CO₂ on net photosynthetic rates of stands of aubergine and amaranthus. *Ann. Bot.* 71, 209–216.
- Hegazy, A., Farid, M., Subiantoro, A. and Norris, S. (2022). Sustainable cooling strategies to minimize water consumption in a greenhouse in a hot arid region. *Agricultural Water Management*, 274, 107960.
- Henderson, S., Gholami, D. & Zheng, Y. 2018, 'Soil moisture sensor-based systems are suitable for monitoring and controlling irrigation of greenhouse crops', *HortScience*, vol. 53, no. 4, pp. 552–559.
- Hur, D.J., Noh, J.H., Lee, H.J. and Song, H.W. (2018) 'Evaluation of stress distribution with wind speed in a greenhouse structure', *Wind Struct*, 27(5), pp. 347-356.
- Ihoume, I., Tadili, R., Arbaoui, N. and Krabch, H. (2023). Design of a low-cost active and sustainable autonomous system for heating agricultural greenhouses: A case study on strawberry (*fragaria vulgaris*) growth. *Heliyon*, 9(3).
- Jackson, R.D., Idso, S.B., Reginato, R.J., Pinter, P.J. 1981. Canopy temperature as crop water stress indicator. *Water Res. Res.*, 17: 1133-1138.
- Jaliyagoda, N., Lokuge, S., Gunathilake, P. M. P. C., Amaratunga, K. S. P., Weerakkody, W. A. P., Bandaranayake, P. C. G. and Bandaranayake, A. U.

- (2023). Internet of things (IoT) for smart agriculture: Assembling and assessment of a low-cost IoT system for polytunnels. PLoS ONE, 18(5).
- Jiao, Y., Chen, C., Li, G., Fu, H., & Mi, X. (2024). Research on the variation patterns and predictive models of soil temperature in a solar greenhouse. Solar Energy, 270, 112267.
- Jin, C. W., Du, S. T., Wang, Y., Condon, J., Lin, X. Y., & Zhang, Y. S. (2009). Carbon dioxide enrichment by composting in greenhouses and its effect on vegetable production. Journal of Plant Nutrition and Soil Science-Zeitschrift Fur Pflanzenernahrung Und Bodenkunde, 172(3), 418-424. <https://doi.org/10.1002/jpln.200700220>.
- Kaiser, E., Ouzounis, T., Giday, H., Schipper, R., Heuvelink, E. & Marcelis, L.F.M. 2019, 'Adding blue to red supplemental light increases biomass and yield of greenhouse-grown tomatoes, but only to an optimum', *Front. Plant Sci.*, vol. 9, no. January, pp. 1–11.
- Khot, S.B. and Gaikwad, M.S. (2016) 'Development of cloud-based light intensity monitoring system for greenhouse using Raspberry Pi'. In 2016 Int. Conf. Comput. Commun. Control Autom. (ICCUBE), pp. 1–4. IEEE.
- Kittas, C., Karamanis, M. & Katsoulas, N. 2005. Air temperature regime in a forced ventilated greenhouse with rose crop. Energy & Buildings, 37(8): 807–812.
- Kocourek, F., Havelka, J., Berankova, J. and Jarošík, V. (1994) 'Effect of temperature on development rate and intrinsic rate of increase of *Aphis gossypii* reared on greenhouse cucumbers', *Entomologia experimentalis et applicata*, 71(1), pp. 59-64.

- Labs, S. 2013, *The evolution of wireless sensor networks*, Version 1.0, Silicon Labs, pp. 1–5.
- Li, H., Li, A., Zhang, L., Hou, Y., Yang, C., Chen, L. and Lu, N. (2023) 'Estimation of wind speed based on Schlieren machine vision system Inspired by greenhouse top vent', *Sensors*, 23(15), p. 6929.
- Li, T. & Yang, Q. 2015, 'Advantages of diffuse light for horticultural production and perspectives for further research', *Front. Plant Sci.*, vol. 6, no. September, pp. 1–5.
- Liang-Ying, Guo, Y.F. & Zhao-Wei. 2015, 'Greenhouse environment monitoring system design based on WSN and GPRS networks', *2015 IEEE Int. Conf. Cyber Technol. Autom. Control Intell. Syst. (IEEE-CYBER 2015)*, China: Shenyang, pp. 795–798.
- Mahesh Chand Singh, J.P. Singh, Sandeep Kumar Pandey, Nikhil Gladwin Cutting, Pankaj Sharma, Varun Shrivastav and Puneet Sharma. 2018. A Review of Three Commonly Used Techniques of Controlling Greenhouse Microclimate. *Int.J.Curr.Microbiol.App.Sci.* 7(01): 3491-3505. doi:<https://doi.org/10.20546/ijcmas.2018.701.411>
- Mahrer, Y. and Avissar, R., 1984. A numerical simulation of the greenhouse microclimate. *Mathematics and computers in simulation*, 26(3), pp.218-228.
- Mainetti, L., Patrono, L. & Vilei, A. 2011, 'Evolution of wireless sensor networks towards the Internet of Things: a survey', *SoftCOM 2011, 19th Int. Conf. Softw. Telecommun. Comput. Netw.*, Split, Croatia, pp. 1–6.
- Majdoubi, H., Boulard, T., Fatnassi, H. and Bouirden, L. (2009) 'Airflow and microclimate patterns in a one-hectare Canary type greenhouse: An

- experimental and CFD assisted study', *Agricultural and Forest Meteorology*, 149(6-7), pp. 1050-1062.
- Marcelis, L.F.M., Broekhuijsen, A.G.M., Meinen, E., Nijs, E.M.F.M. and Raaphorst, M.G.M. (2005) 'Quantification of the growth response to light quantity of greenhouse-grown crops'. In *V Int. Symp. Artif. Light. Hortic.*, 711, pp. 97–104.
- McCree, K.J. (1971) 'The action spectrum, absorptance and quantum yield of photosynthesis in crop plants', *Agric. Meteorol.*, 9, pp. 191–216.
- Mohagheghi, A. and Moallem, M. (2023) 'An energy-efficient PAR-based horticultural lighting system for greenhouse cultivation of lettuce', *IEEE Access*, 11, pp. 8834–8844.
- Mortensen, L.M. and Strømme, E. (1987) 'Effects of light quality on some greenhouse crops', *Sci. Hortic.*, 33(1–2), pp. 27–36.
- Mosharafian, S., Afzali, S., Weaver, G.M., van Iersel, M. and Velni, J.M. (2021) 'Optimal lighting control in greenhouse by incorporating sunlight prediction', *Comput. Electron. Agric.*, 188, p. 106300.
- Mukazhanov, Y., Kamshat, Z., Assel, O., Shayhmetov, N. & Alimbaev, C. 2017, 'Microclimate control in greenhouses', *Int. Multidiscip. Sci. GeoConf. Surv. Geol. Min. Ecol. Manag. (SGEM)*, vol. 17, no. 62, pp. 699–704.
- Muñoz, M., Guzmán, J.L., Sánchez, J.A., Rodríguez, F. & Torres, M. 2019, 'Greenhouse models as a service (GMaaS) for simulation and control', *IFAC-PapersOnLine*, vol. 52, no. 30, pp. 190–195.

- Myster, J. and Moe, R. (1995) 'Effect of diurnal temperature alternations on plant morphology in some greenhouse crops—a mini review', *Scientia Horticulturae*, 62(4), pp. 205-215.
- Nederhoff, E.M., Vegter, J.G., 1994. Photosynthesis of stands of tomato, cucumber and sweet pepper measured in greenhouses under various CO₂ concentrations. *Ann. Bot.* 73, 353–361.
- Neethirajan, S., Jayas, D.S. & Sadistap, S. 2009, 'Carbon dioxide (CO₂) sensors for the agri-food industry-a review', *Food Bioprocess Technol.*, vol. 2, no. 2, pp. 115–121.
- Nelson, P.V. 2003, *Greenhouse operation and management*, Prentice Hall, Upper Saddle River, NJ.
- Ohyama, K., Kozai, T., Toida, H., 2008. Greenhouse cooling with continuous generation of upward-moving fog for reducing wetting of plant foliage and air temperature fluctuations: a case study. *Acta Hortic.* 797, 321–326
- Olle, M. and Viršile, A. (2013) 'The effects of light-emitting diode lighting on greenhouse plant growth and quality', *Agric. Food Sci.*, 22(2), pp. 223–234.
- Onwuka, B., & Mang, B. (2018). Effects of soil temperature on some soil properties and plant growth. *Advances in Plants & Agriculture Research*, 8(1), 34–37.
- Othmane, F., Shu, M. A. F. L., Leandros, M. and Xiaochan, W. (2021). Internet of Things for the Future of Smart Agriculture: A Comprehensive Survey of Emerging Technologies. *IEEE/CAA J. Autom. Sinica*, 8(4), 718-752.
- Panwar, N. L., Kaushik, S. C., & Kothari, S. (2011). Solargreenhouse an option for renewable and sustainable farming. *Renewable and Sustainable Energy Reviews*, 15(8), 3934e3945. <https://doi.org/10.1016/j.rser.2011.07.030>.

- Panwar, N.L., Kaushik, S.C. & Kothari, S. 2011, 'Solar greenhouse an option for renewable and sustainable farming', *Renew. Sustain. Energy Rev.*, vol. 15, no. 8, pp. 3934–3945.
- Pawlowski, A., Sanchez, J.A., Guzman, J.L., Rodriguez, F., Berenguel, M. & Dormido, S. 2016, 'Event-based control for a greenhouse irrigation system', *2016 2nd Int. Conf. Event-Based Control, Commun. Signal Process. (EBCCSP 2016) - Proc.*, Krakow, Poland.
- Rodríguez, S., Gualotuña, T. & Grilo, C. 2017, 'A system for the monitoring and predicting of data in precision agriculture in a rose greenhouse based on wireless sensor networks', *Procedia Comput. Sci.*, vol. 121, pp. 306–313.
- Rong, L., Liu, D., Pedersen, E.F. and Zhang, G. (2015) 'The effect of wind speed and direction and surrounding maize on hybrid ventilation in a dairy cow building in Denmark', *Energy and Buildings*, 86, pp. 25-34.
- Sanchez-Guerrero, M.C., Lorenzo, P., Medrano, E., Castilla, N., Soriano, T., Baille, A., 2005. Effect of variable CO₂ enrichment on greenhouse production in mild winter climates. *Agric. Forest Meteorol.* 132, 244–252.
- Santosh, D.T., K.N. Tiwari, Vikas Kumar Singh and Raja Gopala Reddy, A. 2017. Micro Climate Control in Greenhouse. *Int.J.Curr.Microbiol.App.Sci.* 6(3): 1730-1742.
- Santosh, D.T., K.N. Tiwari, Vikas Kumar Singh and Raja Gopala Reddy, A. 2017. Micro Climate Control in Greenhouse. *Int.J.Curr.Microbiol.App.Sci.* 6(3): 1730-1742. doi:<https://doi.org/10.20546/ijcmas.2017.603.199>
- Schonhof, I., Kläring, H.P., Krumbein, A., Claußen, W. and Schreiner, M. (2007) 'Effect of temperature increase under low radiation conditions on phytochemicals and

- ascorbic acid in greenhouse grown broccoli', *Agriculture, ecosystems & environment*, 119(1-2), pp. 103-111.
- Shamshiri, R., Ishak, W. & Ismail, W. (2013). A Review of Greenhouse Climate Control and Automation Systems in Tropical Regions. *Journal of Agricultural Science and Applications*, 176-183.
- Shamshiri, R.R., Jones, J.W., Thorp, K.R., Ahmad, D., Man, H.C. & Taheri, S. 2018, 'Review of optimum temperature, humidity, and vapour pressure deficit for microclimate evaluation and control in greenhouse cultivation of tomato', *Int. Agrophys.*, vol. 32, no. 2, pp. 287–302.
- Singh, M.C., Singh, J.P. and Singh, K.G., 2018. Development of a microclimate model for prediction of temperatures inside a naturally ventilated greenhouse under cucumber crop in soilless media. *Computers and electronics in agriculture*, 154, pp.227-238.
- Singh, M.C., Singh, J.P. and Singh, K.G., 2022. Mathematical modelling of greenhouse microclimate under vertically trained soilless cropped conditions. *Agricultural Research*, 11(4), pp.672-682.
- Singh, M.C., Yousuf, A. and Singh, J.P., 2016. Greenhouse microclimate modelling under cropped conditions-A review. *Res. Environ. Life Sci*, 9(12), pp.1552-1557.
- Stanghellini, C., Kempkes, F., 2008. Steering of fogging: control of humidity, temperature or transpiration? *Acta Hort.* 797, 61–67.
- Stouffer, R.J. and Wetherald, R.T. (2007) 'Changes of variability in response to increasing greenhouse gases. Part I: Temperature', *Journal of Climate*, 20(21), pp. 5455-5467.

- Takeya, S., Muromachi, S., Maekawa, T., Yamamoto, Y., Mimachi, H., Kinoshita, T. et al. 2017, 'Design of ecological CO₂ enrichment system for greenhouse production using TBAB + CO₂ semi-clathrate hydrate', *Energies*, vol. 10, no. 7, pp. 1–11.
- Tang, Y., Ma, X., Li, M. and Wang, Y. (2020) 'The effect of temperature and light on strawberry production in a solar greenhouse', *Solar Energy*, 195, pp. 318-328.
- Teitel, M., Ziskind, G., Liran, O., Dubovsky, V. and Letan, R. (2008) 'Effect of wind direction on greenhouse ventilation rate, airflow patterns and temperature distributions', *Biosystems Engineering*,¹ 1101(3), pp. 351-369.
- Trudel, M.-J., & Gosselin, A. (1982). Influence of soil temperature in greenhouse tomato production. *HortScience*, 17(6), 928–929.
- Tzounis, A., Katsoulas, N., Bartzanas, T. and Kittas, C. (2017). Internet of Things in agriculture, recent advances and future challenges. *Biosystems Engineering*, 164, 31-48.
- Ullah, I., Fayaz, M., Aman, M. and Kim, D. (2022). Toward Autonomous Farming—A Novel Scheme Based on Learning to Prediction and Optimization for Smart Greenhouse Environment Control. *IEEE Internat of Things Journal*, 9(24), 25300-25323.
- Umesha, B. (2011) 'Effect of weather parameters on growth and yield parameters of tomato under natural poly house', *Indian Journal of Natural Sciences International Bimonthly ISSN*, 976, p. 0997.
- Wang, S., Boulard, T. and Haxaire, R. (1999) 'Air speed profiles in a naturally ventilated greenhouse with a tomato crop', *Agricultural and forest Meteorology*, 96(4), pp. 181-188.

- Willits, D.H. and Peet, M.M. (1998) 'The effect of night temperature on greenhouse grown tomato yields in warm climates', *Agricultural and Forest meteorology*, 92(3), pp. 191-202.
- Wilson, J.S. 2005, *Sensor Technology Handbook*, Elsevier Inc., Burlington, MA.
- Xin, P., Li, B., Zhang, H. and Hu, J. (2019) 'Optimization and control of the light environment for greenhouse crop production', *Sci. Rep.*, 9(1), p. 8650.
- Yongwei Li, Ying Ding, Daoliang Li, Zheng Miao, Automatic carbon dioxide enrichment strategies in the greenhouse: A review, *Biosystems Engineering*, Volume 171, 2018, Pages 101-119, ISSN 1537-5110, <https://doi.org/10.1016/j.biosystemseng.2018.04.018>.
- Zhang, Y., Mahrer, Y. and Margolin, M., 1997. Predicting the microclimate inside a greenhouse: an application of a one-dimensional numerical model in an unheated greenhouse. *Agricultural and forest meteorology*, 86(3-4), pp. 291-297.

**REAL TIME MONITORING OF MICROCLIMATIC PARAMETERS OF
POLYHOUSE USING IOT EMBEDDED SENSOR SYSTEMS**

BY

ABHIRAM BABU (2021-02-029)

BHAVANA P (2021-02-030)

ANJALY ANAND (2021-02-039)

KEERTHI NATH R (2021-02-044)

ABSTRACT

Submitted in partial fulfilment of the requirement for the degree of

BACHELOR OF TECHNOLOGY IN AGRICULTURAL ENGINEERING

Faculty of Agricultural Engineering and Technology

Kerala Agricultural University



**DEPARTMENT OF SOIL AND WATER CONSERVATION ENGINEERING
KELAPPAJI COLLEGE OF AGRICULTURAL ENGINEERING AND FOOD
TECHNOLOGY**

Tavanur-679573, Malappuram

Kerala, India

2025

ABSTRACT

In the light of increasing global challenges such as climate change, rapid urbanization, and the growing demand for food due to population rise, there is an urgent need to implement sustainable and efficient agricultural practices. One promising solution is the application of smart farming technologies that utilize real-time data for decision-making. This project, conducted at KCAEFT, Tavanur between January and May 2025, focuses on the development and deployment of a real-time microclimate monitoring system inside a polyhouse using IoT-embedded sensor technologies. The system is built around a microcontroller-based architecture with ESP32 modules, enabling wireless communication and real-time data visualization. Multiple environmental parameters critical for crop production—such as air temperature, relative humidity, soil temperature, light intensity, and wind speed—were continuously monitored using a network of strategically placed sensors. Data collected was transmitted to an integrated cloud platform, allowing for remote access and timely insights without manual supervision. To ensure accuracy and reliability, sensor calibration was carried out through comparative analysis with standard instruments and digital weather applications such as Wind Compass Pro and Zoom Earth. Though some sensors (e.g., anemometer, soil temperature, and BH1750 light sensor) initially showed minor deviations of recorded data from their true values, the calibration process yielded highly satisfactory results, as reflected by high R^2 values, validating their performance. A well-planned wiring layout ensured minimal energy usage and cost-efficiency, with total wire requirements of 842 meters per module. Visualization tools and analytics helped track trends in microclimatic variations, enabling precise climate monitoring. This project demonstrates a scalable, low-cost, and energy-efficient solution for real-time microclimatic monitoring of polyhouse environments. It provides a robust foundation for future automation, paving the way for smart farming systems that optimize resource usage, reduce labour dependency, and enhance productivity through precision agriculture practices.